Title
The Structural Bases of Stability-Function Tradeoffs in Antibiotic Resistance Enzymes

Author
Thomas, Veena Lily

Publication Date
2009

Peer reviewed|Thesis/dissertation

The Structural Bases of Stability-Function Tradeoffs in Antibiotic Resistance Enzymes

by

Veena Lily Thomas

DISSERTATION

Submitted in partial satisfaction of the requirements for the degree of

DOCTOR OF PHILOSOPHY

in

Pharmaceutical Sciences and Pharmacogenomics

in the

GRADUATE DIVISION

of the

UNIVERSITY OF CALIFORNIA, SAN FRANCISCO

To Jacob Thomas, Kevin Atkinson, and Keith Santarelli, whose unfailing wisdom and undying support through the years has never failed to astound me.

Acknowledgements

The work presented here was aided and abetted by a great deal of scientific and personal support from a number of talented individuals. First I thank Brian Shoichet for taking me into his laboratory and for countless guidance, both directly on this project and on the way I do science. Brian has an infectious enthusiasm for science, and a unique knack for finding and selling the interesting story and paper among the research, something I have tried to emulate. I am not the same person I was when I started graduate school, and Brian is certainly responsible for much of this; my interactions with him have forced me to sharpen my intellect, my critical thinking skills, my vocabulary, my wit, and my taste in music.

Past and present members of the Shoichet Lab were patient teachers in showing me the techniques employed in this research. Kerim Babaoglu went far and beyond his call of duty to teach me crystallography, from crystallization to collection strategy to refinement, and was a great companion on overnight synchrotron trips. I thank Yu Chen as well for crystallographic advice and assistance, as well as discussions on beta-lactamase. Federica Morandi was an encyclopedic resource of AmpC's idiosyncrasies. Ruth Brenk was a great teacher and role model during my early years in the lab. Sandri Soelaiman purified several of the mutants characterized here, in conjunction with Ray Nagatani, as well as set some crystal trays. Andrea McReynolds also worked very hard to make and purify two AmpC mutants studied. Matthew Merski assisted with the molecular biology. Sarah Boyce was always willing to help with chemistry and crystallography questions.

But above and beyond this, members of the Shoichet lab have really created a friendly and fun environment in which to work, and I've enjoyed spending time with them both in and out of the lab (yes, I have left occasionally). Alan Graves was a dear friend and constant companion, a true Southern gentleman, and I miss seeing his bright

smile in the lab every day and our long conversations. Peter Kolb has always been there with a joke, advice, and tea. Michael Keiser brightened each day with poetry, Peasant Pies, and intellectual sparring. Sarah Boyce has become like a sister to me in our little corner of the wet lab, and a great source of support these past two years in particular. Rafaela Ferreira is wise beyond her years and a dear friend and fellow partner in crime.

I would not be the scientist I am today without the mentorship of several faculty members. My high school biology teacher Charles Brightly started my love for biology and led by example; his love of teaching and his students was an inspiration, and he would have been proud to see the completion of this work. I will be forever in debt to my undergraduate research advisor, Prof. Vernon Ingram, for taking me under his wing and having a tremendous impact on the way I do science. Despite being world-renowned for being considered "The Father of Molecular Medicine" for discovering in the 1950s that sickle cell anemia was the result of a single amino acid change in hemoglobin, he was the one who personally trained me how to use a pipette, how to run experiments, and by demanding excellence, phenomenally hard work, and holding me to higher standards than possibly human, instilled in me a philosophy of being a scientist and a work ethic that continues to this day. I owe my direction in graduate school to Prof. Ken Dill; his brilliance, clarity, and statistical thermodynamics class were an inspiration to me and convinced me that I had to pursue thermodynamics, and his excitement and encouragement about my rotation work with him was an incredible boost to a young grad student. Prof. Charles Craik's enthusiasm about… well, everything… was infectious, and he too took a personal interest in my career, and I strove to great heights because I knew he thought I was capable of them. I can never thank him enough for his compassion and humanity towards me, and for championing my best interests, as I struggled with a blood sugar disorder and all of its repercussions. I thank my thesis committee, Prof. David Agard and Prof. Jim Wells, for scientific discussion and ideas, guidance, and personal support; David's razor-sharp mind, forthrightness, and humanity undoubtedly saved me

from venturing down dark research alleys, and Jim's enthusiasm and excitement for this work, clear-minded direction, and willingness to talk kept me going. Prof. Patsy Babbitt's compassion had a larger impact than she may realize; I will always treasure her candor, conversation, and wisdom as she gave me a ride from New Hampshire to Logan Airport.

Others at UCSF have had a tremendous impact on my years in graduate school. I don't know what I would have done without John Chodera; he has been an incredible guiding light, both scientifically and personally, and companion for countless outings and dinners and Sunday night runs to In N' Out. Sarah Shugarts has become the older sister I never had, kindred spirit on the road of darkness, paved with homemade dinners and a bottle (or two…) of wine, and understands me like few do. I thank the board game crew too for taking me in and providing an oasis during a difficult time, especially Gabriel Rocklin for setting me on the right path again, and Tet Matsuguchi for much laughter. Mike Kim was like half of my mind when we TAed the physical chemistry lab course together, and I thank him for being a great teammate. Christina Chaivorapol made sure I was up on all the best restaurants, and Libusha Kelly kept me inspired by her work-life balance. Ray Nagatani kept me on my toes, and Grant Shackelford's dry sense of humor and quiet friendship kept me going. Administratively, both Chris Olson and Lisa Magargal are constant champions for students in navigating the system and adopted me into their respective graduate programs, and go far beyond their job descriptions; without them I'm sure I would have been kicked out of graduate school long ago, or at least still be on medical leave for a blood sugar disorder while UCSF cut off my health insurance because I was on medical leave.

I'm known for saying that there's the family you're born into, and the family you make for yourself – and both deserve mention here. Anything I've accomplished in my life I owe directly to my dad, whose love and devotion to me I can't comprehend. My dad is the wisest person I know, one of the smartest, and since I was small (no jokes here, please) he has been my hero and an inspiration, and now that I am older, a good friend.

My mom stayed home and raised me, and for that I will always be grateful. She has tried to make sure I don't neglect my life outside of science – with limited success, but I thank her for trying – and is responsible for my artistic side. My sister Sapana inspires me every day with her creativity, her intelligence, and her humor – I think she's always tried to live up to the example of her older sister, but I want her to know that I try to live up to hers.

But I'm almost more impressed by the family I've made for myself, for they have stood by me my entire adult life by choice, not by blood. Kevin Callahan, my platonic soulmate and official Class of '98 Best Friend, has been by my side since we were lab partners at 13; he saw in me something that few did, and I shudder to think of the person I would be today if it weren't for having him in my life. To this day he makes sure I am true to myself and the person I am and could be in his eyes. Kevin Atkinson has been my rock through my undergraduate and graduate years, and is perhaps the single biggest influence on the principles that guide the way I live my life; you'd be hard-pressed to find a better human being. Keith Santarelli is my best friend and means more to me than words can say; our parallel lives through our respective graduate careers, unwavering support and advice for each other, and countless phone calls and e-mails shared the highs and pulled me through the lows, even thousands of miles away.

Christian Laggner has fundamentally changed my life these past few months, and has opened my mind, heart, and soul in ways I didn't know were possible. He is my touchstone, my grounding force, my confidant, and extremely good at saving me from myself. It's unfathomable to me that I didn't get to know him sooner, but I look to the future with bright eyes. *Tibi. In omne tempus.*

These years of graduate school and this thesis would not have been possible without the sage wisdom and more support than I can comprehend, through all my years of graduate school and beyond, from the three people who have always believed in me beyond reason: Jacob Thomas, Kevin Atkinson, and Keith Santarelli. I dedicate this thesis to them.

The text of Chapter 1 is a reprint of the material as it appears in:

Thomas, V.L. et al. Structural Consequences of the Inhibitor-Resistant Ser130Gly Substitution in TEM β-Lactamase. *Biochemistry*.44(26):9330-8 (2005)

It appears here with permission from the authors.

The text of Chapter 2 is a reprint of the material as will appear in:

Thomas, V.L. et al. Structural Bases for Stability-Function Tradeoffs in Antibiotic Resistance.*J Mol Biol* (2009); accepted.

It appears here with permission from the authors.

The text of Appendix A is a reprint of the material as it appears in:

Marciano D.C. et al.. Genetic and structural characterization of an L201P global suppressor substitution in TEM-1 beta-lactamase. *J Mol Biol*. 384(1):151-64.. (2008)

It appears here with permission from the authors.

Abstract

The Structural Bases of Stability-Function Tradeoffs in Antibiotic Resistance Enzymes

Veena L. Thomas

Antibiotic use has led to the evolution of antibiotic resistance enzymes able to hydrolyze newer antibiotics, leaving them useless against killing bacteria. Are there biophysical costs to evolving drug resistance? The hypothesis addressed here is that both protein stability and native activity constrain enzyme evolution, and uses the enzyme β-lactamase, the major resistance mechanism against β-lactam antibiotics like penicillin, to investigate this question.

β-lactamase hydrolyzes β-lactam antibiotics, such as penicillin, rendering them ineffective. In response to drugs combating β-lactamase, two types of β-lactamase resistance mutants have emerged in the clinic. Extended-spectrum mutants have gained the ability to break down larger, third-generation antibiotics that were previously impervious to β-lactamase, whereas inhibitor-resistant mutants have decreased inhibition by covalent inhibitors. Each category of resistance mutant was investigated. First, the crystallographic structure of the S130G inhibitor-resistant β-lactamase was determined to 1.4 Ångstrom resolution. Two configurations of a new water molecule were observed in the active site, and explain how this resistance mutant remains active with the presumed catalytic acid for substrate hydrolysis replaced. Substituting this key catalytic residue to gain inhibitor resistance resulted in a mutant enzyme with almost ten-thousand-fold decreased catalytic activity -- a rather Pyrrhic victory, and an example of the biophysical cost enzymes pay for developing drug resistance.

Second, the "stability-function" hypothesis – do drug-resistant mutants, and enzymes in general, sacrifice their inherent stability and ancestral activity as they gain

activity against newer antibiotics or substrates – was investigated in β-lactamase extended-spectrum resistance mutants. The thermodynamic stability and catalytic activity against both third-generation and older antibiotics was determined for five known β-lactamase extended-spectrum mutant enzymes. These mutant enzymes had between 100- to 200-fold increased activity against the antibiotic cefotaxime, but were destabilized by up to 4.1 kcal/mol, consistent with the stability-function hypothesis. Eight structures, including complexes with inhibitors and extended-spectrum antibiotics, were determined by x-ray crystallography. Distinct mechanisms of action were revealed for each mutant, including changes in the flexibility and ground state structures of the enzyme. Understanding biophysical constraints on evolution of drug resistance, and how distant substitutions are structurally transmitted to the active site has broad relevance to drug-resistant systems.

Table of Contents

List of Tables

List of Figures

Introduction

"... from so simple a beginning, endless forms most beautiful and most wonderful have been, and are being, evolved."

-Charles Darwin, The Origin of Species

According to the famous naturalist Charles Darwin, life on earth may have begun in a "warm little pond, with all sorts of ammonia and phosphoric salts, lights, heat, electricity, etc. present, so that a protein compound was chemically formed ready to undergo still more complex changes" [1]. From these deceptively humble beginnings evolved an estimated 5 million to 100 million species of life, though only about 2 million of these have been identified [2]. Included among these are countless curiosities of nature. The Australian echidna, or spiny anteater, forms trains up to eleven animals long when pursuing females for mating, has a four headed-phallus, is an egg-laying mammal, and produces milk but lacks nipples. Its normal body temperature is only 33º C, lower than any other mammal except the platypus, though it can fluctuate by up to 6-8 degrees normally. In the wintertime, they can drop its body temperature down to 4º C while hibernating, when they take one breath every three minutes. It enters REM sleep at 25º C, but stops at 28 or 15º C. The duck-billed platypus, from the other family of monotremes, exhibits similar marvels of evolution; it has ten sex chromosomes, a tail like a beaver, a bill like a duck, and a spur on its hind leg that injects venom into other animals, making it one of the few venomous mammals. They detect their prey by electrolocation, sensing electric fields created by muscle contractions. When first discovered by Europeans around 1800, some speculated it was some sort of elaborate hoax, the pelt stitched together by a skilled taxidermist. Indeed, the duck-billed platypus is often quipped to be evidence that "God has a sense of humor".

Creationist views aside, such examples of macroscopic evolution of species are made possible by evolution of far smaller components: proteins, the molecular

workhorses of cells, which carry out vitally important structural and biochemical processes responsible for life. These polymers of various lengths and sequences of the 20 amino acids fold to minimize their free energy. For enzymes, however, it is even more complex; not only must they fold into stable conformations, but they must also bind a ligand and catalyze a chemical reaction. Hence, enzyme structures are thought to reflect tradeoffs against several orthogonal constraints. Ligand recognition is often counterproductive to stability: the enzyme must leave key interactions unfulfilled to be satisfied upon ligand-binding. This leads to high-energy interactions in active sites, as enzymes cluster like-charged residues and expose hydrophobic areas to water. To maintain its catalytic activity, an enzyme must sacrifice some potential stability it could achieve with another, inactive sequence.

The hypothesis that enzymes trade stability for function was directly tested in T4 lysozyme [3]. Twenty substitutions total were made at two catalytic residues and three ligand-binding residues. Point substitutions at these positions in the active site stabilized the enzyme by up to 2 kcal/mol relative to the WT enzyme, though these mutants were much less active. Alan Fersht found a similar trend: substituting charged catalytic residues with alanines in both barnase [4] and barstar [5] resulted in an increase in enzyme stability but a decrease in relative activity. The structural bases of stability-function trade-offs were determined with substitutions of catalytic residues of AmpC beta-lactamase: whereas active site substitutions decreased activity significantly, they increased stability by mimicking the substrate, relieving both steric and electrostatic strain, and improving complementarity [6].

But enzymes are not evolutionary endpoints; they also gain new properties through gene duplication, random mutations, and natural selection. How does the stability-function hypothesis relate to evolution of new properties? Enzymes have a small margin of stability; gaining new activities through active site modification may destabilize the enzyme [3]. Since an unstable enzyme is an unfolded enzyme, stability may

serve as a constraint on enzyme evolution. Previous research in this lab found that while TEM extended-spectrum β-lactamase resistance mutants have evolved the ability to hydrolyze third-generation cephalosporins that were previously not β-lactam substrates, these mutant enzymes have both decreased stability and decreased activity against their ancestral substrate, penicillin [7].

Are there biophysical and enzymatic constraints and tradeoffs to evolving new enzyme functions and antibiotic resistance? To address this question and understand its generality, we turned to β-lactamases such as AmpC, and TEM-1, major resistance mechanisms against β-lactam antibiotics, such as penicillins and cephalosporins; hydrolysis of their β-lactam ring leaves them ineffective against bacteria. To put this work in context, we first turn to a brief history of β-lactam antibiotics.

From the *NewYork Times* [8]:

> In March 1942, Mrs. Miller was near death at New Haven Hospital suffering from a streptococcal infection, a common cause of death then. She had been hospitalized for a month, often delirious with her temperature spiking to nearly 107, while doctors tried everything available, including sulfa drugs, blood transfusions and surgery. All failed.
>
> As she slipped in and out of consciousness, her desperate doctors obtained a tiny amount of what was still an obscure, experimental drug and injected her with it. Her hospital chart, now at the Smithsonian Institution, registered a sharp overnight drop in temperature, and by the next day she was no longer delirious and soon was eating full meals, one of her doctors reported.

This "obscure, experimental drug" was penicillin, now credited with saving millions of lives since its introduction.

Perhaps the best way to describe the now-famous story of the discovery of penicillin is in the words of Alexander Fleming himself [9], who won the Nobel Prize in 1945 for its discovery:

> In my first publication I might have claimed that I had come to the conclusion, as a result of serious study of the literature and deep thought, that valuable antibacterial substances were made by moulds and that I set out to investigate the problem. That would have been untrue and I preferred to tell the truth that penicillin started as a chance observation. My only merit is that I did not neglect the observation and that I pursued the subject as a bacteriologist. My publication in 1929 was the starting-point of the work of others who developed penicillin especially in the chemical field.
>
> The origin of penicillin was the contamination of a culture plate of staphylococci by a mould. It was noticed that for some distance around the mould colony the staphylococcal colonies had become translucent and evidently lysis was going on. This was an extraordinary appearance and seemed to demand investigation, so the mould was isolated in pure culture and some of its properties were determined….
>
> The result… is very similar to that observed with lysozyme with one very important difference, namely that the microbes which were most powerfully inhibited were some of those responsible for our most common infections. This was a most important difference.

However, even then, before resistance was seen in the clinic, Fleming cautioned against the dangers of potential emergence of antibiotic resistance, and its prevention [9]:

> But I would like to sound one note of warning. Penicillin is to all intents and purposes non-poisonous so there is no need to worry about giving an overdose and poisoning the patient. There may be a danger, though, in underdosage. It is not difficult to make microbes resistant to penicillin in the laboratory by exposing them to concentrations not sufficient to kill them, and the same thing has occasionally happened in the body.
> The time may come when penicillin can be bought by anyone in the shops. Then there is the danger that the ignorant man may easily underdose himself and by exposing his microbes to non-lethal quantities of the drug make them resistant. Here is a hypothetical illustration. Mr. X. has a sore throat. He buys some penicillin and gives himself, not enough to kill the streptococci but enough to educate them to resist penicillin. He then infects his wife. Mrs. X gets pneumonia and is treated with penicillin. As the streptococci are now resistant to penicillin the treatment fails. Mrs. X dies. Who is primarily responsible for Mrs. X's death? Why Mr. X whose negligent use of penicillin changed the nature of the microbe. *Moral:* If you use penicillin, use enough.

Indeed, as early as 1947, the first penicillin-resistant bacterial strain was reported in the clinic, 4 years after the mass-production of penicillin.

There are several mechanisms through which bacterial strains develop resistance to antibiotics, including inactivation or modification of the drug or its target, and modification of porin channels or an increase in efflux pumps, both resulting in decreased permeability of the antibiotic into the bacterial cells. The bacterial enzyme β-lactamase is one example of a resistance mechanism causing drug inactivation; hydrolysis of β-lactam antibiotics, such as penicllin, by β-lactamase renders them useless against killing bacteria.

The class A β-lactamase, TEM-1, was detected in the clinic in 1963, 17 years after penicillin was first approved by the FDA [10] . In response to this resistance enzyme, antibiotics were introduced into the clinic that were not substrates for the wild-type enzyme. In addition, combination therapeutics, consisting of β-lactamase inhibitors in conjunction with antibiotics such as amoxicillin, were also introduced. Unfortunately, this resulted in the emergence of two categories of resistance mutants. Inhibitor-resistant β-lactamase mutants have decreased susceptibility to mechanism-based inhibitors, such as clavulanate, that function by covalently and irreversibly attaching to the catalytic serine in the active site. Extended-spectrum β-lactamase mutants have gained hydrolytic activity the third-generation cephalosporin antibiotics that were previously not substrates for the wild-type enzyme, rendering even these newer antibiotics useless. This has led to a sort-of antibiotics "arms race" between humans and bacteria.

Ironically, what is unfortunate for mankind is fortunate for scientists studying enzyme evolution and how distant mutations affect enzyme active sites: it turns out that β-lactamase is an excellent model system for investigating these questions, not the least of which is because of the wealth of information available about resistance mutations, serving as excellent examples of evolution-in-real-time. Its activity against various antibiotic substrates can be measured easily by spectrophotometric assays, and its inherent thermodynamic stability can be quantified by thermal denaturation, monitored by circular dichroism, since conditions had previously been established under which these enzymes denature reversibly and in a two-state fashion, both prerequisites for

quantitatively measuring changes in enzyme stability. In addition, in theory β-lactamase crystallizes "easily" and expresses "well" (though, as I was soon to discover, for small values of "easily" and "well", as patience approaches zero). These biophysical and biochemical tools allowed us to quantitatively investigate biophysical and biochemical constraints on evolution of new enzyme functions, specifically in regard to antibiotic resistance: as enzymes gain new functions and resistance to antibiotics, do they trade off some of their inherent stability and native enzymatic activity? What are the structural bases for how mutations, often distant from the active site by 10-20 Å, cause antibiotic resistance when the mechanism is not obvious? Even when the mechanism of antibiotic resistance is completely obvious, ie, replacing a catalytic serine to which the mechanism-based inhibitors covalently attach, how does the enzyme remain functional with an important active site residue, implicated in catalysis, replaced? The first two questions are addressed in chapter two of this dissertation, where eight x-ray crystal structures of five extended-spectrum β-lactamase mutants were determined, along with activity and stability measurements, in order to elucidate constraints on evolution of antibiotic resistance. The second question provides the framework for chapter one, where the x-ray crystal structure of an inhibitor-resistant β-lactamase was determined to 1.4 Å resolution in order to determine the mechanism by which it remains catalytically active. It is to these questions that we now turn.

References

1. Darwin, C. (1871). Communication with botanist Joseph Hooker.
2. The National Science Foundation. "Tree of Life" project.
3. Shoichet, B. K., Baase, W. A., Kuroki, R. & Matthews, B. W. (1995). A Relationship Between Protein Stability and Protein Function. *Proc. Nat. Acad. Sci USA.* **92**, 452-456.
4. Meiering, E. M., Serrano, L. & Fersht, A. R. (1992). Effect of active site residues in barnase on activity and stability. *J. Mol. Biol.* **225**, 585-9.
5. Schreiber, G., Buckle, A. M. & Fersht, A. R. (1994). Stability and function: two constraints in the evolution of barstar and other proteins. *Structure* **2**, 945-51.
6. Beadle, B. M. & Shoichet., B. K. (2002). Structural bases of stability-function trade-offs in enzymes. *J. Mol. Biol.* **321**, 285-296.
7. Wang, X., Minasov, G. & Shoichet, B. K. (2002). Evolution of an Antibiotic Resistance Enzyme Constrained by Stability and Activity Trade-Offs. *J. Mol. Biol.* **320**, 85-95.
8. Saxon, W. (1999, June 9). Anne Miller, 90, First Patient Who Was Saved by Penicillin. In *The New York Times*.
9. Fleming, A. (1964). Penicillin. In *Nobel Lectures, Physiology or Medicine 1942-1962*. Elsevier Publishing Company, Amsterdam.
10. Orencia, M. C., Yoon, J. S., Ness, J. E., Stemmer, W. P. & Stevens, R. C. (2001). Predicting the emergence of antibiotic resistance by directed evolution and structural analysis. *Nat Struct Biol* **8**, 238-42.

Gloss to Chapter 1

I barely knew what a crystal structure was when I came to UCSF. I had worked on peptide aggregation biophysics as an undergraduate, but came to graduate school open to new research areas: anything except pipetting, proteins, and bacteria. It is a testament to Brian's infectious enthusiasm for cool science that he somehow convinced me to devote my graduate career to experimental research on whether native activity and stability constrain evolution of bacterial antibiotic resistance proteins. But I was certainly green around the edges when it came to my new research. I remember my initial meeting with Brian to discuss this project, the first step of which would be to investigate evolution of inhibitor-resistant TEM beta-lactamases, to determine if stability constrained their evolution. I told him that it all sounded great, but where did one get these proteins from? After all, with my previous research, we ordered the 42-amino acid peptides on the internet, and they showed up in the mail. Brian just looked at me funny. "Um, you make them," he said. "Oh, great!" I responded. "So, about two weeks?"

Several months, much hard work and optimization, and numerous purifications later, I jumped at Brian's offer of a new side-project: the crystallization and (hopefully) structure-determination of an inhibitor-resistant TEM beta-lactamase, Ser130Gly. Mechanism-based clinical inhibitors of TEM covalently cross-link the catalytic Ser64 to Ser130 in the active site. Inhibitor-resistant substitutions in TEM identified in the clinic are located at multiple positions of the enzyme. However, very few inhibitor-resistant TEM enzymes feature substitutions directly to Ser130, the most obvious substitution for a protein engineer to have designed. In TEM-76, Ser130, an active-site serine to which mechanism-based inhibitors covalently cross-linked, had been substituted with glycine. However, as this serine was also implicated as the catalytic acid in substrate hydrolysis, it was unclear how this clinically relevant mutant enzyme remained active at all – and potentially explained its relative scarcity in the clinic. And the best part? Our

collaborators had determined the kinetics against antibiotic substrates and inhibitors, had shipped us the protein (!), and my mission, should I choose to accept it, was to crystallize it, determine the structure and the mechanism by which it remained catalytically active, and its stability. I jumped at the chance to learn crystallography – it seemed very mysterious and prestigious.

Mysterious, yes. But crystallize it did, and after my first synchrotron trip, I had a data set of TEM S130G to 1.4 Angstrom resolution. Looking back, it's amazing how much better and more intuitive crystallography software has gotten in such a short amount of time. After much wrestling with ShelX (which we later determined was primarily meant for higher resolution data than mine), and O, I got fed up and re-solved the structure in CNS. The resulting structure revealed that a new water molecule replaced the presumed catalytic acid, and likely functioned as the hydrogen donor in substrate hydrolysis. It also revealed unexpected similarities to another inhibitor-resistant TEM mutant, TEM-32, where the cross-linking Ser130 was still present, but had moved significantly relative to the wild-type position – and a new water molecule was also found close to the wild-type Ser130 position. This demonstrated that several inhibitor-resistant substitutions had the same net effect, converging on the cross-linking Ser130.

This chapter originally appeared in *Biochemistry* in 2005.

Chapter 1:
Structural Consequences of the Inhibitor-Resistant Ser130Gly Substitution in TEM β-Lactamase[†, ‡]

Veena L. Thomas[§], Dasantila Golemi-Kotra[‖], Choonkeun Kim[‖], Sergei B. Vakulenko[‖], Shahriar Mobashery[‖]*, Brian K. Shoichet[⊥]*

[§]Graduate Program in Pharmaceutical Sciences and Pharmacogenomics

[⊥]Department of Pharmaceutical Chemistry

University of California, San Francisco

San Francisco, CA 94143

[‖]Department of Chemistry and Biochemistry

University of Notre Dame

Notre Dame, IN 46556

[†]This work was supported by NIH grants GM63815 (to B.K.S.) and AI33170 (to S.M.), and by the Achievement Rewards for College Scientists Foundation and a National Science Foundation predoctoral fellowship (to V.L.T.).

[‡]Atomic coordinates and structure factors have been deposited in the Protein Data Bank at the Research Collaboratory for Structural Bioinformatics at Rutgers University (entry 1YT4).

*Corresponding authors. B.K.S.: Phone: 415-514-4126. Fax: 415-502-1411. E-mail: shoichet@cgl.ucsf.edu. S.M.: Phone: 574-631-2933. Fax: 574-631-6652. E-mail: mobashery@nd.edu.

1.1 Abstract

β-lactamase confers resistance to penicillin-like antibiotics by hydrolyzing their β-lactam bond. To combat these enzymes, inhibitors covalently crosslinking the hydrolytic Ser70 to Ser130 were introduced. In turn, mutant β-lactamases have emerged with decreased susceptibility to these mechanism-based inhibitors. Substituting Ser130 with glycine in the inhibitor-resistant TEM (IRT) mutant TEM-76 (S130G) prevents the irreversible crosslinking step. Since the completely conserved Ser130 is thought to transfer a proton important for catalysis, its substitution might be hypothesized to result in a nonfunctional enzyme; this is clearly not the case. To investigate how TEM-76 remains active, its structure was determined by x-ray crystallography to 1.40 Å resolution. A new water molecule (Wat1023) is observed in the active site, with two configurations located 1.1 Å and 1.3 Å from the missing Ser130 Oγ; this water molecule likely replaces the Ser130 sidechain hydroxyl in substrate hydrolysis. Intriguingly, this same water molecule is seen in the IRT TEM-32 (M69I/M182T), where Ser130 has moved significantly. TEM-76 shares other structural similarities with various IRTs; like TEM-30 (R244S) and TEM-84 (N276D), the water molecule activating clavulanate for crosslinking (Wat1614) is disordered (in TEM-30 it is actually absent). As expected, TEM-76 has decreased kinetic activity, likely due to the replacement of the Ser130 sidechain hydroxyl with a water molecule. In contrast to the recently determined structure of the S130G mutant in the related SHV-1 β-lactamase, in TEM-76 the key hydrolytic water (Wat1561) is still present. The conservation of similar accommodations among IRT mutants suggests that resistance arises from common mechanisms, despite the disparate locations of the various substitutions.

1.2 Introduction

The catalytic activity of the TEM family of class A β-lactamases is a major resistance mechanism against β-lactam antibiotics, such as penicillins (Figure 1A); hydrolysis of the β-lactam ring of these antibiotics renders them ineffective against bacteria. To combat these enzymes, inhibitors against β-lactamase, such as clavulanate, tazobactam, and sulbactam (Figure 1.1, *B-D*), were developed. In turn, inhibitor-resistant TEM β-lactamases (IRTs) have emerged in the clinic with decreased susceptibility to these mechanism-based inhibitors. These inhibitors function by acylating the enzyme's active site. After reacting with the catalytic Ser70, these β-lactam compounds can partition into either the hydrolytic pathway common to β-lactam substrates, or an inactivation pathway culminating in irreversible modification of Ser130, a completely conserved active site residue (*1-5*) (Figure 1.2). Though the crosslinking reaction may occur several hundreds of times less frequently than the competitive hydrolytic pathways, eventually the enzyme is completely and irreversibly inhibited (*6-8*).

The IRT mutant enzymes that have emerged in the clinic typically involve substitutions at several positions, including Met69, Arg275, Asn276, and Arg244 (www.lahey.org/Studies/temtable). To date, atomic resolution structures of five IRT mutants have been determined (*9-11*). The Arg244Ser substitution found in the TEM-30 mutant results in displacement of a water molecule involved in the inactivation chemistry of clavulanate (*3, 10*). This same water molecule was only transiently present in the TEM-84 (N276D) IRT mutant as well (*9*). In both TEM-32 (M69I/M182T) and TEM-34 (M69V), movement of Ser130, a site of covalent attachment, explains the inhibitor-resistant phenotype of these two mutants (*10*). The structures of the wild-type and the IRT TEM-33 (M69L) were observed to be virtually identical (with the exception of the site of mutation). Differences in the structures of the two enzymes became apparent only in the dynamic motions of the mutant and wild-type enzymes during computational

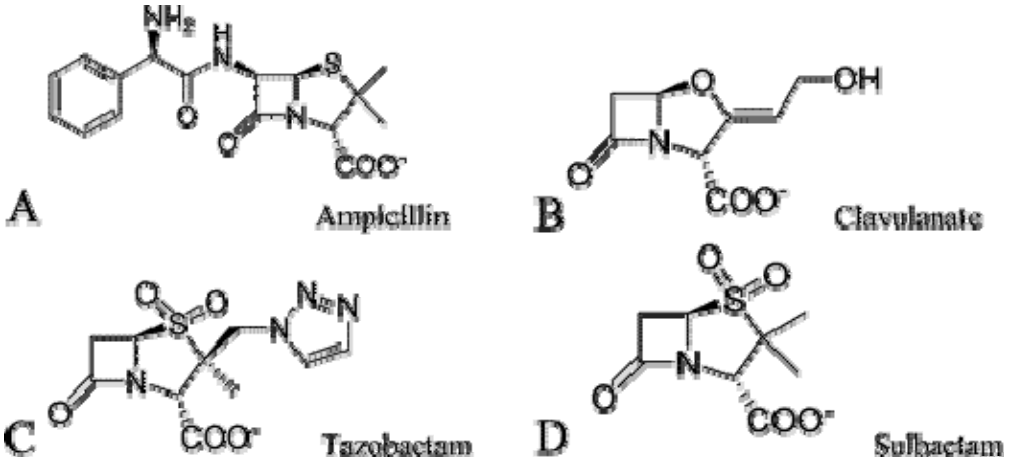

Figure 1.1 Chemical structures of the TEM β-lactamase substrate ampicillin (A) and mechanism-based inhibitors (B-D).

---

simulations (*11*). The primary contributing factor to the IRT phenotype of the TEM-33 enzyme was an increase in the apparent dissociation constants of the pre-acylation complexes with the inhibitors. Though replacing the Ser130 sidechain would seem to be the easiest way to prevent mechanism-based inhibition, its substitution is somewhat rare among clinical isolates. Most of the IRT substitutions are relatively distant from this position, and in this sense seem relatively subtle. For instance, the C_α atoms of Arg244 and Asn276 are located 14 Å and 17 Å from the Ser130 C_α, respectively. In contrast, the IRT mutant TEM-76 has simply replaced the crosslinking Ser130 with glycine, thus disrupting the inhibition reaction. At first glance, the mechanism of this mutant thus seems fairly obvious. The question here is not why this mutant is resistant to inhibition (though we will see that even here there are some subtleties), but rather how it remains active in its turnover of substrates, since Ser130 is thought to be a key catalytic residue.

Ser130 has been implicated as the catalytic acid necessary for protonating the lactam nitrogen leaving group, promoting the opening of the β-lactam ring during substrate hydrolysis (*12, 13*). Thus substitution of this serine with glycine in TEM-76

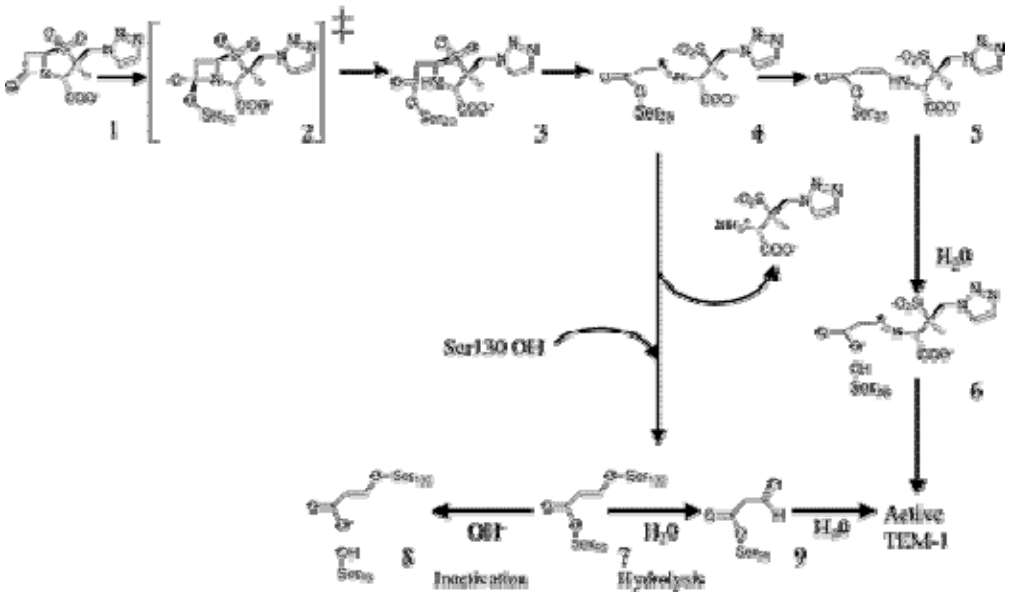

Figure 1.2 Simplified hydrolytic and inhibition pathways of TEM β-lactamase for tazobactam (*1, 11*).

---

might be expected to render the enzyme nonfunctional. As S130G is a naturally evolved mutant enzyme, it is apparent that TEM-76 has somehow compensated for the loss of this active site serine. To understand how this occurs, we have measured the kinetic parameters for activity and inhibition of TEM-76 and have determined its x-ray crystal structure to 1.40 Å resolution. This structure reveals how S130G compensates for the loss of its catalytic acid, and reveals some unexpected similarities with the more subtle mutant enzymes TEM-30, TEM-32, and TEM-84.

1.3 Materials and Methods

I. Construction and purification of TEM-1 β-lactamases

The cloning of the wild-type TEM-1 β-lactamase has been reported**.** To produce the Ser130Gly mutant of TEM-1 β-lactamase, a previously reported construct was used (*14*). In this construct the gene for the wild-type (TEM-1) enzyme was fused to the leader sequence of the outer membrane protein A (OmpA) and cloned into the expression vector pET24a(+) to allow secretion of large amounts of β-lactamase into the growth medium.

The mutant enzyme as prepared with QuikChange Site-Directed Mutagenesis Kit (Stratagene) using two oligonucleotide primers, TEM130Gly-D: gccataaccatg***ggt***gataacactg (the codon for Gly is in italics; the point mutation is in bold) and TEM130Gly-R: cagtgttatcacccatggttatggc that introduced a single mutation into the gene for the TEM-1 β-lactamase resulting in the desired substitution. The mutation was confirmed by sequencing of both strands of the entire gene. The TEM-1 and S130G mutant enzymes were isolated and purified as described previously (*11*).

II. Kinetics Measurements

The steady-state kinetic parameters for penicillins and cephalosporins were determined from nonlinear regression plots. The experimental data were fitted using GRAFIT software. The assays were carried out in 100 mM sodium phosphate buffer, pH 7.0, at room temperature, monitoring hydrolysis of penicillin G at 240 nm ($\Delta\varepsilon_{240}$ = 570 $M^{-1}cm^{-1}$), ampicillin at 235 nm ($\Delta\varepsilon_{235}$ = 820 $M^{-1}cm^{-1}$), cephaloridine at 267 nm ($\Delta\varepsilon_{267}$ = 1000 $M^{-1}cm^{-1}$) and nitrocefin at 482 nm ($\Delta\varepsilon_{267}$ = 17400 $M^{-1}cm^{-1}$). In all cases the substrate concentrations were such that they flanked the K_m values.

Inactivation constants for clavulanate, sulbactam, and tazobactam were calculated for the S130G mutant enzyme as per method described by Imtiaz *et al (3)*. Inactivation experiments with the mutant enzyme were initiated by the addition of a portion of a stock solution of clavulanate or sulbactam (10–160 μM final concentrations) to the enzyme (1 μM) solutions. For tazobactam the final concentration in the inactivation experiment ranged from 9 to 53 μM. Incubation was stopped by dilution of 10 μL aliquots of incubation mixture into 1 mL assay containing 0.8 mM penicillin G, at various time intervals. The residual enzyme activity in the aliquot was monitored until complete depletion of the substrate resulted. A progressive increase of the activity of the enzyme was observed initially, attributed to its recovery from the transiently inhibited species. The highest steady-states rates, in the course of substrate hydrolysis, were used in

calculation of the remaining enzyme activity.

The apparent K_I values for all three compounds were calculated for the S130G mutant enzyme by the method of Dixon (*15*). Two concentrations of the substrate penicillin G, typically 400 and 700 or 800 μM, were used. A series of assay mixtures containing both substrate and various concentrations of the inactivators (0.2-2 mM for clavulanate, 52-570 μM for sulbactam, and 11-500 μM for tazobactam) were prepared in 100 mM sodium phosphate buffer, pH 7.0. An aliquot of the stock solution of the enzyme was added to afford a final concentration of 60 nM of S130G mutant, in a total volume of 1.0 mL, followed by the immediate measurement of enzyme activity. The rates were measured for the first 5% of substrate turnover.

The partition ratios (k_{cat}/k_{inact}), for clavulanate, sulbactam and tazobactam were determined by the titration method (*16*). Several buffered mixtures containing various molar ratios of [I]/[E] of each of the inhibitors with S130G mutant enzyme were incubated at 4 °C overnight (ca. 20 hr). The molar ratio [I]/[E] for the experiment with clavulanate was from 4 to 1300, for sulbactam from 4 to 800, and for tazobactam from 4 to 400. The remaining activity of the enzyme was assayed under conditions of the excess substrate, with penicillin G.

The rate constants for recovery of the enzyme activity (k_{rec}) from the transiently inhibited species for the S130G mutant enzyme incubated with each of the compounds were measured at the molar ratio ([I]/[E]) that displayed a long delay prior to the linear steady-state hydrolysis of penicillin G. These experiments were performed under conditions of excess substrate, as described by Koerber and Fink (*17*). The calculations of the constants were performed according to the method of Glick *et al (18).*

III. Crystallization and structure determination

TEM S130G crystals were grown in hanging drops over a well solution of 1.4M NaH_2PO_4/K_2HPO_4, pH 8.3. A volume of 2 μL of 20 mg/mL protein in 50 mM KPi buffer

was mixed with 2 μL of well solution and the resulting 4 μL drop was seeded with microcrystals of TEM M182T (*19*). Crystals grew within five weeks. Crystals were soaked in 25% sucrose in 1.6M $KNaP_i$ as cryoprotectant for 10-30 seconds and then frozen in liquid nitrogen. Diffraction data were collected from a single crystal on the 8.3.1 beamline at the Advanced Light Source (Berkeley, CA) at a wavelength of 1.0332 Å. A total of 169 frames were integrated, and 149,639 reflections were scaled and merged using the DENZO/SCALEPACK package (*20*). The data are 98.9% complete to 1.40 Å resolution (43,334 unique reflections, Table 1.1). Crystals belong to the space group $P2_12_12_1$, with unit cell dimensions of 41.60, 59.71, and 88.36 Å, which are similar to the WT crystals (*21*). An initial structure was obtained by the molecular replacement EPMR using the M182T TEM mutant (Protein Data Bank accession code 1JWP) apo structure as an initial search model. Five percent of the data (2126 reflections) was set aside randomly as the test set. Following rigid body refinement in CNS 1.1 (*22*)**,** the S130G structure was refined by cycles of Cartesian and B-factor refinement. Water molecules were recognized and placed in the structure by CNS 1.1 on the basis of positive F_o-F_c density at a minimum contour level of 2σ, confirmed by visual inspection, and only those with B factors <60 $Å^2$ were retained. Multiple conformations of protein sidechains and water molecules were added to interpret features of an F_o-F_c electron density map.

IV. Thermal denaturation

The S130G enzyme was denatured by raising the temperature in 0.1 ˚C increments at a ramp rate of 2 ˚C/min in 200 mM potassium phosphate buffer, pH 7.0, using a Jasco 715 spectropolarimeter with a Peltier effect temperature controller and an in-cell temperature monitor (*23*)**.** Denaturation was marked by an obvious transition in the far-UV CD (223 nm) signal. Consistent with previous stability work with TEM enzymes, all melts were reversible and apparently two-state, as judged by the sharp transition in the denaturation

Table 1.1 Data and refinement statistics for S130G crystal structure

Unit cell parameters (Å)	41.60 59.71 88.36
Resolution (Å)	20.0 – 1.40 (1.45 – 1.40)*
Unique reflections	43,334 (4225)
Total observations	149,639
Working set / test set	40,386 / 2126 reflections
R-merge (%)	4.2 (38.4)
Completeness (%)	98.9 (97.8)
$\langle I \rangle / \langle \sigma(I) \rangle$	15.42 (2.37)
Number of residues	263
Number of water molecules	327
Space group	$P2_12_12_1$
RMSD bond lengths (Å)	0.010
RMSD bond angles (°)	1.90
Alternate conformations	14
R-factor (%)	18.30
R-free (%)	22.40

*Values in parentheses are for the highest resolution shell.

curve. Temperature of melting (T_m) and van't Hoff enthalpy of unfolding (ΔH_{vh}) values were calculated using EXAM (*24*). The free energy of unfolding relative to WT was calculated using the method of Becktel and Schellman: $\Delta\Delta G_u = \Delta T_m * \Delta S_u^{WT}$ (*25*). A positive value of $\Delta\Delta G_u$ indicates a stability gain. The ΔS_u^{WT} was 0.43(±0.02) kcal mol^{-1} K^{-1} (*19*).

1.4. Results

I. Kinetic parameters for turnover of substrates and for inhibition of TEM-1 and S130G β-lactamases.

We investigated the turnover of two penicillins and two cephalosporins with both the TEM-1 and its S130G mutant variant (Table 1.2). Whereas K_m values increased for both ampicillin (6-fold) and benzylpenicillin (14-fold) for the mutant protein, they decreased slightly for nitrocefin (2.5-fold) and cephaloridine (2.3-fold). However, the catalytic rate constants (k_{cat}) of S130G for these β-lactam antibiotics all decreased significantly; the effect ranges from a 9-fold decrease in k_{cat} for ampicillin to a 2300-fold decrease for cephaloridine. This decrease in hydrolytic ability of the mutant enzyme is responsible for the decrease in the pseudo second-order rate constant k_{cat}/K_m for all substrates measured; for instance, the k_{cat}/K_m for S130G is only 0.05% that for TEM-1 against benzylpenicillin. Considering that k_{cat}/K_m values for the wild-type enzyme were at the high levels of 10^6 to nearly 10^8 $M^{-1}s^{-1}$, it would appear that some sacrifice in catalysis does take place on mutation of Ser130 to glycine, but the levels of activity are still sufficient for the manifestation of resistance.

We also investigated the parameters for interaction with the three clinically used mechanism-based inhibitors clavulanate, tazobactam and sulbactam (Table 1.3). These analyses follow the procedures described earlier (*3, 9, 11*). Somewhat unexpectedly, the k_{cat} values for the turnover of these inhibitors (the compounds serve both as inhibitors and substrates) by the mutant enzyme were actually improved, but the values for the S130G

Table 1.2: Kinetics parameters for the TEM-1 wild Type and S130G Mutant

	K_m (mM)		k_{cat} (S^{-1})		k_{cat} / K_m (M^{-1} S^{-1})	
	TEM-1	S130G	TEM-1	S130G	TEM-1	S130G
Ampicillin	0.02	0.13 ± 0.01	1530	170 ± 4	7.7×10^7	$(1.3 \pm 0.1) \times 10^6$
Benzylpenicillin	0.02	0.28 ± 0.02	2000	15 ± 1	1.0×10^8	$(5 \pm 0.4) \times 10^4$
Nitrocefin	0.22	0.09 ± 0.01	920	10 ± 1	4.2×10^6	$(1.0 \pm 0.1) \times 10^5$
Cephaloridine	0.93	0.39 ± 0.05	1500	0.7 ±0.1	1.6×10^6	$(1.7 \pm 0.2) \times 10^3$

mutant enzyme approach those for typical substrates (Table 1.2). The first-order rate constants for enzyme inactivation (k_{inact}) were also somewhat improved in each case for the mutant enzyme. The increases in the values for k_{cat} were relatively larger than those for k_{inact} (sulbactam being the exception). As a consequence, the partition ratios (k_{cat}/k_{inact}) for the clavulanate and tazobactam were elevated somewhat for the mutant variant, but the parameter for sulbactam actually decreased by 5.3-fold. The partition ratio is an indication of the efficiency of the enzyme inactivation chemistry; the lower the number, the better the inactivation chemistry. Therefore, the mutant enzyme is less prone to inactivation by clavulanate and tazobactam.

Furthermore, the apparent K_I values for the non-covalent preacylation complexes measured for the S130G mutant enzyme were consistently and significantly elevated over those measured for the wild-type enzyme (Table 1.3). This observation indicated that saturation of the active site of the mutant enzyme by these agents is substantially less likely to take place for the S130G enzyme. We acknowledge that the mathematical expressions for k_{cat} and k_{inact} for the cases of mechanism-based inhibitors are complicated, made up of multiple microscopic rate constants that define the various steps. Similarly, K_m is a complex factor. For examples of these mathematical expressions, please consult Mobashery et al (*26*). It is conceivable that within the short period of measurements for the competition experiments, a significant catalytic commitment to turnover would take place and indeed what is measured as K_I may actually approximate the K_m for the given inhibitor. An increased apparent K_I value might thus result from an increased deacylation

Table 1.3 Inhibition parameters for the TEM-1 Wild-Type and S130G Mutant

Enzyme	Inhibitor	$k_{cat}(s^{-1})$	$k_{inact}(s^{-1})$	$K_I(\mu M)$	k_{cat}/ k_{inact}	$k_{rec}(s^{-1})$
Wild-Type[4]	Clavulanate	0.21 ± 0.03	$(1.7 \pm 0.03) \times 10^{-3}$	0.4	125 ± 36	$(8.4 \pm 0.1) \times 10^{-3}$
	Sulbactam	1.95 ± 0.15	2.0×10^{-4}	1.6	1×10^{4}	$(1.12 \pm 0.02) \times 10^{-2}$
	Tazobactam	1.4 ± 0.9	$(3 \pm 2) \times 10^{-3}$	$(2 \pm 1) \times 10^{-2}$	475 ± 42	$(7.23 \pm 0.05) \times 10^{-3}$
S130G mutant	Clavulanate	4.6 ± 1.0	$(2.9 \pm 0.6) \times 10^{-3}$	105 ± 20	1600 ± 100	$(1.2 \pm 01) \times 10^{-2}$
	Sulbactam	49 ± 22	$(2.6 \pm 1.0) \times 10^{-2}$	220 ± 15	1900 ± 450	$(9.5 \pm 0.1) \times 10^{-4}$
	Tazobactam	22 ± 13	$(3.5 \pm 1.3) \times 10^{-2}$	95 ± 15	630 ± 90	$(5.2 \pm 0.1) \times 10^{-3}$

vs acylation rate constants, a true increase in the dissociation constant, or both. Regardless of whether it is the K_I or the K_m that is being evaluated, the consequence is the same: the IRT β-lactamase does not experience saturation with the given inhibitor until a higher concentration of the inhibitor is achieved, with the attendant manifestations of poorer inhibition of the enzyme. Therefore, it is plausible that elevated apparent K_I values play an important role in manifestation of the IRT phenotype in organisms that harbor the S130G substitution.

We parenthetically comment here that the substitution at position 130 is not influencing the recovery from the portion of the enzyme that has been inhibited by the transiently inhibited species (***5***, Figure 1.2). The recovery from inhibition (k_{rec}) by this species in each case (Table 1.3) is insignificantly influenced by the mutation.

II. X-ray crystallography.

The crystallographic structure of TEM-76 was determined to 1.40 Å resolution. The quality of the data and refinement are described in Table 1.1. The structure closely resembles that of the wild-type and pseudo-wild-type proteins (the isofunctional stabilized M182T variant, WT*, used here for structural comparisons) (*19*); the root mean

squared deviation of all C_α atoms was 0.26 Å to the latter. Ramachandran analysis of the structure showed that 93% of residues were in most favored regions, with 7% in additionally allowed regions. The final R-factors for the working set (R_{cryst}) and the test set (R_{free}) are 18.3% and 22.4%, respectively. At this resolution, interesting features in the density can be seen. Holes in the density of sidechain phenyl rings are clearly visible when contoured at 2.0σ (Figure 3A). Fourteen residues could be modeled in an alternate conformation based on positive F_o-F_c density (Figure 1.3B).

Whereas the S130G structure resembles that of the WT* overall, in the active site several changes at key positions were apparent in the difference electron density maps. A new water molecule (Wat1023) was modeled into the active site (Figure 1.3C) based on positive F_o-F_c electron density at a contour level of 3σ. Wat1023 was modeled in two configurations (Wat1023A and Wat1023B) due to residual positive F_o-F_c electron density at a contour level of 3σ. The two conformations of this water molecule are 1.5 Å apart. Simulated annealing omit F_o-F_c electron density maps for the alternate conformations of Wat1023 showed strong electron density for this water molecule at a contour level of 4.0σ (Figure 1.3C), with distinct density still present at a contour level of 5.0σ. The B-factors of these waters are as follows: Wat1023A=9.9, Wat1023B=12.4. The two conformations of the new active site water molecule, Wat1023A and Wat1023B, are located 1.1 Å and 1.3 Å respectively from the position that the missing Oγ of the wild-type Ser130 occupies. A second conformation of the active site residue Lys234 was modeled based on unambiguous features in F_o-F_c electron density maps at a contour level of 3σ. This second conformation is rotated relative to the canonical wild-type conformation; this moves the N_ζ atom of this new conformation 1.5 Å away from the position observed in the WT* structure. Correspondingly, the N_ζ atom of Lys73 has moved 0.5 Å relative to the WT* TEM structure; this increases the Lys73 N_ζ – Ser70 Oγ distance from 2.9 Å in WT* to 3.4 Å in TEM-76, breaking this key hydrogen bond

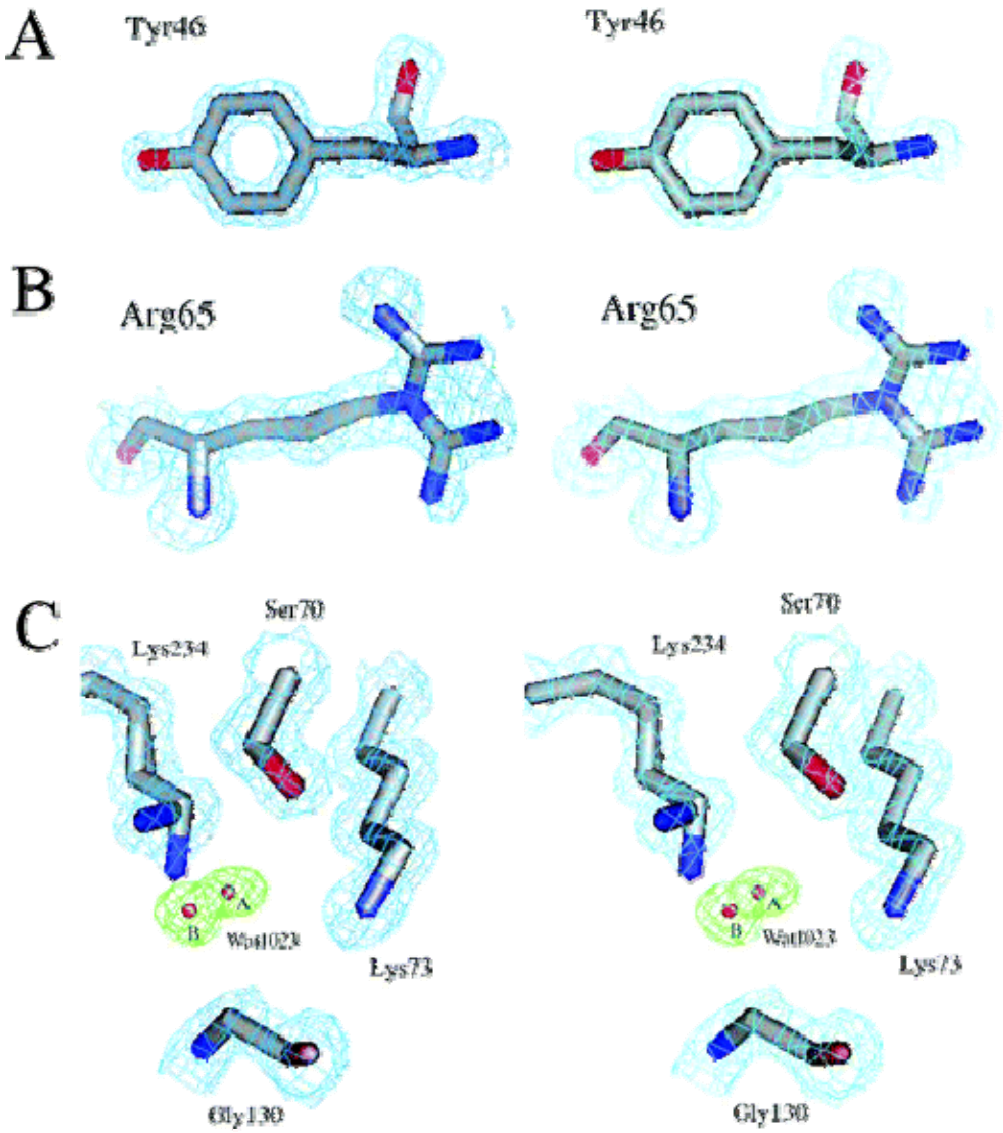

Figure 1.3 Electron density of the characteristic regions of the S130G structure. Carbon, nitrogen, oxygen, and sulfur atoms are colored gray, blue, red, and orange respectively. (A-D) Quality of the S130G β-lactamase mutant crystal structure at 1.40 Ångstrom resolution. (A) Stereoview of Tyr46 structure and $2F_o$-F_c electron density contoured at 2σ (cyan). (B) Stereoview of the alternative conformations modeled for Arg65 superimposed on the $2F_o$-F_c electron density map (cyan) at 1σ. (C) Stereoview of Asn170 superimposed on the $2F_o$-F_c map (cyan) at 2σ. Oxygen and nitrogen atoms can be distinguished on the basis of electron density volumes. (D) Stereoview of Arg259 overlaid on the $2F_o$-F_c electron density contoured at 2σ (cyan) and the $2F_o$-F_c electron density map (green, 2.5σ). Positive density corresponding to hydrogen atoms on the sidechain can be seen. (E) Electron density for the S130G active site. The final $2F_o$-F_c map (cyan) contoured at 1.5σ is overlaid with simulated annealing omit electron density at 4.0σ (green) for the new active site water (Wat1023A/Wat1023B).

(Table 1.4). A similarity with the WT* structure was the presence of the hydrolytic water (Wat1561), which was modeled into F_o-F_c positive electron density visible at a 3σ contour level (Figure 1.4). Based on results with the analogous S130G mutant in SHV, the presence of this water was surprising (see Discussion). In addition, the Ser130Gly substitution results in a local expansion of the binding site; the Ser70-Ser130 C_α-C_α distance has increased from 6.7 Å in WT* to 7.3 Å in S130G, a difference of 0.6 Å.

III. Thermal stability of S130G mutant.

Ser130 is hypothesized to have both a kinetic and structural role in class A β-lactamases (*21, 27, 28*); the Ser130Gly substitution in *Streptomyces albus* G β-lactamase resulted in decreased stability, though this was not a thermodynamic measurement (*28*). TEM-1 has previously been shown to reversibly denature in a two-state fashion (*23*), and the thermal stability of the TEM S130G mutant was determined in a similar manner. TEM-76 has a melting temperature of 52.3°C, a stabilization of 0.8 degrees relative to wild-type enzyme, and a stability gain of 0.34 kcal/mol, using the method of Schellman (*25*). The van't Hoff enthalpy has decreased from 139.5 kcal/mol in wild-type TEM-1 (*19*) to 115.0 kcal/mol for S130G, which slightly complicates the interpretation of this stability result. Nevertheless, it seems clear that this mutant is more stable in the region of its T_m than the WT enzyme.

Table 1.4: Selected distances in TEM-76 (S130G), TEM-32 (M69I/M182T), and WT*.

	Distance (Å)		
	TEM-76	TEM-32	WT*[a]
Catalytic water[b] - Ser70 O_γ	2.6	2.8	2.8
Catalytic water - Glu166 $O_\varepsilon 2$	2.3	2.5	2.7
Catalytic water - Asn170 N_δ	3.2	2.7	2.6
Oxyanion hole water[c] - Ser70 O_γ	2.8	3.0	2.7
Oxyanion hole water - Ser70 N	3.0	2.9	2.8
Oxyanion hole water - Ala237 N	2.9	3.2	3.1
Oxyanion hole water - Ala237 O	2.7	2.6	2.8
C3 water[d] - Arg244 NH2	2.7	2.9	2.8
C3 water - Ser235 O_γ	3.7	3.1	2.8
Ser70 O_γ - Lys73 N_ζ	3.4	3.1	2.8
Ser70 O_γ - Ser130 O_γ	NP[e]	5.5	3.2
Ser130 O_γ - Lys73 N_ζ	NP	5.4	3.8
Ser130 O_γ - Lys234 N_ζ	NP	3.3	2.8
Active site water[f] - Ser70 O_γ	2.9	2.7 (1^{st})[g] 3.2 (2^{nd})	NP
Active site water - Lys73 N_ζ	2.8	2.9	NP
Active site water - Lys234 N_ζ	3.0	2.9	NP
Active site water - Lys234 N_ζ(B)	2.9	NP	NP
Active site water(B) - Ser70 O_γ	3.1	NP	NP
Active site water(B) - Lys73 N_ζ	3.8	NP	NP
Active site water(B) - Lys234 N_ζ	3.7	NP	NP
Active site water(B) - Lys234 N_ζ(B)	4.0	NP	NP
Lys73 N_ζ - Asn132 $O_\delta 1$	3.0	3.0	3.0

[a]PDB 1JWP
[b]The catalytic water is numbered Wat1561 in TEM-76, Wat6 in TEM-32, and Wat57 in WT*.
[c]The oxyanion hole water is numbered Wat1012 in TEM-76, Wat5 in TEM-32, and Wat196 in WT*.
[d]This water, expected to interact with C3 carboxylate of β-lactams, is numbered Wat1614 in TEM-76, Wat7 in TEM-32, and Wat99A in WT*.
[e]Not present.
[f]The active site water is numbered Wat1023A/Wat1023B in TEM-76 and Wat85 in TEM-32.
[g]Measured from the alternate conformations of Ser70 seen in TEM-32.

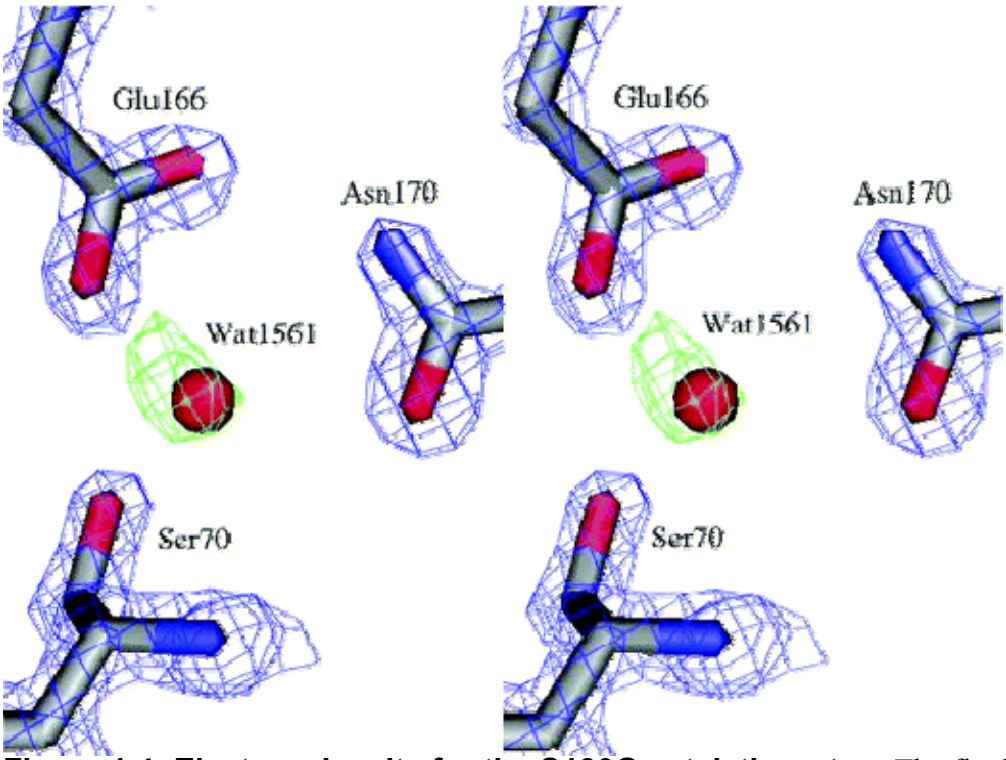

Figure 1.4: Electron density for the S130G catalytic water. The final $2F_o$-F_c map (blue) at 2σ for the enzyme sidechains is overlaid with the F_o-F_c electron density map (green, 3σ) prior to modeling the catalytic water.

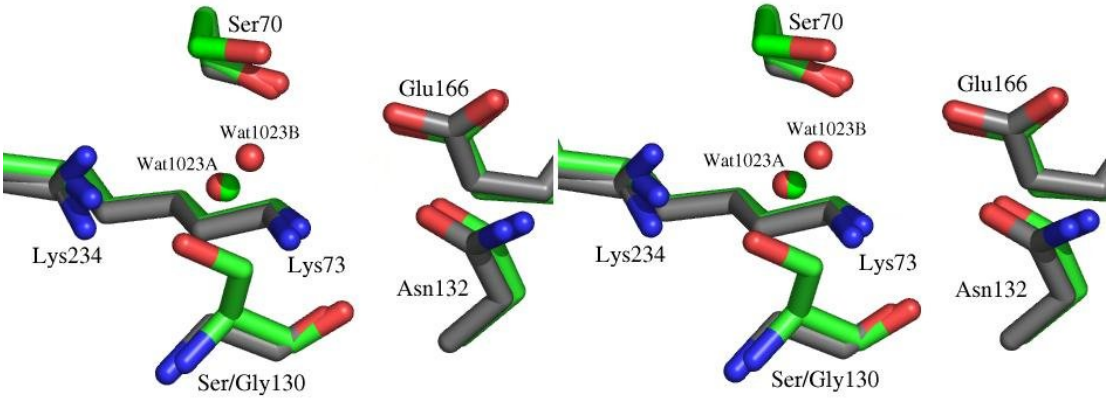

Figure 1.5: Active site overlay of S130G mutant (carbons in gray) with TEM-32 (M69I/M182T) (carbons in green). Nitrogen, oxygen, and sulfur atoms are colored blue, red, and orange respectively. Active site waters are shown as spheres in red (S130G) or green (TEM-32).

1.5. Discussion

Over 25 inhibitor-resistant TEM β-lactamase mutants have been clinically isolated to date, many involving substitutions distant from the catalytic center. The Ser130Gly substitution might conceptually be the simplest to understand; eliminating the Ser130 O_γ prevents irreversible covalent attachment of the inhibitor to this residue, thus disrupting the inactivation pathway. In nature, however, substitution of the strictly conserved Ser130 occurs in only three out of 25 IRTs, and then only to a glycine residue (www.lahey.org/Studies/temtable), consistent with a mechanistic role for this residue. What we would like to address here is how the S130G mutant remains functional at all, and how the structural perturbations caused by truncating the crosslinking residue resemble those seen in more subtle, and arguably more successful, inhibitor-resistant variants.

Like other IRT variants, the inhibitor resistance gained by S130G comes with decreased hydrolytic ability against β-lactam substrates (*29-32*). If Ser130 acts as the catalytic acid in substrate hydrolysis, how does S130G remain active? The two conformations of Wat1023 (Wat1023A/Wat1023B), the new active site water, are located 1.1 Å and 1.3 Å from the missing Ser130 Oγ, respectively (Figure 3C) and likely replace Ser130 as the proton source. Replacement of this Ser130 Oγ by a water molecule previously had been predicted on the basis of molecular modeling results (*33*). Though S130G is less efficient than TEM-1 at hydrolyzing β-lactam substrates – the rate of catalysis has decreased ten-fold for ampicillin, and almost 150-fold for benzylpenicillin – what remains of the catalytic competence is sufficient to confer antibiotic resistance on the host bacteria *in vivo*. This could explain why only Ser130 substitutions to glycine naturally occur, since a substitution to any other residue would be too large to easily accommodate a new water molecule in this position in the active site; in fact, the S130A

mutant is much less active than the S130G enzyme, as evidenced by their relative k_{cat}/K_m values (*28*).

One basis for the resistance conferred by Ser130Gly seems obvious; the deletion of the crosslinking residue. Unexpectedly, this "most obvious" of IRT mutants shares mechanistic and structural similarities with several of the more subtle IRTs previously characterized. Like TEM-33 (M69L), the apparent equilibrium K_I values have increased dramatically for S130G (Table 1.3), reflecting diminished active site saturation by the inhibitors. Structurally, the mutant resembles some of the accommodations observed in TEM-32 (Figure 1.5, Table 1.4). In TEM-32 (M69I/M182T), the χ_1 angle of Ser130 has changed by 64 degrees, placing the O_γ of Ser130 2.2 Å away from the canonical Ser130 O_γ conformation. This rotation of Ser130 away from the active site allows incorporation of a new water molecule. Interestingly, this new TEM-32 water molecule is only 0.20 Ångstroms from one conformation of the new TEM-76 water molecule (Wat1023A); both of these mutants have acquired the same water molecule to offset displacement – or replacement – of Ser130. In addition, Lys234 has moved relative to the wild-type protein in both TEM-32 and TEM-76. In class A β-lactamases, the Lys234 sidechain normally hydrogen bonds to the hydroxyl group of Ser130. The Ser130Gly substitution causes Lys234 to adopt a novel second conformation not present in the pseudo-wild-type structure at 0.85 Å resolution (*34*). In the primary Lys234 conformation, the side chain hydrogen bonds to the new active site water molecule replacing the Ser130 hydroxyl group. Due to the partial occupancy of this new water molecule, the Lys234 sidechain adopts a second conformation where it hydrogen bonds to the backbone carbonyl of Ile127; this Lys234-Ile127 hydrogen bond is present in TEM-32 as well.

Another such structural perturbation causing inhibitor resistance is increased disorder of the conserved water molecule (Wat1614) hydrogen-bonded to the guanidinium group of Arg244 and the carbonyl group of Val216; this water molecule is

the source of the proton necessary for ring-opening in clavulanate inactivation (Figure 1.2, Table 1.4) (*2, 3*). In TEM-76, the B-factor of this water molecule has increased relative to the stabilized wild-type apo structure (33.2 in S130G, compared to 17.1 in WT* at 1.75Å resolution). At least two other IRT mutants appear to have gained inhibitor resistance by similar means; in both the TEM-84 (N276D) and TEM-30 (R244S) x-ray structures, this water molecule could not be crystallographically refined (*9, 10*). Disrupting the inactivation pathway for mechanism-based inhibitors likely increases partitioning of the inhibitors through the hydrolytic pathway, reducing overall inhibition.

The structure of the S130G mutant was recently determined to 1.8 Å in SHV β-lactamase (*35*), which has 68% sequence identity to TEM-1 and is closely related structurally; their structures have a C_α RMSD of 1.4 Å, and the catalytically important residues have an RMSD of only 0.23 Å (*36, 37*). Despite these similarities, the Ser130Gly substitution in TEM leads to related, but nevertheless different, conformational changes compared to SHV S130G. Similar to TEM-76, a new water molecule is found less than 1 Å away from the missing Ser130 hydroxyl group in SHV S130G. The Ser130Gly substitution in both TEM and SHV results in a binding site expansion, as evidenced by the 0.6 Å increase in both the Ser70-Ser130 and Lys73-Ser130 C_α-C_α distances. Substitution of Ser130 with glycine in SHV leads to a rotation of the Ser70 hydroxyl group so that it breaks highly conserved hydrogen bonds to Lys73 and the catalytic water molecule and hydrogen bonds to the water molecule within the oxyanion hole instead. No such reorientation of Ser70 is seen in TEM-76; however, rotation of Lys73 achieves some of the same effect, breaking the hydrogen bond with Ser70. Though the TEM-1 and SHV-1 binding sites align closely, Ser70 has a different orientation in each. Interestingly, rotation of Ser70 in SHV S130G causes it to adopt the same conformation seen in wild-type TEM, though different from native SHV-1; perhaps

this explains why this catalytic serine does not further reorient in the TEM S130G mutant.

One of the most striking observations in the SHV S130G mutant is the departure of the Glu166-activated water molecule, which is thought to be critical for catalysis. In the TEM S130G structure reported here, this key catalytic water is clearly present (Figure 4), though perhaps less ordered than in the WT* structure. Overall this key water is still pre-organized for hydrolysis and still contacts its primary activating residues, including the deacylation catalytic base Glu166.

In closing, we return to our initial questions: how does S130G tolerate the loss of a key catalytic functionality, and what are the structural bases for loss of activity versus both substrates and inhibitors? The structural replacement of the O_γ of Ser130 by Wat1023 explains how the enzyme remains active at all and offers another example of the extraordinary chemical plasticity of enzymes. The enzyme appears to lose activity based on the relative inefficiency of a bound water versus a serine O_γ, and movement of Lys73. The decreased activity of S130G does not appear to result from diminished overall stability of the folded enzyme, which, if anything, is actually somewhat stabilized relative to WT. What is intriguing is that the accommodations observed in S130G are qualitatively similar to those observed in IRT mutants whose substitutions often occur at sites less directly correlated with the sites of crosslinking. Like TEM-33 (M69L), S130G suffers from elevated apparent K_I values. TEM-30 (R244S) also results in a displacement of Wat 1614, as does TEM-84 (N276D). Similarly, TEM-32 (M69I/M182T) results in a displacement of Ser130, the appearance of a water molecule equivalent to Wat1023A, and a conformational change in Lys234. However, TEM-32 has acquired resistance to inhibitors with only a modest (5-fold) reduction in k_{cat} for substrates compared to S130G. In S130G, nature would appear to have made the most intuitive mutation, but also among the least successful based on catalytic activity and prevalence. The bases of action of the

many other action-at-a-distance IRTs, such as TEM-38 (M69V/R275L) and TEM-39 (M69L/W165R/N276D) which, like TEM-30 and TEM-32, result in relatively resistant, relatively active IRTs, appears ever more interesting in light of the conserved accommodations of this simplest of IRT mutants, S130G.

1.6. Acknowledgements

We thank Yu Chen, Ruth Brenk, Federica Morandi and Alan Graves for reading the manuscript, and Yu Chen for crystallographic advice and assistance.

1.7 References

1. Kuzin, A. P., Nukaga, M., Nukaga, Y., Hujer, A., Bonomo, R. A., and Knox, J. R. (2001) Inhibition of the SHV-1 beta-lactamase by sulfones: crystallographic observation of two reaction intermediates with tazobactam, *Biochemistry 40*, 1861-1866.

2. Yang, Y., Janota, K., Tabei, K., Huang, N., Siegel, M. M., Lin, Y. I., Rasmussen, B. A., and Shlaes, D. M. (2000) Mechanism of inhibition of the class A beta -lactamases PC1 and TEM-1 by tazobactam. Observation of reaction products by electrospray ionization mass spectrometry, *J. Biol. Chem. 275*, 26674-26682.

3. Imtiaz, U., Billings, E. M., Knox, J. R., Manavathu, E. K., Lerner, S. A., and Mobashery, S. (1993) Inactivation of class A beta-lactamases by clavulanic acid: the role of arginine-244 in a proposed nonconcerted sequence of events, *J. Am. Chem. Soc. 115*, 4435-4442.

4. Brown, R. P., Aplin, R. T., and Schofield, C. J. (1996) Inhibition of TEM-2 beta-lactamase from Escherichia coli by clavulanic acid: observation of intermediates by electrospray ionization mass spectrometry, *Biochemistry 35*, 12421-32.

5. Bush, K., and Mobashery, S. (1998) How beta-lactamases have driven pharmaceutical drug discovery. From mechanistic knowledge to clinical circumvention, *Adv Exp Med Biol 456*, 71-98.

6. Knowles, J. R. (1985) Penicillin Resistance - the Chemistry of Beta-Lactamase Inhibition, *Accounts of Chemical Research 18*, 97-104.

7. Fisher, J., Charnas, R. L., and Knowles, J. R. (1978) Kinetic studies on the inactivation of Escherichia coli RTEM beta- lactamase by clavulanic acid, *Biochemistry 17*, 2180-2184.

8. Charnas, R. L., and Knowles, J. R. (1981) Inactivation of RTEM beta-lactamase from Escherichia coli by clavulanic acid and 9-deoxyclavulanic acid, *Biochemistry 20*, 3214-3219.

9. Swaren, P., Golemi, D., Cabantous, S., Bulychev, A., Maveyraud, L.,

Mobashery, S., and Samama, J. P. (1999) X-ray structure of the Asn276Asp variant of the Escherichia coli TEM-1 beta-lactamase: direct observation of electrostatic modulation in resistance to inactivation by clavulanic acid, *Biochemistry 38*, 9570-6.

10. Wang, X., Minasov, G., and Shoichet, B. K. (2002) The structural bases of antibiotic resistance in the clinically derived mutant beta-lactamases TEM-30, TEM-32, and TEM-34, *J Biol Chem 277*, 32149-56.

11. Meroueh, S. O., Roblin, P., Golemi, D., Maveyraud, L., Vakulenko, S. B., Zhang, Y., Samama, J. P., and Mobashery, S. (2002) Molecular dynamics at the root of expansion of function in the M69L inhibitor-resistant TEM beta-lactamase from Escherichia coli, *J Am Chem Soc 124*, 9422-30.

12. Lamotte-Brasseur, J., Dive, G., Dideberg, O., Charlier, P., Frere, J. M., and Ghuysen, J. M. (1991) Mechanism of acyl transfer by the class A serine beta-lactamase of Streptomyces albus G, *Biochem J 279*, 213-21.

13. Atanasov, B. P., Mustafi, D., and Makinen, M. W. (2000) Protonation of the beta-lactam nitrogen is the trigger event in the catalytic action of class A beta-lactamases, *Proc Natl Acad Sci U S A 97*, 3160-5.

14. Vakulenko, S., and Golemi, D. (2002) Mutant TEM beta-lactamase producing resistance to ceftazidime, ampicillins, and beta-lactamase inhibitors, *Antimicrob Agents Chemother 46*, 646-53.

15. Dixon, M. (1953) The determination of enzyme inhibitor constants, *Biochem J 55*, 170-1.

16. Silverman, R. (1988) in *Mechanism-based Enzyme Inactivation: Chemistry and Enzymology* pp 22, CRC Press, Boca Raton.

17. Koerber, S. C., and Fink, A. L. (1987) The analysis of enzyme progress curves by numerical differentiation, including competitive product inhibition and enzyme reactivation, *Anal Biochem 165*, 75-87.

18. Glick, B. R., Brubacher, L. J., and Leggett, D. J. (1978) A graphical method for extracting rate constants from some enzyme-catalyzed reactions not monitored to completion, *Can J Biochem 56*, 1055-7.
19. Wang, X., Minasov, G., and Shoichet, B. K. (2002) Evolution of an Antibiotic Resistance Enzyme Constrained by Stability and Activity Trade-Offs, *J. Mol. Biol. 320*, 85-95.
20. Otwinowski, Z., and Minor, W. (1997) Processing of X-ray diffraction data collected in oscillation mode., *Methods Enzymol. 276*, 307-326.
21. Strynadka, N. C., Adachi, H., Jensen, S. E., Johns, K., Sielecki, A., Betzel, C., Sutoh, K., and James, M. N. (1992) Molecular structure of the acyl-enzyme intermediate in beta-lactam hydrolysis at 1.7 A resolution, *Nature 359*, 700-5.
22. Brünger, A. T., Adams, P. D., Clore, G. M., DeLano, W. L., Gros, P., Grosse-Kunstleve, R. W., Jiang, J. S., Kuszewski, J., Nilges, M., Pannu, N. S., Read, R. J., Rice, L. M., Simonson, T., and Warren, G. L. (1998) Crystallography & NMR system: A newsoftware suite for macromolecular structure determination, *Acta Crystallogr. D 54*, 905-921.
23. Wang, X., Minasov, G., and Shoichet, B. K. (2002) Noncovalent Interaction Energies in Covalent Complexes: TEM-1 Beta-Lactamase and Beta-Lactams, *Proteins 47*, 86-96.
24. Kirchhoff, W. H. (1993), NIST.
25. Becktel, W. J., and Schellman, J. A. (1987) Protein stability curves., *Biopolymers 26*, 1859-77.
26. Mobashery, S., Ghosh, S. S., Tamura, S. Y., and Kaiser, E. T. (1990) Design of an effective mechanism-based inactivator for a zinc protease, *Proc Natl Acad Sci U S A 87*, 578-82.
27. Juteau, J. M., Billings, E., Knox, J. R., and Levesque, R. C. (1992) Site-saturation mutagenesis and three-dimensional modelling of ROB-1 define a substrate binding role of Ser130 in class A beta-lactamases, *Protein Eng 5*, 693-701.
28. Jacob, F., Joris, B., Lepage, S., Dusart, J., and Frere, J. M. (1990) Role

of the conserved amino acids of the 'SDN' loop (Ser130, Asp131 and Asn132) in a class A beta-lactamase studied by site-directed mutagenesis, *Biochem J 271*, 399-406.

29. Aumeran, C., Chanal, C., Labia, R., Sirot, D., Sirot, J., and Bonnet, R. (2003) Effects of Ser130Gly and Asp240Lys substitutions in extended-spectrum beta-lactamase CTX-M-9, *Antimicrob Agents Chemother 47*, 2958-61.

30. Delaire, M., Labia, R., Samama, J. P., and Masson, J. M. (1992) Site-directed mutagenesis at the active site of Escherichia coli TEM-1 beta-lactamase. Suicide inhibitor-resistant mutants reveal the role of arginine 244 and methionine 69 in catalysis, *J Biol Chem 267*, 20600-6.

31. Chaibi, E. B., Sirot, D., Paul, G., and Labia, R. (1999) Inhibitor-resistant TEM beta-lactamases: phenotypic, genetic and biochemical characteristics, *J. Antimicrob. Chemother. 43*, 447-458.

32. Helfand, M. S., Bethel, C. R., Hujer, A. M., Hujer, K. M., Anderson, V. E., and Bonomo, R. A. (2003) Understanding resistance to beta-lactams and beta-lactamase inhibitors in the SHV beta-lactamase: lessons from the mutagenesis of SER-130, *J Biol Chem 278*, 52724-9.

33. Lamotte-Brasseur, J., Jacob-Dubuisson, F., Dive, G., Frere, J. M., and Ghuysen, J. M. (1992) Streptomyces albus G serine beta-lactamase. Probing of the catalytic mechanism via molecular modelling of mutant enzymes., *Biochem J 282*, 189-195.

34. Minasov, G., Wang, X., and Shoichet, B. K. (2002) An ultrahigh resolution structure of TEM-1 beta-lactamase suggests a role for Glu166 as the general base in acylation, *J Am Chem Soc 124*, 5333-40.

35. Sun, T., Bethel, C. R., Bonomo, R. A., and Knox, J. R. (2004) Inhibitor-resistant class A beta-lactamases: consequences of the Ser130-to-Gly mutation seen in Apo and tazobactam structures of the SHV-1 variant, *Biochemistry 43*, 14111-7.

36. Kuzin, A. P., Nukaga, M., Nukaga, Y., Hujer, A. M., Bonomo, R. A., and

Knox, J. R. (1999) Structure of the SHV-1 beta-lactamase, *Biochemistry 38*, 5720-7.

37. Jelsch, C., Mourey, L., Masson, J. M., and Samama, J. P. (1993) Crystal structure of Escherichia coli TEM1 beta-lactamase at 1.8 A resolution., *Proteins 16*, 364-383.

Gloss to Chapter 2

After the TEM inhibitor-resistant S130G paper was accepted, I switched gears and systems to return to the original question at hand: do protein stability and native catalytic activity constrain evolution of new enzyme functions, specifically in regards to antibiotic resistance? What are the structural bases by which mutations far from the active site affect catalytic properties? To address these questions, we turned to AmpC β-lactamase, a long-standing model system of the lab. AmpC is an emerging problem in the clinic, as it has now been mobilized onto plasmids. It shares no measurable sequence identity with the class A β-lactamases, such as TEM-1, though both use a catalytic serine and two mechanistically important lysines in their active site. Several extended-spectrum mutations are already known in class C β-lactamases, both from the clinic and *in vitro* evolution and selection from other laboratories. By making the analogous mutations in AmpC, and determining the gain of new activity against third-generation cephalosporin antibiotics that were not previously substrates for the wild-type enzyme, and measuring the native activity and protein stability, we hoped to investigate the generality of what was determined for TEM-1: as this enzyme gained new activity, it sacrificed some of its ancestral activity against penicillin and its inherent stability.

They say that by the end of graduate school, one can reproduce the first two years in about two months – and this project is likely no exception. After much heartache wrestling with making the affinity columns used in the purification, optimizing PCR conditions for mutagenesis, unsuccessful ligations and transformations, and expression of destabilized mutants – we had these mutant proteins in our hand ready for investigation. Further characterization revealed that two mutations found in other class C beta-lactamases did not confer extended spectrum activity when their analogous mutation was made in AmpC – and thus were excluded from further analysis and inclusion in this study (See Appendix 2.A).

The characterization of the remaining five extended-spectrum AmpC β-lactamase mutant enzymes showed that they were in line with our hypothesis – as these mutant enzymes have gained activity against extended-spectrum antibiotics, by about 100- to 200-fold, they have correspondingly sacrificed some of their native activity, by about 3- to 15- fold, and their stability, by up to 4.1 kcal/mol.

If successful generation of these mutant proteins proved to be the bottleneck in this project, coaxing these proteins to crystallize was certainly not easy either. Though crystallization conditions have been well-worked out for the wild-type enzyme, several of these mutant proteins proved recalcitrant to crystallization under these conditions, and we turned to many crystallization screens. Thousands of drops set, several crystals frozen and brought to the synchrotron, only to be painfully revealed as salt crystals, and a lot of dashed hopes later, I obtained crystal structures of all the mutant proteins under investigation.

I don't think there's anything in the world quite like seeing the first electron density maps of a protein you've spent months, or even years, trying to crystallize. It's like peering straight inside the enzyme, coaxing it to reveal its secrets as to how it functions – and realizing that at that moment, you are the only person in the world who knows what this protein looks like. I've compared it to staying up all night to finish a book when you're dying to know the ending – many late nights were spent at my desk, battling eye strain, to finally understand the story behind how these distant mutations confer extended-spectrum activity to these enzymes. In several cases, the resulting structures shed insight as to why they were so hard to crystallize – V298E causes a domino effect of structural changes, resulting in an active site loop flipping out. T70I, after a year and a half of crystallization attempts, finally formed a single crystal when set with a transition-state analog inhibitor – and of two monomers, miraculously one was apo, and one was holo, and the two structures were completely different. In the apo structure, about 25 residues in the "omega loop" region, forming one wall of the active

site, have become disordered and cannot be resolved, and the beta-turn forming the oxyanion hole has flipped into the active site. This increased flexibility and disorder in the apo structure potentially explains why this mutant was so difficult to crystallize in the absence of ligand bound. However, in the holo structure bound to a transition-state analog inhibitor, this loop adopts a distinct conformation, and the oxyanion hole reforms – one example of increased increased flexibility in these extended-spectrum mutant AmpC enzyme structures. The crystal structures determined here reveal that the extended-spectrum substitutions, though located throughout the protein structure, primarily have the same ultimate effect – they enlarge the active site to allow the accommodation of the larger, third-generation cephalosporin antibiotics that were not substrates for the wild-type enzyme.

The resulting work paints a portrait of how stability constrains evolution of new enzyme functions, and how distant mutatations can transmit their effects back to an active site up to 20 Angstroms away. This chapter was accepted to the *Journal of Molecular Biology* in 2009.

Chapter 2:
Structural Bases for Stability-Function Tradeoffs in Antibiotic Resistance

Veena L. Thomas[a, b], Andrea C. McReynolds[b, †], Brian K. Shoichet[b,*]

[a]Graduate Program in Pharmaceutical Sciences and Pharmacogenomics, University of California, San Francisco; San Francisco, California, 94158-2518

[b]Department of Pharmaceutical Chemistry, University of California San Francisco, Byers Hall, Room 508D, 1700 4th Street, San Francisco, CA 94158-2550

[†]Current address: UT Southwestern Medical Center at Dallas, 6001 Forest Park Rd.Room ND7.202, Dallas, TX 75390-9041

[*]Corresponding author: shoichet@cgl.ucsf.edu, phone: 415-514-4126, fax: 415-514-4260

Keywords: protein stability; AmpC beta-lactamase; antibiotic resistance; evolution; action-at-a-distance

2.1 Abstract

Pre-organization of enzyme active sites for substrate recognition typically comes at a cost to the stability of the folded form of the protein, and consequently enzymes can be dramatically stabilized by substitutions that attenuate the size and pre-organization "strain" of the active site. How this stability-activity trade-off constrains enzyme evolution has remained less certain, and it is unclear whether one should expect major stability insults as enzymes mutate towards new activities, or how these new activities manifest structurally. These questions are both germane and easy to study in β-lactamases, which are evolving on the timescale of years to confer resistance to an ever-broader spectrum of β-lactam antibiotics. To explore whether stability is a substantial constraint on this antibiotic resistance evolution, we investigated extended-spectrum mutants of class C β-lactamases which had evolved new activity versus third-generation cephalosporins. Five mutant enzymes had between 100- to 200-fold increased activity against the antibiotic cefotaxime in enzyme assays, and the mutant enzymes all lost thermodynamic stability – from 1.7 to 4.1 kcal/mol – consistent with the function-stability hypothesis. Intriguingly, several of the substitutions were 10 – 20 Å from the catalytic serine; the question arose how they conferred extended-spectrum activity. Eight structures, including complexes with inhibitors and extended-spectrum antibiotics, were determined by x-ray crystallography. Distinct mechanisms of action are revealed for each mutant, including changes in the flexibility and ground state structures of the enzyme. These results explain the structural bases for the antibiotic resistance conferred by these substitutions, and their corresponding decrease in protein stability, which will constrain the evolution of new antibiotic resistance.

2.2 Introduction

To engineer a protein for stability, among the surest places to make substitutions is the active site. This will appear paradoxical to many, because these active-site substitutions typically reduce the activity of the mutant protein, and an inactive-but-stable mutant enzyme is rarely sought. Still, this trading of activity for stability illustrates a point: active sites are typically those regions in proteins that manifest the most internal strain. In active sites, polar groups are sequestered from water [1; 2], like-charged residues cluster together, residues adopt strained conformations [3], and hydrophobic patches are exposed [4]. As Warshel [1; 2] and others [5; 6] have suggested, this strain pre-organizes the active site for ligand recognition and catalysis, and is paid for at the time of folding by the net overall stability conferred by the rest of the protein. The conversion of active-site "strain" into increased stability was first tested in barnase [7], barstar [8], T4 lysozyme [9], and AmpC ß-lactamase [10], where point substitutions increased enzyme stability by up to 4 kcal/mol, or 30% of net overall stability. Subsequent studies are consistent with the idea that residues important for function may be suboptimal for stability [11; 12; 13; 14; 15; 16], and that enzymes may be substantially stabilized by active site substitutions that attenuate the activity [17; 18; 19].

If there is by now much support for the idea that enzymes can be stabilized by active site substitutions, the "stability-function hypothesis" [9], the logical corollary, that they will often lose stability as they gain activity, has been more controversial. In a study of the antibiotic resistance enzyme TEM-1 ß-lactamase, we found that clinically selected gain-of-activity mutants lost stability to the point where a secondary site substitution occurred, far from the active site, that restored stability and allowed further destabilizing gain-of-resistance mutants to evolve [20; 21; 22] Subsequently, Weinreich and colleagues showed that the pathways to stable and active TEM mutants was epistatic and cooperative, consistent with a stability constraint on enzyme evolution [23]. On the other

hand, Arnold has argued that the apparent stability-activity trade-offs may be unrelated, simply reflecting differing constraints: enzymes evolved for activity will give up stability because it is not being as strongly selected, whereas an enzyme being evolved for stability may give up activity for the same reason. Although there is agreement that enzymes that are stabilized [24; 25], or buffered against unfolding by chaperones [26], are more evolvable, consensus has not emerged around a correlation between stability and activity in enzyme evolution.

These two views may be reconcilable. At its heart, the stability-activity trade-off hypothesis is about competing physical interactions in the active site. For those enzymes that evolve new activity by increasing active site pre-organization, for instance by increasing active site size to accommodate larger substrates, trade-offs in stability seem physically necessary. However, not all gain-of-function mutants fit this pattern. For instance, a thermophilic enzyme selected for activity may give up its stability simply because this is not being selected for [27]. Similarly, one can imagine a protein that evolves to recognize a simpler substrate, one that requires less pre-organization than its ancestral substrate; in this case, the mutant enzyme might well gain *both* activity and stability relative to the ancestral protein. But for situations where a new active site is being created, or an established one enlarged or further pre-organized, then by physical necessity we expect stability, unless otherwise compensated, to be sacrificed.

The experimental support for stability-activity trade-offs in enzyme evolution rests largely on a study in TEM-1 β-lactamase [20], and it seemed worthwhile to explore generality in another enzyme. We turned to the class C β-lactamase AmpC which, though also a β-lactamase, diverged from the class A enzymes hundreds of million years ago, with the two families sharing no measurable sequence identity and differing from each other in size, domain organization, and in mechanistic details [28; 29; 30]. AmpC-family

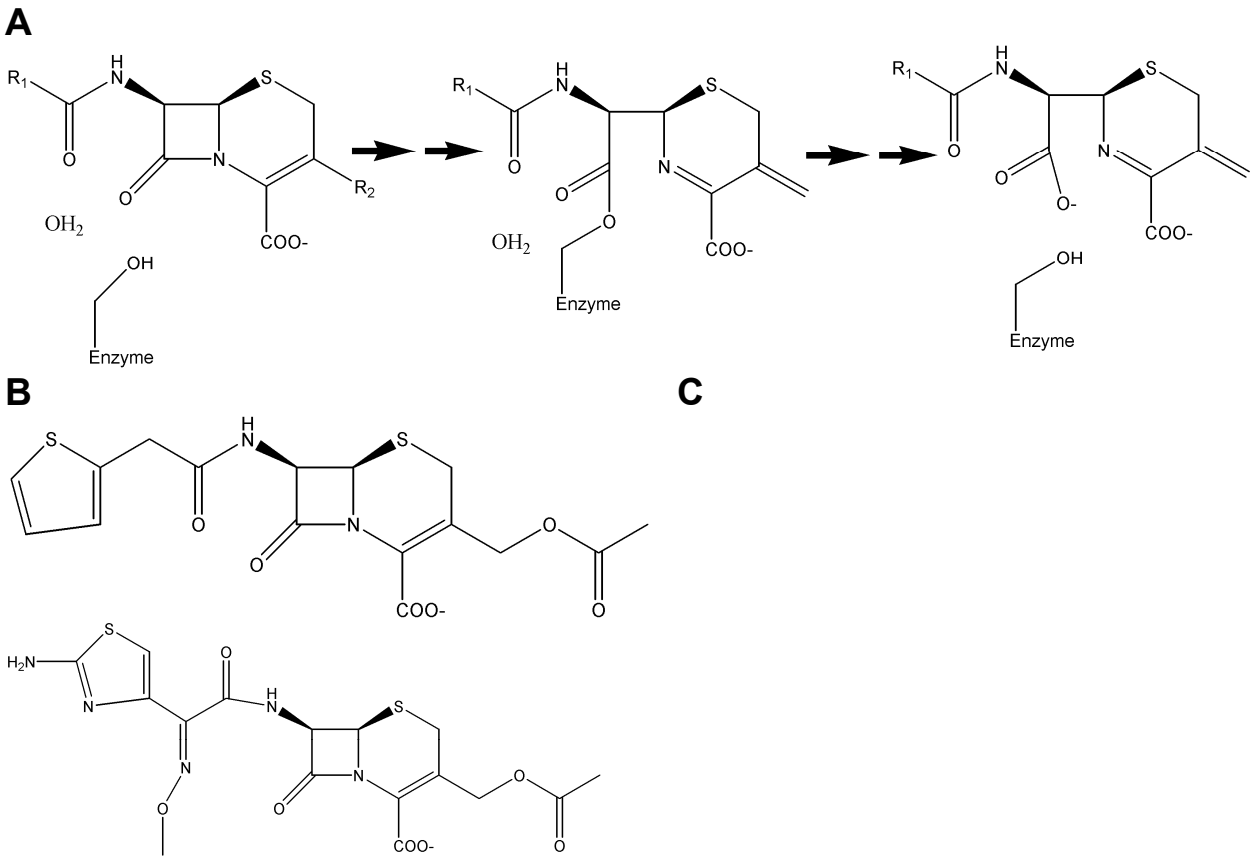

Figure 2.1 Beta-lactamase reaction mechanism and representative antibiotic substrates. (a) Reaction mechanism of AmpC ß-lactamase. (b) The first-generation cephalosporin antibiotic cephalothin. (c) The third-generation cephalosporin antibiotic cefotaxime.

---

enzymes confer resistance to β-lactam antibiotics (Figure 2.1A and B), and are key resistance determinants in hospital acquired pathogens, especially to the cephalosporin β-lactams. "β-lactamase stable" 3rd generation cephalosporins, such as ceftazidime and cefotaxime (Figure 2.1C), were introduced in the early 1980s to overcome resistance conferred largely by class A β-lactamases, but they are also poor substrates for AmpC, whose active site is essentially too small to accommodate them. Thus, when these large 3rd generation cephalosporins form covalent adducts with AmpC they are forced into a conformation that is incompetent for catalysis, due to steric clashes between their bulky R1 side chain and residues Val211 and Tyr221 [31]. "Extended-spectrum" β-lactamase

(ESBL) mutants with increased hydrolytic activity against third-generation cephalosporins have subsequently appeared, both in the clinic [32; 33; 34; 35] and as the product of *in vitro* evolution and mutagenesis [36; 37; 38; 39]. Because these mutant enzymes were evolving to recognize substrates that were too large for the native active site, but in which catalysis would retain the same location and same chemistry, they seemed like good templates to explore for stability-activity trade-offs.

Here we investigate five extended-spectrum mutants of AmpC (Figure 2.2), asking the following questions. Are these mutants in fact better enzymes for the 3rd generation cephalosporins and are not simply, for instance, over-expressed in resistant cells? Does any gain of activity come with a concomitant loss of stability? Since stability-activity trade-offs are formulated as biophysical compensations, is the stability change thermodynamic, as reflected by reversible two-state thermal denaturation? The stability-function hypothesis applies to improved substrate complementarity arising from the introduction of structural defects or increasing residue pre-organization; to investigate this we determine x-ray crystal structures of the five mutant enzymes. These structures also reveal how substitutions that are distant from the active site, as occur with resistance mutations in many enzymes [40; 41; 42], can transduce their perturbations to the active site, and thereby increase catalytic activity.

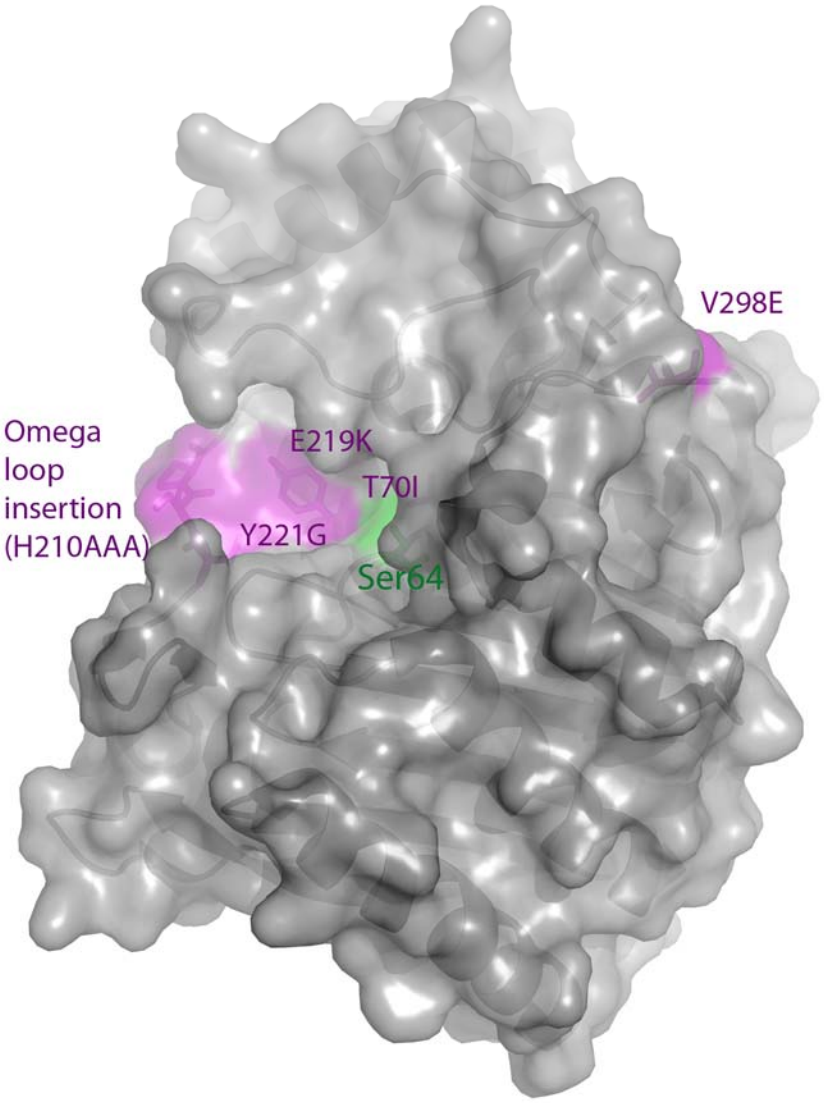

Figure 2.2 ESBL substitutions under investigation in AmpC β-lactamase, shown in purple. The catalytic serine is shown in green.

2.3 Results

I. Function-stability tradeoffs

Five ESBL mutants – V298E [39], the "omega loop insertion" (H210AAA) [32; 33; 34], T70I [36], Y221G [37], and E219K [35; 38], were made by site-directed mutagenesis and purified to apparent homogeneity, and the kinetic constants k_{cat} and K_m against the first-generation cephalosporin cephalothin, and the third-generation cefotaxime, were determined. All of the ESBLs had increased activity against cefotaxime relative to wild-type AmpC, as measured by k_{cat}, typically by 100- to 200-fold (Table 2.1, Figure 2.3A). Normally, one would use k_{cat}/K_m to compare the relative activities of the WT and mutant enzymes, but for class C β-lactamases this value is misleading. Since the acylation rate constant (k_2) for β-lactams is fast on the scale of the pre-covalent disassociation constant (k_{-1}), the K_m values for these enzymes does not reflect a disassociation constant, but rather the deacylation rate constant ($k_3 = k_{cat}$) divided by the acylation rate constant (k_2). Thus k_{cat}/K_m collapses to simply k_2, making what would ordinarily be considered the "specificity constant" misleading [43]. Because k_{cat} is slow for the WT enzyme, (k_{cat} = 0.0448 s^{-1} for cefotaxime in wild-type AmpC, [44]), K_m values are typically too low to be measured, and IC_{50} is typically used as proxy for K_m [44; 45]. For these enzymes, k_{cat} comparisons are more informative. This can be illustrated by example. For WT AmpC, the k_{cat} for cefotaxime is 0.0448 s^{-1}, and the IC_{50}-derived K_m is 0.8 μM, resulting in a k_{cat}/K_m of 5.6 x 10^4 M^{-1} s^{-1}. For V298E, k_{cat} is 4.4 sec^{-1} (Table 2.1), and the K_m is 79 μM – resulting in the same k_{cat}/K_m value as the wild-type enzyme. However, 50 nM of V298 will hydrolyze 50 μM of ceftazidime, a physiologically relevant concentration, in minutes, while WT AmpC at the same concentration would take close to half a day. This gain in new activity against cefotaxime was accompanied by a corresponding loss of native activity against cephalothin, typically from 3- to 8-fold, but as high as 100-fold in the case of Y221G (Table 2.1, Figure 2.3A).

Mutation	C_α-C_α dist. to Ser64 (Å)	Melting temp (T_m)	ΔT_m (°C)	$\Delta\Delta H$ (kcal/ mol)	$\Delta\Delta G$ (kcal/ mol)	Cephalothin		Cefotaxime	
						K_m (µM)	k_{cat} (s^{-1})	K_m (µM)	k_{cat} (s^{-1})
WT	NA	54.6	-----	182	----	27	420	0.8	0.0448
T70I	10.0	51.5	-3.1	142	-1.74	53	53.9	295	9.2
V298E	21.0	47.2	-7.4	102	-4.14	32	90.6	79	4.4
E219K	9.3	48.6	-6.0	180	-3.36	24	84.6	77	6.9
Y221G	4.6	50.8	-3.8	199	-2.13	99	4.2	337	8.0
Ω loop insertion (res. 210)	14.5	51.3	-3.3	183	-1.85	23	134	53	8.7

Table 2.1 Kinetic and thermodynamic parameters of AmpC ESBL mutants

The stability of the ESBL mutants was determined by thermal denaturation, monitored by far-UV circular dichroism. To determine thermodynamic stability of these mutant enzymes, it is necessary to demonstrate their reversibility and two-state behavior upon thermal unfolding. Extensive previous work suggests that wild-type and mutant AmpC enzymes denature reversibly and in a two-state manner [46]: they reversibly denature both by rapid cooling and by slow re-annealing from the folded state in temperature melts, the T_m and ΔH_u are very similar when measured by far-UV CD, near-UV CD, and by fluorescence, the T_m is unaffected by ramp rates between 0.5 and 2º C/min, and the transition itself is well-fit by a two-state model [46]. Thermal denaturation of each extended-spectrum AmpC mutant monitored by far-UV was also consistent with a reversible, two-state model. Melting curves showed clear two-state behavior, with a clear and sharp transition at the melting temperature (Figure 2.3B). Denaturation was reversible, ranging from 90 to 100 percent of CD signal regained after quick cooling of the denatured enzymes. The thermal denaturation of a representative mutant, Y221G,

A

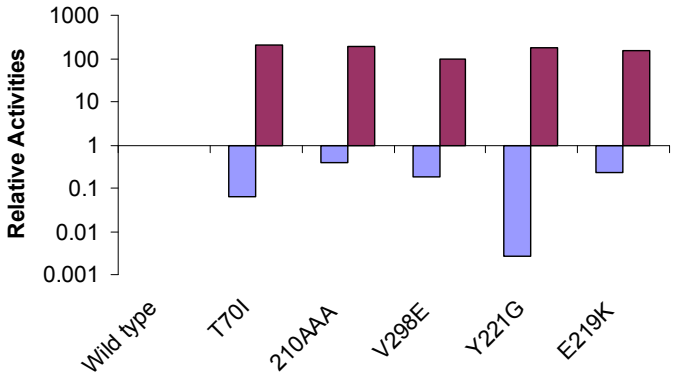

B

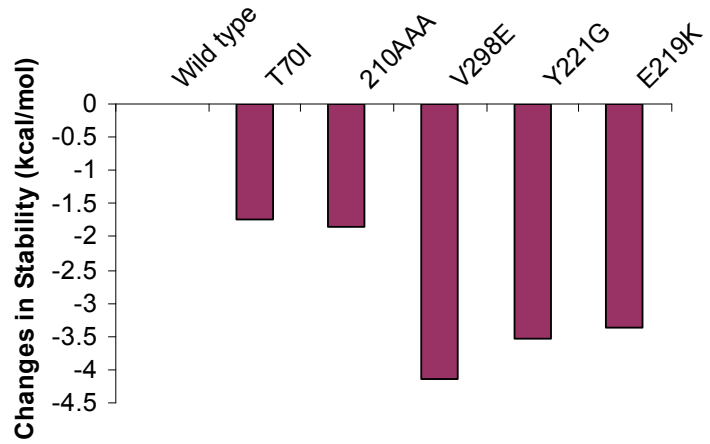

C

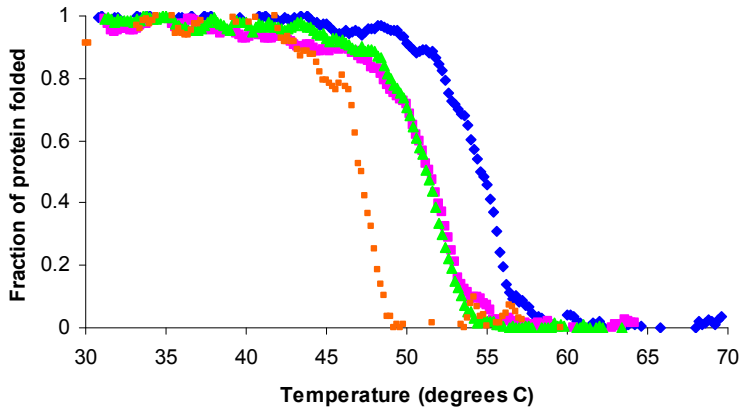

Figure 2.3: Relative enzyme activities and thermodynamic stabilities of AmpC ESBL mutants. (a) Relative activities of AmpC ESBLs against the first-generation cephalosporin cephalothin and the third-generation cephalosporin cefotaxime. (b) Characteristic thermal denaturation curves of selected AmpC ESBL mutants relative to the wild-type enzyme (c) The differential stabilities of AmpC ESBL mutants relative to wild-type.

monitored by fluorescence emission also showed a sharp transition with the same T_m of 50.8°C as when monitored by far-UV (Supplementary Material Figure S1A). A second ESBL mutant, the omega loop insertion, also showed a sharp transition with a T_m of 52.1°C (compared to a T_m of 51.3°C by CD) when monitored by far-UV (Supplementary Material Figure S1B). We therefore assume that these mutants, like the wild-type enzyme, denature in a reasonable approximation to reversible, two-state behavior, allowing us to determine true thermodynamic differences in enzyme stability relative to the wild-type enzyme.

The thermodynamic stability of all five ESBLs was decreased relative to the wild-type enzyme (Table 2.1, Figure 2.3C). Melting temperatures of these mutant enzymes diminished by between 3.1°C to 7.4°C, corresponding to a decrease in stability of 1.7 to 4.1 kcal/mol, a substantial change in stability for single substitutions, particularly since the overall stability of the wild-type enzyme is only 14 kcal/mol [46].

II. V298E apo structure

The structure of the V298E mutant enzyme was determined by x-ray crystallography to 2.64 Å resolution (R_{work}=18.4%, R_{free}=23.4%, Table 2). Well-defined $2F_o$-F_c electron density at a contour level of 1σ was seen for most residues in the structure, with the exception of residues 285-296 (Figure 4, Supplementary Material Figure S2). The resulting structure reveals a "domino effect" of structural changes, starting at the point of substitution, and transmitted to the active site, 20 Å away (Figure 2.4). Val298 is found in a mini-hydrophobic core of the wild-type enzyme; when substituted to a glutamate, Glu298 moves to enable its interaction with solvent, opening up a cavity in the hydrophobic core (Figure 2.4). The sidechain of Trp260 adopts a conformation where it can fill this cavity. The new position of Glu298 clashes with the position of Pro297 in the

wild-type enzyme; to avoid this clash, Pro297 swings out. This residue is on one end of a loop forming one wall of the active site; when it adopts this new conformation, it presumably takes the rest of the loop with it, as density is lost for residues 285-296 in this structure (Figure 2.4). The positions of key active site residues resemble that of the wild-type AmpC structure, with the exception of Tyr150, which adopts a new conformation where it hydrogen-bonds with Lys315. As an aside, we observed strong positive F_o-F_c density connecting

atom $C_{\varepsilon 2}$ of Tyr150 and atom N_ζ of Lys67. We also observed this feature in the omega loop insertion apo crystal structure (below), and a similar feature was observed in the crystal structure of the omega loop insertion GC1 from *E. cloacae.*[32] In the GC1 structure this feature was left unmodeled but attributed to a reaction with sodium azide present in the crystallographic buffer; we have also chosen not to model this feature.

III. Omega loop insertion apo structure

The three-residue omega loop insertion was originally identified as a clinical isolate in the class C P99 β-lactamase from *E. cloacae* and was subsequently characterized [32; 33; 34; 47]. In addition, two structures of this extended-spectrum class C β-lactamase were determined, both the apo form [32], and in complex with a cefotaxime phosphonate transition-state analog [33]. Inspired by this work, we decided to study the thermodynamic implications of this substitution, and for consistency, made the analogous mutation in AmpC. Since it was determined that the length, not the identity, of the insertion was crucial in imparting catalytic activity, and an insertion of three alanines had comparable extended-spectrum activity [34; 47]; we used an insertion of three alanine residues after His210 to represent the omega loop insertion. The structure of the apo omega loop insertion structure was determined to 1.64 Å resolution by x-ray crystallography

Protein	**V298E**	**Omega loop insertion**	**T70I/ BZB**	**Y221G**	**Y221G/ cefotaxime**	**E219K**	**E219K/ benzo(b) thiophene**
Data collection							
Space group	$P2_1$	C2	C2	C2	C2	C2	C2
Cell dimensions							
a, b, c (Å)	81.271 75.852 84.086	117.582 77.926 98.050	114.162 77.361 91.747	117.717 76.789 98.693	117.80 77.58 98.89	118.247 76.876 116.492	117.06 77.41 97.24
α, β, γ (°)	90.00 115.96 90.00	90.00 115.96 90.00	90.00 122.12 90.00	90.00 116.62 90.00	90.00 118.60 90.00	90.00 130.89 90.00	90.0 115.58 90.0
Resolution (Å)	30.0-2.64 (2.70-2.64)*	30.0-1.64 (1.68-1.64)	30.0-2.64 (2.70-2.64)	30.0-1.90 (1.95-1.90)	60.02-2.30 (2.42-2.30)	30.0-1.84 (1.88-1.84)	30.0-1.63 (1.67-1.63)
R_{merge} (%)	8.9	6.1	7.1	6.8	10.6	9.4	6.1
$I / \sigma I$	8.0 (2.0)	8.7 (2.3)	7.8 (2.1)	7.7 (2.1)	4.5 (2.3)	5.1 (2.2)	8.4 (2.0)
Completeness (%)	100.0 (100.0)	100.0 (99.9)	98.4 (97.0)	99.9 (99.9)	96.9 (96.2)	94.0 (93.2)	99.9 (100.0)
Refinement							
No. reflections	28,233 (2080)	92,466 (6818)	34,977 (2548)	58,776 (4295)	32,017 (2363)	60,887 (4418)	92,583 (4868)
R_{work}/R_{free} (%)	18.4 / 23.4	17.0 / 19.7	19.6 / 24.7	15.7 / 19.7	19.6 / 24.8	17.4 / 21.7	17.6 / 20.8
No. atoms							
Protein	5577	6297	5316	5541	5610	5549	5565
Ligand/ion	6	0	12	74	28	10	44
Water	119	278	249	577	187	737	865
B-factors (Å^2)							
Protein	24.8	15.3	27.90	17.36	29.96	18.49	16.48
Ligand/ion	52.8	44.3	32.75	42.7	45.7	39.10	23.93
Water	37.358	36.9	30.81	30.71	30.79	27.65	28.41
r.m.s. deviations							
bond lengths (Å)	0.013	0.016	0.011	0.015	0.013	0.015	0.010
bond angles (°)	1.494	1.486	1.414	1.460	1.437	1.465	1.383

Table 2.2 Crystallographic statistics *Values in parenthesis represent highest resolution shells

A

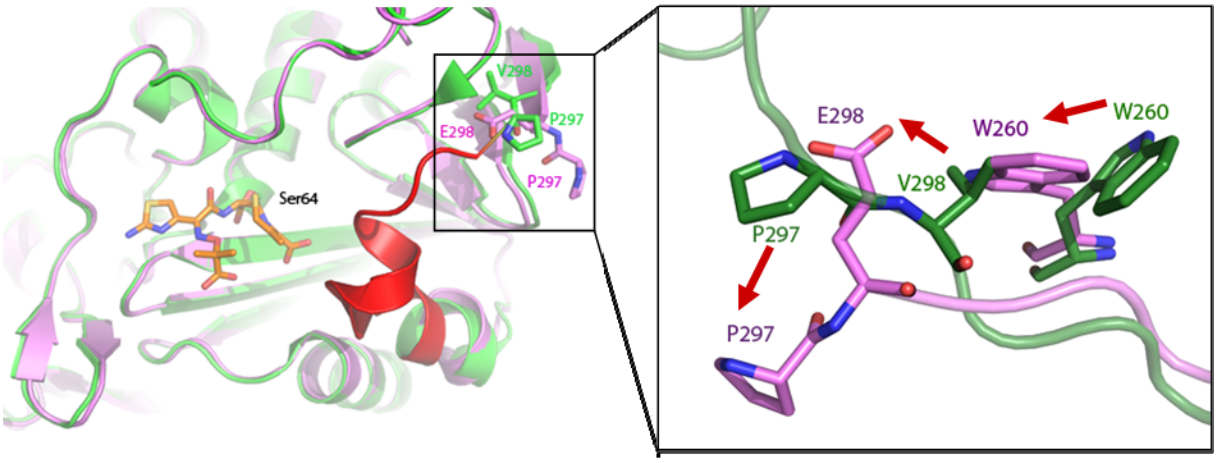

Figure 2.4: The x-ray crystal structure of V298E to 2.6 Å resolution, showing an overview of changes in the V298E mutant (purple) compared to the WT protein (green). Density is lost for the region of the loop shown in red, presumed to have flipped out. Structural changes are shown at the point of mutation (inset), with the mutant protein (purple) overlaid on the WT protein (green).

(R_{work}=17.0%, R_{free}=19.7%, Table 2). Overall, the omega loop insertion structure resembles the wild-type structure, the RMSD for C_α atoms are 0.16 Å. However, in the region of the omega loop, at the terminus of the active site, the changes are substantial. In the mutant, the insertion causes the omega loop to adopt a new conformation (Figures 2.5A and 2.5B); the C_α of Pro216 has moved by 8.9 Å, relative to the wild-type Pro213. Similarly, Val211 has moved by 8.5 Å, and has in essence been replaced by Ala211. In addition, the Tyr221 OH has moved by 1.1 Å, and the Tyr221 C_δ, the atom thought to sterically clash with a catalytically competent conformation of third-generation cephalosporins, has shifted by 0.6 Å. Well-defined $2F_o$-F_c electron density at a contour level of 1 σ was seen for most residues in the structure, with the exception of residues 287-293 in the A monomer (the positions cannot be resolved for residues 285-290 in the

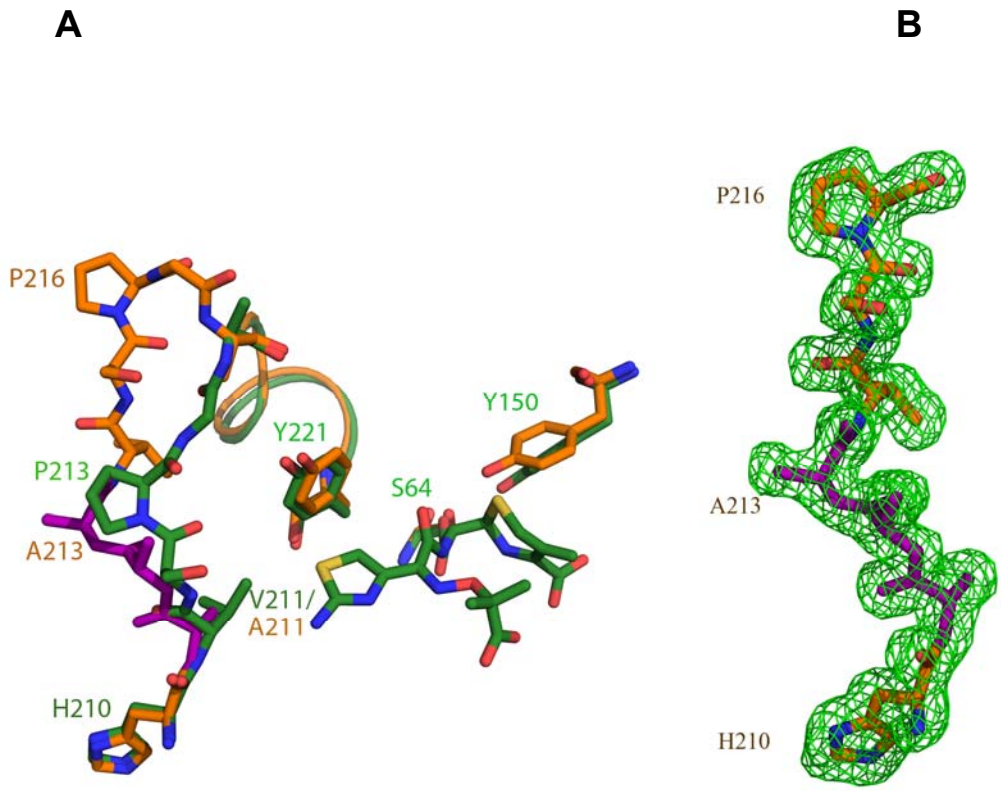

Figure 2.5: The x-ray structure of the "omega loop insertion" mutant (H210AAA) to 1.6 Å resolution. (a) The omega loop insertion structure (orange, 3 alanine insertion in purple) overlaid on the WT protein (green). (b) F_o-F_c omit density for residues 210-216 shown at 3σ.

A monomer of the wild-type enzyme). The key active site residues resemble that of the wild-type AmpC structure, with the exception of Tyr150, which adopts a new conformation where it hydrogen-bonds with Lys315.

IV. T70I apo and holo structures

T70I was crystallized out of a buffer containing the transition-state analog benzo(b)thiophene-2-boronic acid (BZB, K_i 27 nM) [48], after repeated attempts to grow apo T70I crystals failed. The structure of T70I was determined by x-ray crystallography to 2.14 Å resolution (R_{work}=19.6%, R_{free}=24.7%, Table 2). Like all AmpC structures, the protein, though functionally a monomer, crystallized with two monomers in the asymmetric unit. Surprisingly, one monomer was an apo structure, and the other had the

transition-state analog bound to the active site, and each monomer adopted different conformations (Figure 2.6). In the apo monomer no electron density was seen for residues 193-221, comprising the omega loop of the enzyme. In addition, the β-turn from residues 318-322 has flipped into the active site, disorganizing the region around the oxyanion hole formed by the backbone nitrogens of the catalytic Ser64 and Ala318 (Figure 2.6A). The active site of the T70I/benzo(b)thiophene structure (Figure 2.6B), conversely, resembles that of the WT AmpC/benzo(b)thiophene structure [48]. In addition, unlike in the apo structure, strong electron density is seen for residues 193-221 at 1σ, allowing the positions for these residues to be determined (Figure 2.6B). This region now adopts a slightly different conformation than it does in the wild-type AmpC structure, predominately in the region from residues 211-216 (Figure 2.6B); it enlarges the active site in some regions, though is closer to the active site in others.

V. E219K apo and holo structures

The E219K apo structure was determined to 1.84 Å resolution (R_{work}=17.4%, R_{free}=21.7%, Table 2.2), and its complex with the transition-state analog inhibitor benzo(b)thiophene-2-boronic acid was determined to 1.63 Å resolution (R_{work}=17.6%, R_{free}=20.8%, Table 2.2). After an initial round of refinement using the wild-type enzyme as a model, negative F_o-F_c density was seen at 3σ for Glu219, with nearby positive F_o-F_c density at 3σ resembling a lysine. This residue was computationally mutated to a lysine and the structure was further refined. $2F_o$-F_c density was unambiguous at the point of substitution for Lys219 in both the final structures, verifying the substitution (Supplementary Material figure S3A). The position of this side chain in both structures resembles that of Glu219 in the wild-type structure, pointing into solvent (Supplementary Material figure S3B). In the wild-type enzyme, the side chain of Glu219 hydrogen-bonds to its own backbone amide nitrogen. Substitution of this residue to a lysine removes this interaction, and the K219 backbone nitrogen now hydrogen-bonds with the backbone

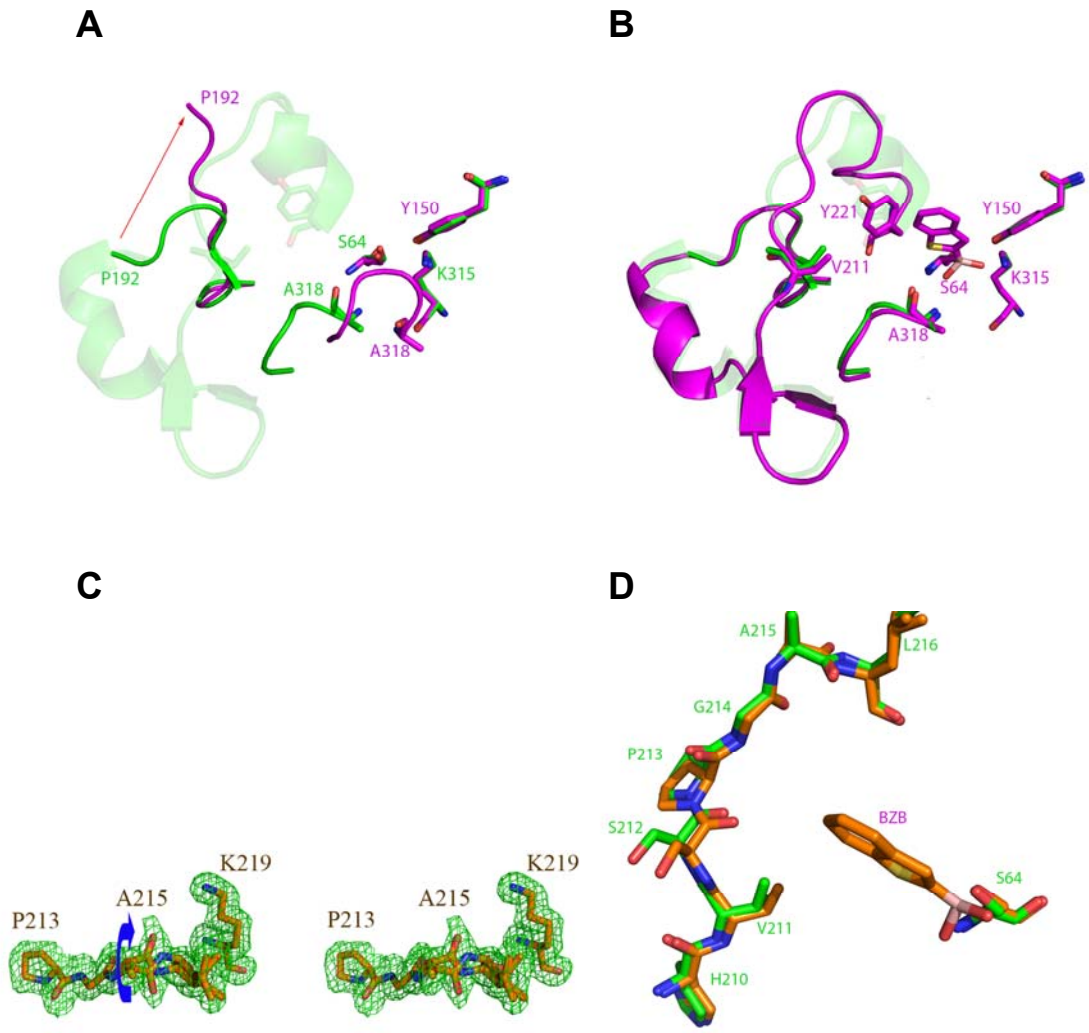

Figure 2.6: Flexibility induced in extended-spectrum mutants T70I and E219K. (a) The T70I apo structure (purple) overlaid on the WT structure (green). Density is lost from residues 193-221 in the omega loop (shown in transparent green) in the T70I structure. (b) The T70I/benzo(b)thiophene (BZB) structure (purple) overlaid on the WT structure (green). Residues 193-221, lost in the T70I structure but present in the T70I/benzo(b)thiophene structure, are shown in cartoon. (c) Stereo view of the x-ray crystal structure of E219K/BZB to 1.63 Å resolution. F_o-F_c omit density is shown at 3σ. Arrow highlights the two conformations of residues 215-216, distinguished by a peptide flip. (d) The omega loop and active site of E219K/BZB (orange) overlaid with that of the wild-type AmpC structure (green), showing the conformational differences in the 211-213 region. The position of BZB is shown in the active site.

carbonyl of Leu216, which has moved closer to it (Figure 2.6C). This in turn affects the conformation of residues 215-216. In the WT structure, the backbone nitrogen of Asp217 hydrogen-bonds with the backbone carbonyl of Ala215. With the carbonyl of Leu216 now engaged with the backbone nitrogen of Lys219, residues 215-216 now adopt two conformations, with the peptide backbone flipped relative to each other (Figure 2.6C). Also, residues 211-213, also in the omega loop, now adopt a different conformation than in the wild-type AmpC structure (Figure 2.6D).

VI. Y221G apo structure

The Y221G apo structure was determined to 1.90 Å resolution (R_{work}=15.7%, R_{free}=19.7%, Table 2.2). Few structural changes are seen in Y221G compared to the WT AmpC structure. Substitution of Tyr221 to a glycine creates a cavity, which alleviates the steric clash that occurs with the catalytically competent conformation of the third-generation cephalosporins (below). This opens up space in the active site that is only partially filled by Asp217 adopting a new conformation and moving into its place.

VII. Y221G/cefotaxime structure

Y221G crystals were soaked into a 1.7 M KPi, pH 8.7, 50 mM cefotaxime, solution for one hour and then flash-frozen to obtain a structure of the Y221G/cefotaxime complex. The structure of the Y221G/cefotaxime complex was determined by x-ray crystallography to 2.3 Å resolution (R_{work}=19.6%, R_{free}=24.8%, Table 2.2). Strong $2F_o$-F_c electron density was seen for the ligand at 1σ in the B monomer, and in an F_o-F_c omit map at 3σ (Figure 2.7A). We compared the Y221G/cefotaxime structure to the crystal structure of wild-type AmpC in complex with the closely related third-generation cephalosporin ceftazidime (Figure 2.7B, [31]). Cefotaxime, which for the Y221G mutant enzyme has become a good substrate, adopts a different conformation than does ceftazidime in its complex with WT AmpC (Figure 2.7B), where the third generation

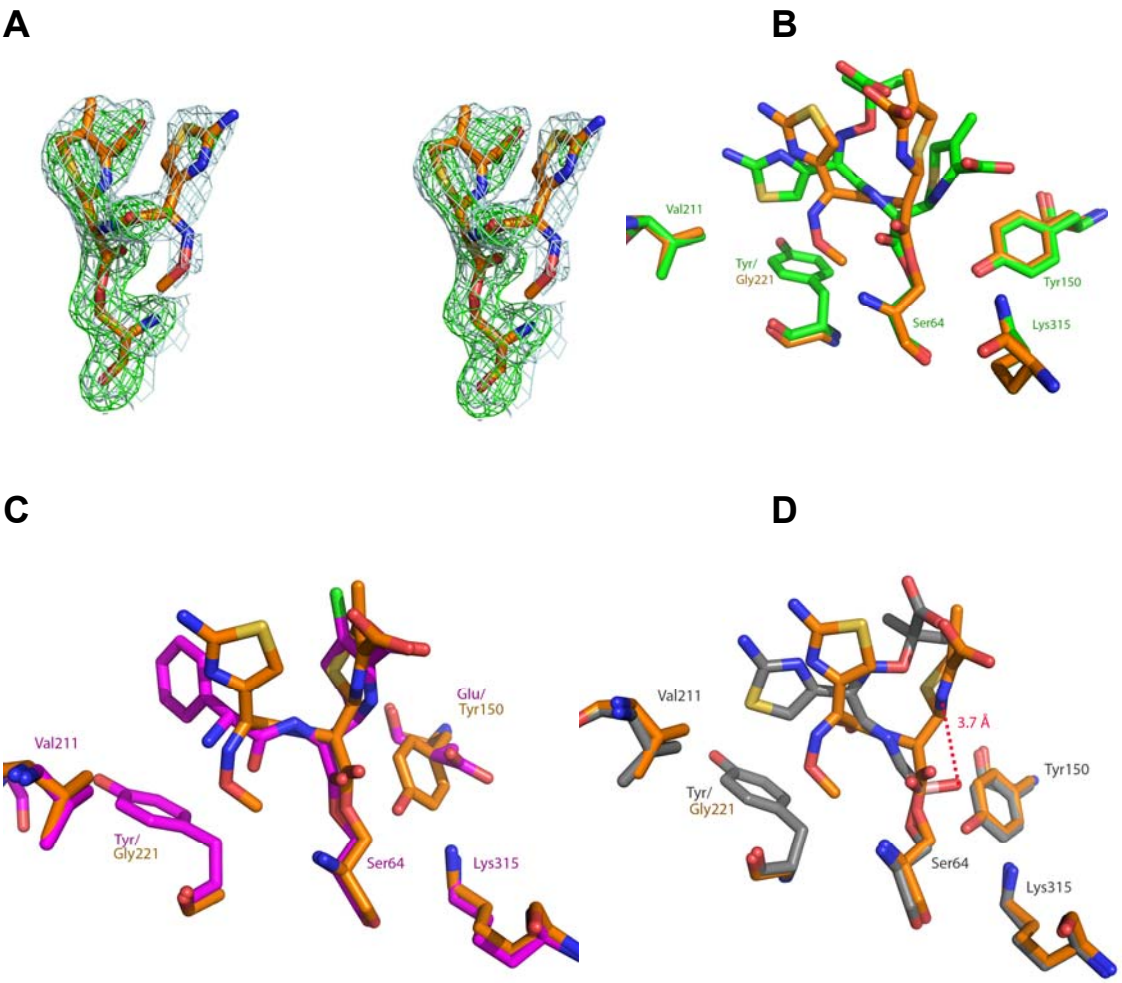

Figure 2.7: X-ray structure of Y221G/cefotaxime (2.3 Å). (a) Stereo view of quality of density of cefotaxime in the active site of Y221G. $2F_o$-F_c density (blue) is shown at a contour level of 1σ, and F_o-F_c.omit density (green) is shown at a contour level of 3σ. (b) The Y221G/cefotaxime structure (orange) overlaid with the WT/ceftazidime structure (green). (c) The Y221G/cefotaxime structure (orange) overlaid with the WT/loracarbef structure (purple). (d) The Y221G/cefotaxime structure (orange) overlaid with the WT/ceftazidime deacylation transition state analog (gray).

---

cephalosporin is such a poor substrate that it functions as a covalent inhibitor. The new conformation of cefotaxime in the active site of Y221G resembles that of good substrates, such as loracarbef, in WT AmpC[49] (Figure 2.7C). Cefotaxime's adoption of the loracarbef-like structure in the Y221G complex appears to make it competent for catalysis. In contrast with the AmpC/ceftazidime structure, where the lactam nitrogen of

substrate is only 1.8 Å from where the attacking water is expected to be in the deacylation high-energy intermediate, in the Y221G/cefotaxime structure this same nitrogen has moved 3.7 Å from the putative water position, making it competent for catalysis (Figure 2.7D, [31]). This movement is, in turn, allowed by the introduction of the cavity in Y221G, increasing the volume of the active site and its ability to accommodate 3rd generation cephalosporins.

2.4 Discussion

Two key observations emerge from this study. First, each of the five mutant enzymes has achieved its two-orders of magnitude activity gains at the cost of substantial stability loss. The minimum stability loss is 1.7 kcal/mol (3.3°C), for T70I, whereas V298E loses 4.1 kcal/mol (7.4°C), fully 30% of the net stability of the native protein. Second, the crystal structures reveal that the substitutions, though distant from one another by up to 30 Å, have the same overall effect, enlarging the active site by introducing physical defects, allowing the mutant enzymes to accommodate the large, third-generation cephalosporins. We consider these points in turn.

I. Destabilization of the mutant enzymes

The stability insults conferred by these gain-of-function substitutions are easily appreciated. In V298E, substituting a charged residue into a well-packed hydrophobic core causes a cascade of conformational changes that are revealed in the x-ray structure of the mutant enzyme (Figure 2.4). Similarly, in Y221G, the substitution introduces a straight-forward structural defect, creating a hole in the protein structure and loss of van der Waals interactions that are only partially fulfilled by movement of Asp217 into this region. In the H210AAA insertion mutant, the expanded omega loop conformation reduces packing, van der Waals interactions, hydrogen bonding, and hydrophobic surface area burial (Figure 2.5). Finally, both T70I and E219K lose hydrogen bonds that

ordinarily stabilize this same omega-loop region of the enzyme. In WT AmpC, the hydroxyl of Thr70 hydrogen bonds with the backbone carbonyl of Glu219 in this loop, while in the structure of T70I this interaction has been lost and not replaced, leading to substantial conformational change in the mutant protein (Figure 2.6). In E219K, the substitution of the lysine disrupts a hydrogen bond that, in the WT enzyme, the native glutamate side chain made to its own backbone nitrogen, which otherwise has no partner in the WT structure. This internal hydrogen-bond stabilizes the loop conformation adopted in this region of the structure and its loss is likely responsible for the destabilization of E219K. Thus, all five mutant enzymes are textbook illustrations of how to disrupt protein structure and stability, should that ever be one's goal.

II. Translating stability loss into activity gain

The activity that these mutants need to gain is the ability to hydrolyze β-lactam substrates that are too large for the native active site, the 3rd generation cephalosporins. Each of the mutants accomplishes this by introducing structural insults to the integrity of the protein. Three mechanisms may be considered through which these stability defects are translated into increased activity: by changing the ground state of the enzyme, by changing enzyme flexibility, or by changing its dynamics. Here, we will not further distinguish between flexibility and dynamics, as our structural and thermodynamic results are insufficiently resolved to do so, but will simply refer to both under the rubric of "flexibility", understanding that dynamics may play a role.

Perhaps the simplest mutant to understand is Y221G, which changes the ground state, apo conformation of the enzyme to accommodate 3rd generation cephalosporins. Tyr221 is a highly conserved residue whose presence forces 3rd generation cephalosporins into a catalytically incompetent conformation, owing to a steric clash with their large R1 side chains (above). Substitution of Tyr221 by a glycine allows the β -

lactam to relax into a catalytically competent conformation. Thus, in the Y221G/cefotaxime complex (Figure 2.7), this third-generation cephalosporin adopts a conformation resembling that adopted by good substrates in WT x-ray structures (Figure 2.7C). Similarly, the x-ray structure of H210AAA reveals a well-resolved, larger conformation for the omega loop, indicating a change in the ground state for this mutant enzyme. This insertion effectively replaces Val211 with an alanine; Val211 is the second residue, in addition to Tyr221, that in WT AmpC clashes with the R1 side chain of 3rd generation cephalosporins. This structure is largely consistent with that of the enzyme that inspiring our work on this mutant, the clinically isolated GC1 ESBL from *E. cloacae* [32; 33; 34; 47]. One difference between the two structures is that the GC1 apo structure revealed local disorder in residues 213-215 [32], which includes one residue of the insertion, suggesting increased flexibility relative to that of the P99 enzyme. Conversely, in the AmpC apo structure the omega loop adopts a new, well-ordered conformation that expands active site volume (Figure 2.5).

The V298E mutant falls into the same category of affecting the ground state conformation of the enzyme—enlarging it—though here flexibility may also play a role. The introduction of a glutamate into the hydrophobic core of the protein is a gross structural insult, and to relieve this the enzyme undergoes substantial reorganization, flipping the now Glu298 into bulk solvent. This perturbation, 21 Å from the catalytic serine, begins a cascade of structural changes, starting with a flip of Trp260 into the hole created by the movement of Glu298. What used to be the loop defined by residues 285 to 296, which in the WT structure formed a bounding wall of the active site, is both moved outwards and disordered—it has largely disappeared from the electron density maps—reflecting both increased active site volume and, potentially, flexibility. The net effect is to increase the volume of the active site, improving its ability to accommodate the catalytically competent conformation of the bulky 3rd generation cephalosporins. This,

then, provides a relatively rare structural view into a phenomenon common to resistance enzymes as diverse as dihydrofolate reductase [42], HIV protease [40], HIV reverse transcriptase [50], and BCR-ABL kinase [41] —the occurrence of resistance substitutions far from the active site.

The mutant enzymes T70I and E219K appear to gain activity against 3rd generation cephalosporins via increased flexibility. The T70I apo structure has two notable conformational changes relative to WT: notwithstanding the 2.14 Å resolution to which it was determined, density is missing for residues 193-221 in the active site "omega loop", and an active site ß turn (residues 318-322) has flipped conformations to disrupt the catalytically critical oxyanion hole, formed by the backbone nitrogens of Ser64 and Ala318. Since this mutant enzyme is catalytically active, the x-ray structure can only represent one conformation accessible to the protein, suggesting that it is more flexible. Indeed, in the complex with the transition-state analog BZB, the active site of T70I resolves into a conformation that is again catalytically competent, resembling the native active site in conformation and overall volume. These observations are consistent with activity being gained by increased flexibility in T70I, which appears to be much more plastic on ligand binding than does the WT enzyme[51]. The situation with E219K is more subtle. We observe little substantial conformational change in either the E219K apo or inhibitor-bound structure relative to WT AmpC, though the mutant is 150-fold more active against cefotaxime. The loss of the internal hydrogen bond between the side chain and backbone nitrogen of residue 219 appears to loosen the structure, with the 215-216 peptide bond adopting a second conformation in the holo structure, while residues 211-213 also undergo a conformational change (Figure 2.6D). Neither of these conformations are seen in a 1.07 Å structure of WT AmpC [52] that revealed other inherent conformational states, suggesting increased flexibility in the E219K enzyme, again in the omega loop region.

How do these results fit with the stability-activity trade-off model? At the simplest level, the observation that the AmpC ESBLs have in every case lost stability is consistent with the model. At atomic resolution, too, the structural underpinnings of the "stability-function" hypothesis are confirmed—larger, more difficult substrates are recognized by the introduction of stability defects that increase either the ground-state size of the AmpC active site, or its ability to flex when confronted by the larger substrates.

It is this physical basis of the model that is key to understanding where the "stability-function" hypothesis is relevant, and how it may be reconciled with the observations of other groups. Clearly, stability-activity trade-offs are not linked by physical law; one can imagine substitutions that increase stability without effect on activity—indeed, the stability restoring mutant in TEM-1 ESBLs, M182T, is an example of such, [20; 22] and the evolution of thermophilic mutants that do not sacrifice activity is another [27]. Nor does the evolution of new function necessarily require stability sacrifices. Indeed, results from this study suggest that an enzyme could mutate to a new substrate profile and ***gain*** stability. Thus, for all five mutant enzymes studied here, the k_{cat} values for smaller 1st generation substrates, such as cephalothin, is actually *reduced*, typically by 3- to 8-fold, and by 100-fold for Y221G, for the destabilized mutants (Table 2.1). The same increase in active site volume and flexibility that allows the larger 3rd generation cephalosporins to be accommodated by the AmpC ESBL mutants decreases complementarity for smaller substrates, which fit the native active site snugly. If one inverts the evolution of AmpC, and imagines that Y221G is the native enzyme, then one would be able to evolve a "mutant" that has the WT sequence with 100-fold ***greater*** activity for the smaller cephalothin, and substantially improved stability. This would be a case where the active site has shrunk and new interactions with the rest of the folded

protein have been (re)introduced, consistent with the physical model underlying the "stability-function" hypothesis.

Still, this case remains the exception that proves the rule. In enzymes evolving under the pressure of antimicrobial or antineoplastic chemotherapy, such as dihydrofolate reductase [42], HIV protease [40], BCR-ABL tyrosine kinase [41], HIV reverse transcriptase [50], and ß-lactamases, gain-of-function and many inhibitor-resistant mutants are likely to sacrifice stability, not because stability is a necessary correlate to activity, by some implied law, but rather because introduction of structural defects or further pre-organization into active sites typically reduce stability. It is a testament to the importance of stability in enzyme evolution that "restabilizing" and "recatalyzing" substitutions have been found *in vivo* to compensate for activity and stability losses occurring as a side effect of primary drug-resistance substitutions [20; 21; 22; 53]. The role of stability as a constraint in enzyme evolution [23; 26] may well have implications for strategies to reduce resistance evolution under chemotherapeutic pressure [26].

2.5 Materials and Methods

I. Construction and purification of AmpC β-lactamases

Mutants of AmpC were created using the overlap extension polymerase chain reaction [54]. Both WT and mutant enzymes were expressed and purified as described [49; 55], except Y221G, where the cells were lysed using a Microfluidizer M-110 at 18,000 psi in 50 mM Tris-HCl, pH 7, and the lysate was purified. The mutant enzymes were purified from an m-aminophenylboronic acid affinity column [55].

II. Kinetic measurements

The activity of each mutant enzyme was determined by its hydrolysis of the β-lactam substrate cephalothin (Sigma, St Louis, MO) in a 50 mM Tris-HCl buffer containing

0.01% Triton-X at pH 7.0. Reaction rates were measured in a Hewlett–Packard HP-8453 spectrometer. Values of k_{cat} and K_m were determined from Michaelis-Menten plots, and parameters were fit using Kaleidagraph (Synergy, Reading, PA). The extinction coefficients used were: AmpC: 2.45 OD/mg/mL/cm; cephalothin: $\Delta\varepsilon_{265}$ = -8790 M^{-1} cm^{-1}; cefotaxime: $\Delta\varepsilon_{260}$= -6710 M^{-1} cm^{-1}. At high substrate concentrations, 1 mm pathlength cuvettes were used to obtain kinetic data.

III. Crystallization and structure determination

AmpC extended-spectrum mutants were crystallized in the following conditions: V298E: 30% PEG 8000, 0.1M sodium cacodylate, 0.2 M ammonium sulfate, pH 6.5; omega loop insertion: 1.7M KPi, pH 8.0; T70I/benzo(b)thiophene 2-boronic acid (BZB) and E219K/BZB: 1.7M KPi, pH 8.7, 360 μM BZB; Y221G and E219K: 1.7M KPi, pH 8.7. Y221G was also soaked in 50mM cefotaxime, 1.7 M KPi, pH 8.7, for 1 hour. Diffraction was measured at beamline 8.3.1 at the Advanced Light Source (Lawrence Berkeley National Labs, Berkeley, CA). Reflections were indexed, integrated and scaled using MOSFLM [56] and SCALA in CCP4 [57]. Molecular replacement was accomplished with Molrep in CCP4 [57], using the appropriate apo structure, typically the wild-type structure (1KE4) as a search model. Model building and refinement was completed with Coot [58] and REFMAC5 [59] in the CCP4 suite [57].

IV. Thermal Denaturation

Enzymes were denatured by raising the temperature in 0.1 °C increments at a ramp rate of 2 °C/min in 50 mM potassium phosphate (pH 6.8), 50 mM potassium chloride, 38% (v/v) ethylene glycol buffer, using a Jasco 715 spectropolarimeter with a Peltier-effect temperature controller and an in-cell temperature monitor [46]. Denaturation was marked by an obvious transition in the far-UV CD (223 nm) signal. Consistent with previous work with AmpC enzymes, which demonstrated reversible, two-state behavior (see Results) [10;

[46], all mutant enzyme melts were reversible and apparently two-state, as judged by >90% return of CD signal upon quick cooling following denaturation, and a clear, sharp transition in the denaturation curve. Denaturation of two representative mutant enzyme (Y221G and H210AAA) was also measured by the intensity of the integrated fluorescence emission for all wavelengths above 300 nm, exciting at 280 nm, using a fluorescence detector on the Jasco instrument, and compared to thermal denaturation monitored by far-UV to investigate two-state behavior. Temperature of melting (T_m) and van't Hoff enthalpy of unfolding (ΔH_{vh}) values were calculated using EXAM [60]. The free energy of unfolding relative to WT was calculated using the method of Becktel and Schellman: $\Delta\Delta G_u = \Delta T_m \Delta S_u^{WT}$ [61]. A negative value of $\Delta\Delta G_u$ indicates a stability loss. The $\Delta S_u^{WT}$was 0.56 kcal mol^{-1} K^{-1} [46].

V. PDB Accession codes

X-ray crystal structure coordinates have been deposited in the Protein Data Bank with the following accession codes: V298E = 3IXD; H210AAA = 3IWI; T70I/BZB = 3IXG; Y221G = 3IWO; Y221G/CTX = 3IXH; E219K = 3IWQ; E219K/BZB = 3IXB.

2.6. Acknowledgements

This work was supported by NIH grants GM63813 (to BKS). VLT was partly supported by a National Science Foundation Predoctoral Fellowship. We thank Sandri Soelaiman and Ray Nagatani for some mutagenesis, protein purification and setting crystal trays, Kerim Babaoglu, Yu Chen, and Pascal Egea for crystallographic assistance, Christian Laggner for advice and assistance with chemical intuition, Matthew Merski for molecular biology assistance, and Sarah Boyce and Jens Carlsson for reading this manuscript.

2.7 References

1. Warshel, A. (1978). Energetics of Enzyme Catalysis. *Proc. Natl. Acad. Sci. USA* **75**, 5250-5254.
2. Warshel, A., Sussman, F. & Hwang, J.-K. (1988). Evaluation of Catalytic Free Energies in Genetically Modified Proteins. *J. Mol. Biol.* **201**, 139-159.
3. Herzberg, O. & Moult, J. (1991). Analysis of the Steric Strain in the Polypeptide Backbone of Protein Molecules. *Proteins* **11**, 223-229.
4. Clackson, T. & Wells, J. A. (1995). A hot spot of binding energy in a hormone-receptor interface. *Science* **267**, 383-386.
5. Richards, F. M. (1974). The interpretation of protein structures: total volume, group volume distributions and packing density. *J. Mol. Biol.* **82**, 1-14.
6. Williams, R. J. (1972). The Entatic State. *Cold Spring Harbor Symposia on Quantitative Biology* **36**, 53-62.
7. Meiering, E. M., Serrano, L. & Fersht, A. R. (1992). Effect of active site residues in barnase on activity and stability. *J. Mol. Biol.* **225**, 585-9.
8. Schreiber, G., Buckle, A. M. & Fersht, A. R. (1994). Stability and function: two constraints in the evolution of barstar and other proteins. *Structure* **2**, 945-51.
9. Shoichet, B. K., Baase, W. A., Kuroki, R. & Matthews, B. W. (1995). A Relationship Between Protein Stability and Protein Function. *Proc. Nat. Acad. Sci USA.* **92**, 452-456.
10. Beadle, B. M. & Shoichet., B. K. (2002). Structural bases of stability-function trade-offs in enzymes. *J. Mol. Biol.* **321**, 285-296.
11. Ota, M., Isogai, Y. & Nishikawa, K. (1997). Structural requirement of

highly-conserved residues in globins. *FEBS Lett* **415**, 129-33.

12. Mukaiyama, A., Haruki, M., Ota, M., Koga, Y., Takano, K. & Kanaya, S. (2006). A hyperthermophilic protein acquires function at the cost of stability. *Biochemistry* **45**, 12673-9.
13. Hargrove, M. S. & Olson, J. S. (1996). The stability of holomyoglobin is determined by heme affinity. *Biochemistry* **35**, 11310-8.
14. Chen, Y. C. & Lim, C. (2008). Common physical basis of macromolecule-binding sites in proteins. *Nucleic Acids Res* **36**, 7078-87.
15. Liang, S., Zhang, J., Zhang, S. & Guo, H. (2004). Prediction of the interaction site on the surface of an isolated protein structure by analysis of side chain energy scores. *Proteins* **57**, 548-57.
16. Ota, M., Kinoshita, K. & Nishikawa, K. (2003). Prediction of catalytic residues in enzymes based on known tertiary structure, stability profile, and sequence conservation. *J Mol Biol* **327**, 1053-64.
17. Kidokoro, S., Miki, Y., Endo, K., Wada, A., Nagao, H., Miyake, T., Aoyama, A., Yoneya, T., Kai, K. & Ooe, S. (1995). Remarkable activity enhancement of thermolysin mutants. *FEBS Lett.* **367**, 73-6.
18. Zhi, W., Srere, P. A. & Evans, C. T. (1991). Conformational stability of pig citrate synthase and some active-site mutants. *Biochemistry* **30**, 9281-9286.
19. Garcia, C., Nishimura, C., Cavagnero, S., Dyson, H. J. & Wright, P. E. (2000). Changes in the apomyoglobin folding pathway caused by mutation of the distal histidine residue. *Biochemistry* **39**, 11227-37.

20. Wang, X., Minasov, G. & Shoichet, B. K. (2002). Evolution of an Antibiotic Resistance Enzyme Constrained by Stability and Activity Trade-Offs. *J. Mol. Biol.* **320**, 85-95.

21. Huang, W. & Palzkill, T. (1997). A natural polymorphism in beta-lactamase is a global suppressor. *Proc Natl Acad Sci U S A* **94**, 8801-6.

22. Sideraki, V., Huang, W., Palzkill, T. & Gilbert, H. F. (2001). A secondary drug resistance mutation of TEM-1 beta-lactamase that suppresses misfolding and aggregation. *Proc Natl Acad Sci U S A* **98**, 283-8.

23. Weinreich, D. M., Delaney, N. F., Depristo, M. A. & Hartl, D. L. (2006). Darwinian evolution can follow only very few mutational paths to fitter proteins. *Science* **312**, 111-4.

24. Bloom, J. D., Labthavikul, S. T., Otey, C. R. & Arnold, F. H. (2006). Protein stability promotes evolvability. *Proc Natl Acad Sci U S A* **103**, 5869-74.

25. Bloom, J. D. & Arnold, F. H. (2009). In the light of directed evolution: pathways of adaptive protein evolution. *Proc Natl Acad Sci U S A* **106 Suppl 1**, 9995-10000.

26. Tokuriki, N. & Tawfik, D. S. (2009). Chaperonin overexpression promotes genetic variation and enzyme evolution. *Nature* **459**, 668-73.

27. Giver, L., Gershenson, A., Freskgard, P. O. & Arnold, F. H. (1998). Directed evolution of a thermostable esterase. *Proc Natl Acad Sci U S A* **95**, 12809-13.

28. Massova, I. & Mobashery, S. (1998). Kinship and Diversification of Bacterial Penicillin-Binding Proteins and Beta-Lactamases. *Antimicrob. Agents Chem.* **42**, 1-17.

29. Galleni, M., Lamotte-Brassear, J., Raquet, X., Dubus, A., Monnaie, D., Knox, J. R. & Frere, J.-M. (1995). The Enigmatic Catalytic Mechanism of Active-Site Serine Beta-lactamases. *Biochemical Pharmacology* **49**, 1171-1178.

30. Matagne, A., Misselyn-Bauduin, A. M., Joris, B., Erpicum, T., Granier, B. & Frere, J. M. (1990). The diversity of the catalytic properties of class A beta-lactamases. *Biochem J* **265**, 131-46.

31. Powers, R. A., Caselli, E., Focia, P. J., Prati, F. & Shoichet, B. K. (2001). Structures of ceftazidime and its transition-state analogue in complex with AmpC beta-lactamase: implications for resistance mutations and inhibitor design. *Biochemistry* **40**, 9207-14.

32. Crichlow, G. V., Kuzin, A. P., Nukaga, M., Mayama, K., Sawai, T. & Knox, J. R. (1999). Structure of the extended-spectrum class C beta-lactamase of Enterobacter cloacae GC1, a natural mutant with a tandem tripeptide insertion. *Biochemistry* **38**, 10256-61.

33. Nukaga, M., Kumar, S., Nukaga, K., Pratt, R. F. & Knox, J. R. (2004). Hydrolysis of third-generation cephalosporins by class C beta-lactamases. Structures of a transition state analog of cefotoxamine in wild-type and extended spectrum enzymes. *J Biol Chem* **279**, 9344-52.

34. Nukaga, M., Taniguchi, K., Washio, Y. & Sawai, T. (1998). Effect of an amino acid insertion into the omega loop region of a class C beta-lactamase on its substrate specificity. *Biochemistry* **37**, 10461-8.

35. Matsumura, N., Minami, S. & Mitsuhashi, S. (1998). Sequences of homologous beta-lactamases from

clinical isolates of Serratia marcescens with different substrate specificities. *Antimicrob Agents Chemother* **42**, 176-9.

36. Raimondi, A., Sisto, F. & Nikaido, H. (2001). Mutation in Serratia marcescens AmpC beta-lactamase producing high- level resistance to ceftazidime and cefpirome. *Antimicrob Agents Chemother* **45**, 2331-9.

37. Zhang, Z., Yu, Y., Musser, J. M. & Palzkill, T. (2001). Amino acid sequence determinants of extended spectrum cephalosporin hydrolysis by the class C P99 beta-lactamase. *J Biol Chem* **276**, 46568-74.

38. Tsukamoto, K., Ohno, R., Nukaga, M. & Sawai, T. (1992). The effect of amino acid substitution at position 219 of Citrobacter freundii cephalosporinase on extension of its substrate spectrum. *Eur J Biochem* **207**, 1123-7.

39. Morosini, M. I., Negri, M. C., Shoichet, B., Baquero, M. R., Baquero, F. & Blazquez, J. (1998). An extended-spectrum AmpC-type beta-lactamase obtained by in vitro antibiotic selection. *FEMS Microbiol Lett* **165**, 85-90.

40. Muzammil, S., Ross, P. & Freire, E. (2003). A major role for a set of non-active site mutations in the development of HIV-1 protease drug resistance. *Biochemistry* **42**, 631-8.

41. Shah, N. P., Nicoll, J. M., Nagar, B., Gorre, M. E., Paquette, R. L., Kuriyan, J. & Sawyers, C. L. (2002). Multiple BCR-ABL kinase domain mutations confer polyclonal resistance to the tyrosine kinase inhibitor imatinib (STI571) in chronic phase and blast crisis chronic myeloid leukemia. *Cancer Cell* **2**, 117-25.

42. Volpato, J. P. & Pelletier, J. N. (2009). Mutational 'hot-spots' in mammalian, bacterial and protozoal

dihydrofolate reductases associated with antifolate resistance: sequence and structural comparison. *Drug Resist Updat* **12**, 28-41.

43. Dubus, A., Wilkin, J. M., Raquet, X., Normark, S. & Frere, J. M. (1994). Catalytic mechanism of active-site serine beta-lactamases: role of the conserved hydroxy group of the Lys-Thr(Ser)-Gly triad. *Biochem J* **301**, 485-94.

44. Trehan, I., Morandi, F., Blaszczak, L. C. & Shoichet, B. K. (2002). Using steric hindrance to design new inhibitors of class C beta-lactamases. *Chem Biol* **9**, 971-80.

45. Mazzella, L. J. & Pratt, R. F. (1989). Effect of the 3'-leaving group on turnover of cephem antibiotics by a class C beta-lactamase. *Biochem J* **259**, 255-60.

46. Beadle, B. M., McGovern, S. L., Patera, A. & Shoichet, B. K. (1999). Functional analyses of AmpC beta-lactamase through differential stability. *Protein Sci* **8**, 1816-24.

47. Nukaga, M., Haruta, S., Tanimoto, K., Kogure, K., Taniguchi, K., Tamaki, M. & Sawai, T. (1995). Molecular evolution of a class C beta-lactamase extending its substrate specificity. *J Biol Chem* **270**, 5729-35.

48. Powers, R. A., Blazquez, J., Weston, G. S., Morosini, M. I., Baquero, F. & Shoichet, B. K. (1999). The complexed structure and antimicrobial activity of a non-beta-lactam inhibitor of AmpC beta-lactamase. *Protein Sci* **8**, 2330-7.

49. Patera, A., Blaszczak, L. C. & Shoichet, B. K. (2000). Crystal structures of substrate and inhibitor complexes with AmpC -lactamase: Possible implications for substrate-assisted catalysis. *J. Am. Chem. Soc.* **122**, 10504-10512.

50. Ghosn, J., Chaix, M. L. & Delaugerre, C. (2009). HIV-1 resistance to first- and second-generation non-nucleoside reverse transcriptase inhibitors. *AIDS Rev* **11**, 165-73.

51. Beadle, B. M., I. Trehan, Focia, P. & Shoichet, B. K. (2002). Structural Milestones in the Pathway of an Amide Hydrolase: substrate, acyl, and product complexes of cephalothin with AmpC b-lactamase. *Structure* **10**, 413-424.

52. Chen, Y., Minasov, G., Roth, T. A., Prati, F. & Shoichet, B. K. (2006). The deacylation mechanism of AmpC beta-lactamase at ultrahigh resolution. *J Am Chem Soc* **128**, 2970-6.

53. Schock, H. B., Garsky, V. M. & Kuo, L. C. (1996). Mutational anatomy of an HIV-1 protease variant conferring cross-resistance to protease inhibitors in clinical trials. Compensatory modulations of binding and activity. *J Biol Chem* **271**, 31957-63.

54. Ho, S. N., Hunt, H. D., Horton, R. M., Pullen, J. K. & Pease, L. R. (1989). Site-directed mutagenesis by overlap extension using the polymerase chain reaction. *Gene* **77**, 51-9.

55. Usher, K. C., Blaszczak, L. C., Weston, G. S., Shoichet, B. K. & Remington, S. J. (1998). Three-dimensional structure of AmpC beta-lactamase from Escherichia coli bound to a transition-state analogue: possible implications for the oxyanion hypothesis and for inhibitor design. *Biochemistry* **37**, 16082-92.

56. Leslie, A. G. W. (1992). Recent changes to the MOSFLM package for processing film and image plate data. *Joint CCP4 + ESF-EAMCB Newsletter on Protein Crystallography* **26**.

57. (1994). The CCP4 suite: programs for protein crystallography. *Acta Crystallogr D Biol Crystallogr* **50**, 760-3.

58. Emsley, P. & Cowtan, K. (2004). Coot: model-building tools for molecular graphics. *Acta Crystallogr D Biol Crystallogr* **60**, 2126-32.

59. Murshudov, G. N., Vagin, A. A. & Dodson, E. J. (1997). Refinement of macromolecular structures by the maximum-likelihood method. *Acta Crystallogr D Biol Crystallogr* **53**, 240-55.

60. Kirchoff, W. (1993). *EXAM: A two-state thermodynamic analysis program*, Gaithersburg, Maryland.

61. Becktel, W. J. & Schellman, J. A. (1987). Protein stability curves. *Biopolymers* **26**, 1859-77.

A

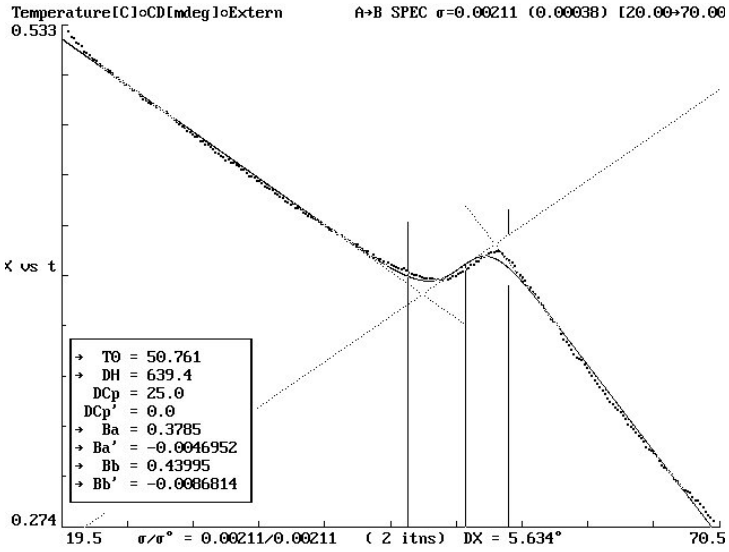

B

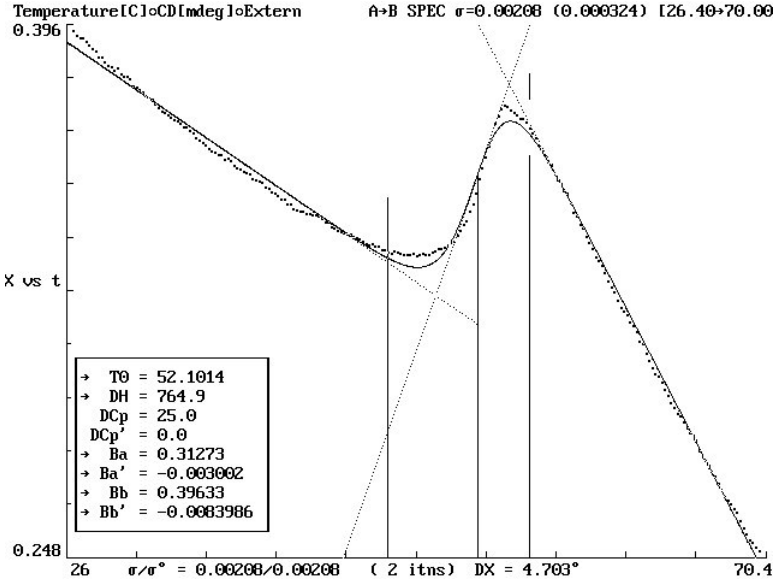

Supplementary Material Figure S1: Thermal denaturation of two representative AmpC extended-spectrum mutants, Y221G (Figure S1A) and the omega loop insertion (Figure S1B) monitored by fluorescence, as analyzed by EXAM.

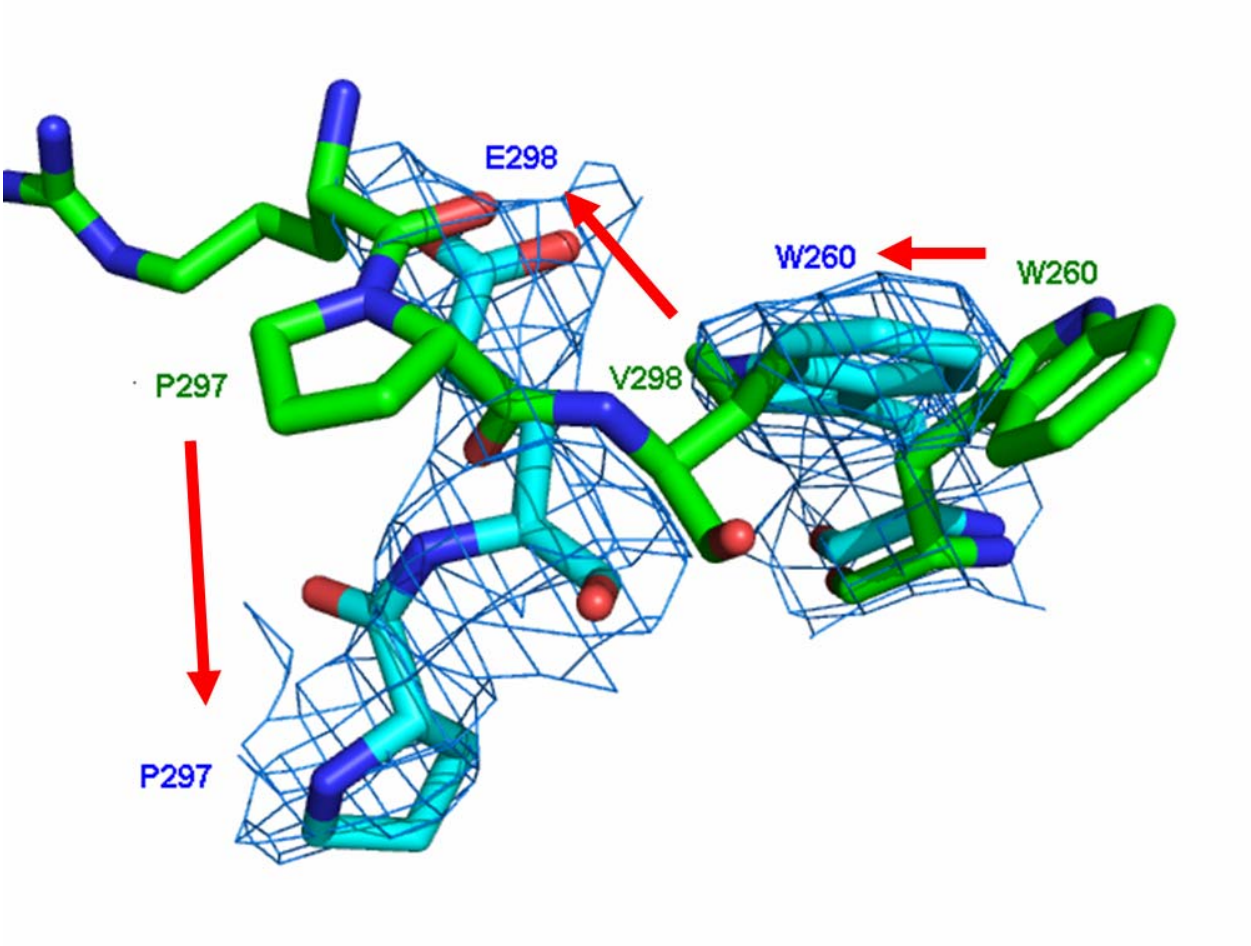

Supplementary Material Figure S2: Quality of density figure for the x-ray crystal structure of V298E to 2.6 Å resolution (cyan), overlaid with the wild-type AmpC structure (green). $2F_o$-F_c electron density for V298E shown at 1σ.

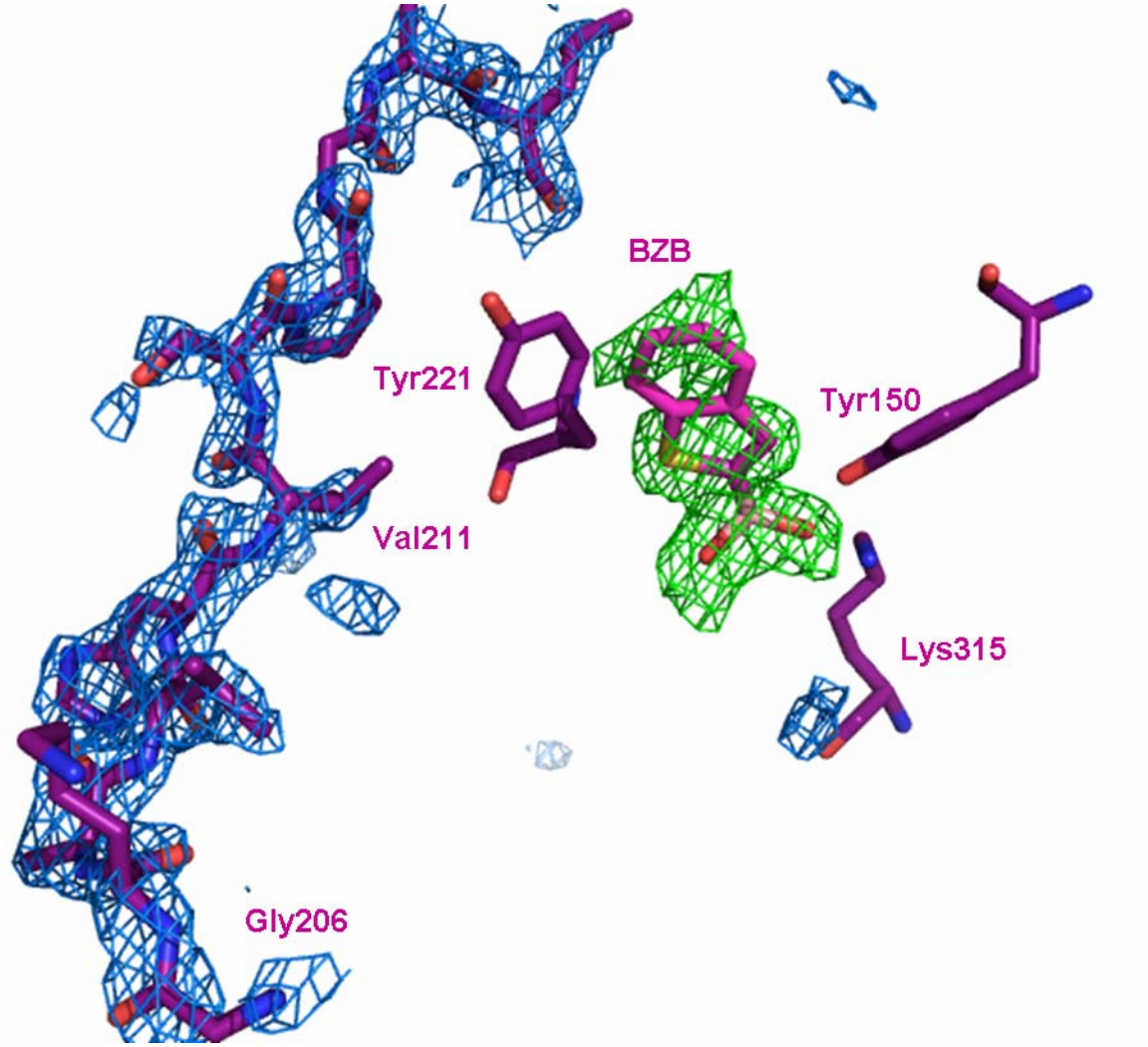

Supplementary Material Figure S3: Quality of density figure for the x-ray structure of T70I/BZB (purple) to 2.14 Å resolution. $2F_o$-F_c density (blue) at 1σ is shown for residues 206-216 (density is lost from residues 193-221 in the omega loop in the T70I apo structure. F_o-F_c omit density for BZB (green) shown at 2σ.

A

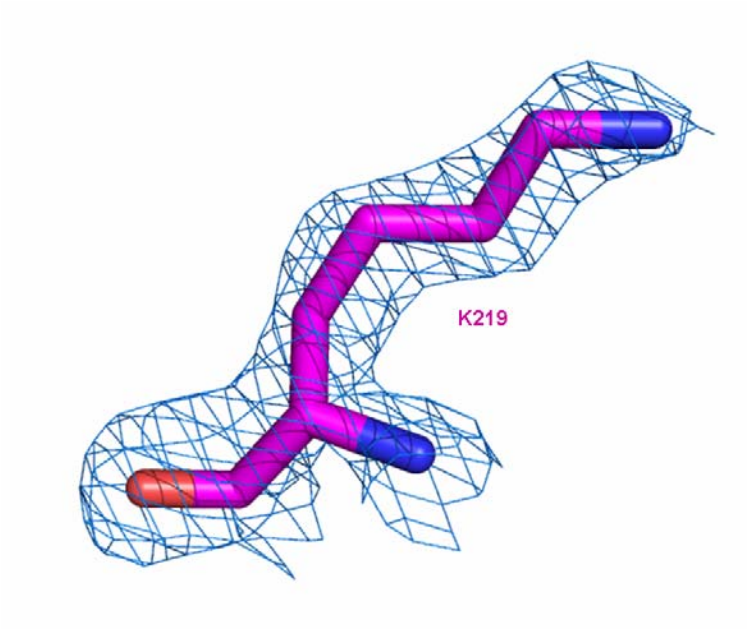

B

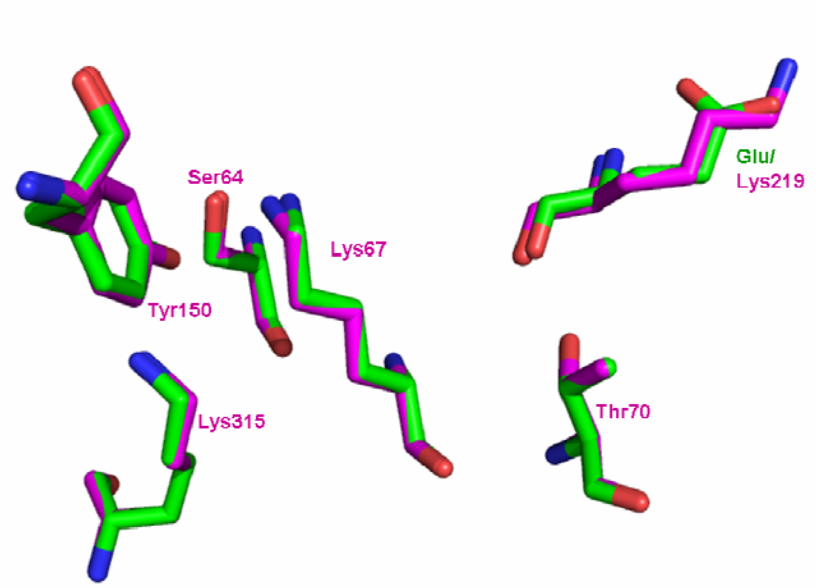

Supplementary Material Figure S4: The x-ray crystal structure of E219K to 1.84 Å resolution. (a) $2F_o$-F_c initial omit density 1σ from the initial rigid body refinement, using a model with residue 219 removed. Density for the lysine at position 219 is unambiguous. (b) The active site of E219K (magenta) overlaid with that of the wild-type AmpC structure (green).

Appendix to Chapter 2

The following appendix consists of data from two mutant AmpC β-lactamases made and purified – L293P and the six-residue deletion Δ289-294 – based on published work that these two mutations respectively conferred extended-spectrum activity to homologous class C β-lactamases. However, when the analogous mutations were made in AmpC β-lactamase, it was found that they do not confer extended-spectrum activity to AmpC – and thus we excluded them from further analysis and from this publication in Chapter 2. I present the data here for the record.

	WT rate (AU/sec)	L293P rate (AU/sec)	xWT rate
Cefepime			
100 μM	4.33×10^{-4}	7.16×10^{-4}	1.65x
10 μM	7.89×10^{-5}	4.33×10^{-4}	5.49x
Ceftazidime			
100 μM	1.04×10^{-3}	1.98×10^{-4}	0.19x
10 μM	2.40×10^{-4}	2.57×10^{-4}	1.07x
Cefotaxime			
100 μM	5.22×10^{-4}	2.22×10^{-4}	0.42
10 μM	2.42×10^{-4}	3.20×10^{-5}	0.13

Table 2.A.1 L293P kinetics against three extended-spectrum β-lactam antibiotics. This demonstrates that this mutant does not substantially confer extended-spectrum activity to AmpC β-lactamase. We do however note that higher relative levels of activity are seen at lower substrate concentrations. 0.84 μM enzyme was used in each assay. Due to the high amounts of protein that would be required to do a full Michaelis-Menten curve, due to its limited activity, this was not pursued.

	WT (AU/sec)	Δ289-294 (AU/sec)	xWT rate
100 μM substrate:			
Cefepime	8.43×10^{-4}	6.70×10^{-4}	0.79x
Ceftazidime	1.85×10^{-3}	3.16×10^{-4}	0.17x
Cefotaxime	1.26×10^{-3}	8.47×10^{-5}	0.07x

Table 2.A.2 Δ289-294 kinetics against three extended-spectrum β-lactam antibiotics. This demonstrates that this mutant does not substantially confer extended-spectrum activity to AmpC β-lactamase. ~2 μM enzyme was used in each assay. Due to the high amounts of protein that would be required to do a full Michaelis-Menten curve, due to its low activity, this was not pursued.

Mutation	**K_m (μM)**	**k_{cat} (s^{-1})**	**k_{cat}/K_m (M^{-1} s^{-1})**
WT	27	420	1.56×10^7
L293P	1.0	3.4	3.27×10^6
Fold change against cephalothin			4.8x decrease

Table 2.A.3 L293P kinetics against cephalothin. This demonstrates its loss of activity against its native substrate.

Mutation	Melting temp (T_m), (^oC)	ΔT_m (^oC)	ΔH (kcal/mol)	$\Delta\Delta G$ (kcal/mol)
L293P	49.9	-4.7	162.0	-2.63
Δ289-294	46.9	-7.7	215.6	-4.31

Table 2.A.4 Protein stability measurements for L293P and Δ289-294. This demonstrates their loss of stability relative to the wild-type AmpC b-lactamase.

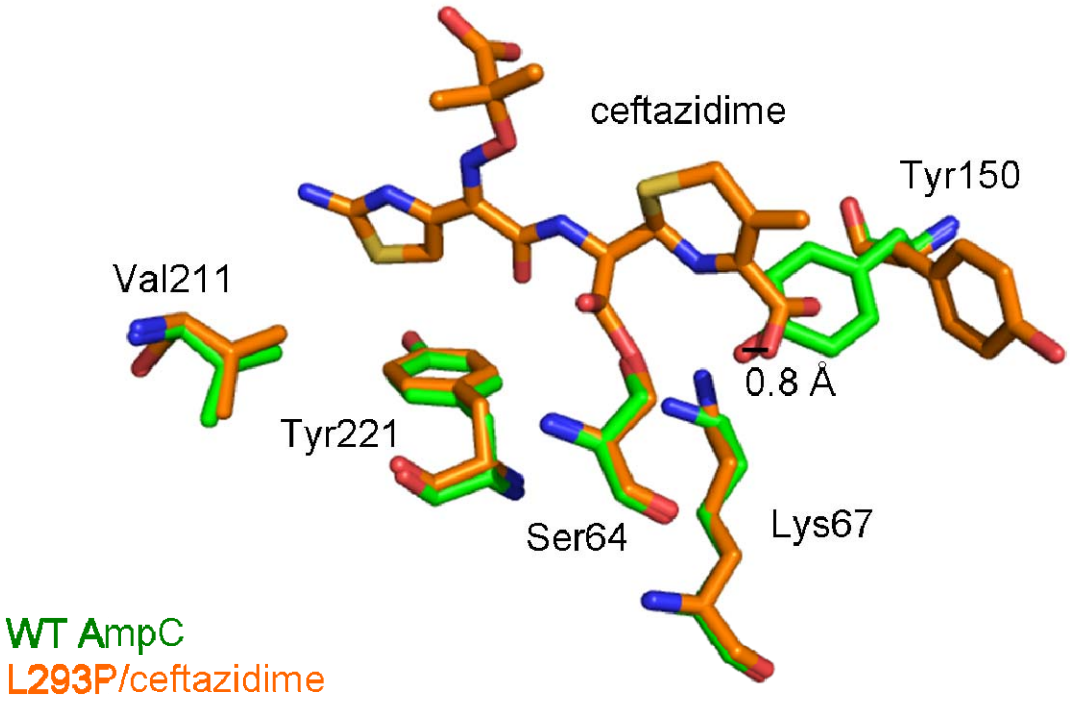

Figure 2.A.1 The 2.29 Å resolution crystal structure of L293P in complex with ceftazidime. This crystal structure shows a never-before observed movement of the active site Tyr150, implicated as the catalytic base for deacylation, out of the active site in the presence of ceftazidime. This movement of Tyr150 is not observed in the apo structure of L293P that I determined to 1.90 A resolution (data not shown). Intriguingly, the hydroxyl group of Tyr150 has essentially been replaced by the carboxylate of ceftazidime. However, since L293P does not appear to have increased activity against ceftazidime (Table 2.A.1), at least not at higher substrate concentrations, it is unclear whether this is an example of substrate-assisted catalysis, or merely capturing an inhibited state of the enzyme.

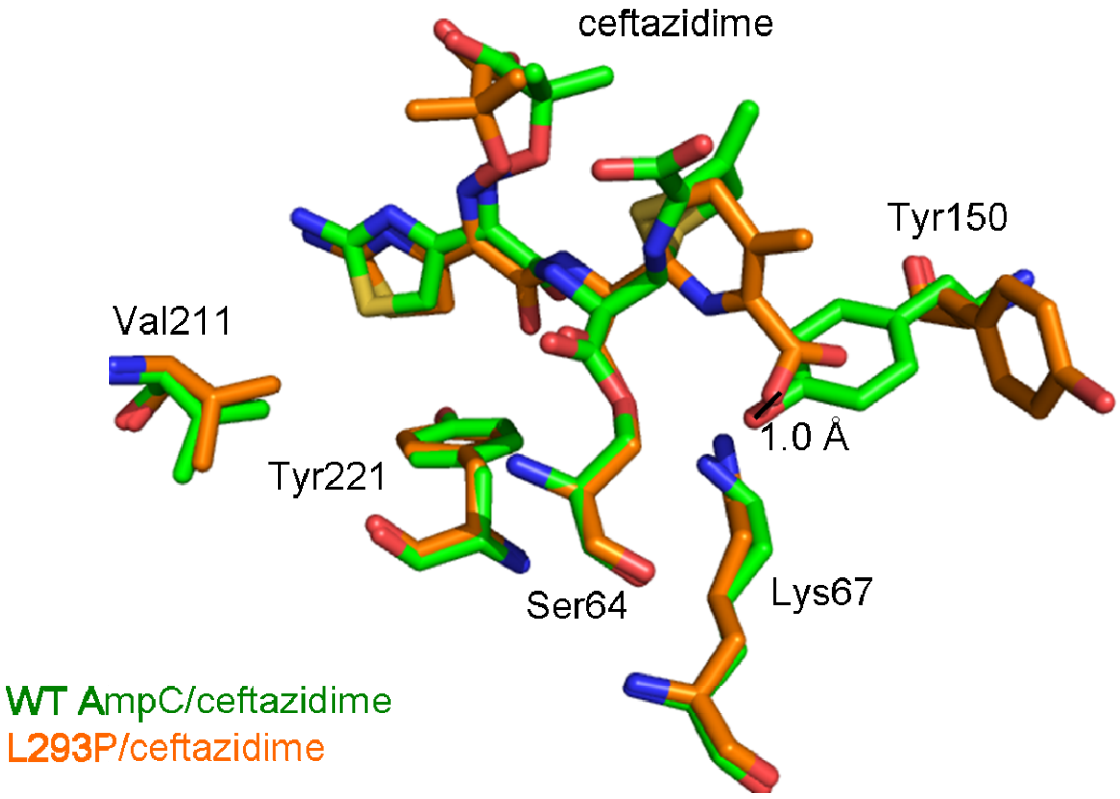

Figure 2.A.2 The 2.29 Å resolution crystal structure of L293P in complex with ceftazidime, overlaid with the WT AmpC/ceftazidime structure. In addition to the movement of the active site Tyr150 (discussed in Figure 2.A.1), this also demonstrates the difference in conformation of ceftazidime in the active site of wild-type AmpC vs. L293P.

Chapter 3:
Discussion, Implications, and Future Directions

3.1 Protein stability and evolvability

What factors contribute to protein evolvability? In particular, as enzymes fold to minimize their free energy, protein stability emerges as a natural potential constraint on enzyme evolvability, especially as proteins are inherently only marginally stable. Destabilized proteins have an increased concentration of unfolded protein relative to folded protein; if a protein is even transiently unfolded, it is more subject to aggregation, degradation by proteases, and etc *in vivo*. Thus even decreases in protein stability that convert to relatively small changes in the amount of protein unfolded by the strictly thermodynamic definition of K_u = [fraction unfolded]/[fraction folded] = $e^{(-dGu/RT)}$ translate to a far larger downstream effect in vivo once aggregation and degradation are taken into account; one example of this is seen in a stabilized class A extended-spectrum β-lactamase mutant, where β-lactamase variants that are isofunctional in vitro at room temperature, except that one is stabilized by 2.7 kcal/mol, show equal hydrolysis for β-lactam hydrolysis *in vivo* at 25 degrees C, but the more stabilized variant is much more effective at hydrolysis *in vivo* at 41º C [1].

Previous work on the "stability-function" hypothesis [2; 3] revealed that substitutions at key active site residues can trade preorganization enabling ligand recognition and catalysis, and thus catalytic activity, and regain stability lost by the presence of a preorganized active site. Thus it seemed logical biophysically that evolution of new enzyme functions, with a further increase in active site preorganization, may further destabilize proteins – and thus we turned to extended-spectrum mutants of AmpC β-lactamase to study this "function-stability" hypothesis, that enzymes with a further increase in function may correspondingly sacrifice some of their inherent stability. In contrast with previous work suggesting that there may be few tradeoffs for evolution of

new enzyme functions [4], this work suggests that thermodynamic stability may constrain enzyme evolution, in line with other work [1].

3.2 Allostery and the conformational ensemble

How mutations and modifications far from the active site function to modulate the catalytic activity of enzymes is also an area of considerable interest and research effort. The definition of allostery was extended in the 1990s to include nonligand modifications, such as protein mutations distant from the active site [5]. How, in general, do mutations function and transmit effects at large distances (20-30 Å) across a protein? We can imagine structural changes transmitting through subsequent interactions in adjacent residues, through a "domino effect". We can also envision a situation where adjacent residues are thermodynamically linked, and energy is transmitted across them in a "Newton's Cradle" effect, forming an allosteric network [6]. Lockless and Ranganathan have developed an elegant sequence-based approach to discover residue pairs statistically, and thus likely functionally or structurally, coupled through evolution by examining homologous protein families [7]. Ota and Agard used simulations of anisotropic thermal diffusion to confirm an intramolecular signaling pathway in PDZ-95 originally predicted by sequence covariation [6].

Proteins likely do not exist as a single, static structure, the traditional view – in the "new view" of proteins, originally proposed by Baldwin and Dill for protein folding (citation), and later extended by Tawfik to native state ensembles (Tawfik 2003), proteins likely exist as a conformational ensemble of states with similar free energy. Benkovic has proposed that allosteric effectors may function by shifting the distribution of this conformational ensemble [5]. It can also be hypothesized that mutations may shift the equilibrium of the ensemble towards alternative, pre-existing structures and functions, and thus may promote evolution of new enzyme functions [8]. Especially in the case of evolution of AmpC extended-spectrum mutants, where the wild-type enzyme inherently

has very low, but non-negligible activity against these third-generation cephalosporin antibiotics, it is tempting to speculate that these mutations may function by shifting the distribution of the conformational ensemble. This idea would be in line with previous work demonstrating that mutations can have substantial effects on increasing activity of promiscuous functions, with only minor effects on their native activity [4]. Indeed, this trend is mimicked in our own work, where extended-spectrum mutants of AmpC typically have gained activity against third-generation cephalosporins by 100- to 200-fold, and have decreased native activity by typically 5- to 15-fold, though as much as 400-fold. But is there any evidence that these mutations may function by altering the distribution of the conformational ensemble?

Three mechanisms can be considered through which distant mutations can affect catalytic properties: through a change in the ground state of the enzyme, through a change in enzyme flexibility, or a change in enzyme dynamics. Each scenario has a unique thermodynamic profile: changes in the enzyme apo structure, such as a larger active site, correspond to a shifted minimum in free energy of the folded protein. An increase in enzyme flexibility would correspond to an altered free energy difference between two conformations in the ensemble, whereas increased dynamics would correspond to a lowered energy barrier between two such conformations. Hybrids between these scenarios can also be imagined.

If we interpret the resulting AmpC extended-spectrum mutant enzyme crystallographic structures within this framework, we see examples of each of these three scenarios: change in ground state, increase in flexibility, and increase in dynamics. In the simplest case, the Y221G structure, substitution of Tyr221 by a glycine changes the ground state of the enzyme, providing more space in the active site, and alleviating a steric clash proposed to inhibit deacylation of third-generation cephalosporins from the active site of the wild-type enzyme. We see little change in the Y221G enzyme structure between the apo structure and the complex structure with cefotaxime, but see that the

third-generation cephalosporin can now adopt a conformation resembling good substrates, which would alleviate the steric clash thought to occur between the former lactam nitrogen of the third-generation cephalosporin and the presumed position of the deacylating water in the transition state.

The V298E crystallographic structure appears to indicate an increase in active site volume through both a hybrid change in the enzyme ground state and an increase in dynamics. We see a "domino effect" of structural changes stemming from the point of substitution, 21 Å away from the catalytic serine, with the net result of a larger active site volume. In addition, we cannot resolve the position of 12 residues in the 290s active site loop (in the wild-type structure, this occurs for six residues), but these residues likely adopt a different conformation than they do in the wild-type structure.

The omega loop insertion crystallographic apo structure suggests its mechanism of action functions through simply a change in the ground state structure, but preliminary evidence from the crystallographic structure upon soaking with cefotaxime suggests that the story may not be so simplistic, and that this mutant may actually function through an increase in enzyme flexibility. The omega loop insertion structure shows a well-resolved, larger conformation for the omega loop, and replacement of Val211 by the first, smaller alanine of the insertion may be sufficient to impart extended-spectrum activity. However, soaking the crystals with cefotaxime in an attempt to obtain a complex structure showed a marked increase in disorder of this loop region; this region was very-well ordered, with low B-factors, in both the wild-type apo and ceftazidime complex structures, and the apo omega loop insertion structure. It appears that the omega loop insertion protein may undergo a conformational change in this region upon binding and hydrolyzing cefotaxime, though these results are admittedly preliminary, and there is insufficient positive density in the active site to conclusively place the ligand.

This evidence is consistent with, though distinct from, evidence from a related enzyme in the literature: the GC1 extended-spectrum beta-lactamase, found in the clinic,

with a three-residue insertion in the omega loop at positions 211-213 relative to that of the wild-type P99 beta-lactamase from which it was derived (Pratt/Knox 2004). Our own "omega loop insertion" is the insertion of three alanine residues at the homologous location in AmpC, and AmpC and GC1 are 70% identical, and have 82% sequence homology (Powers/Shoichet citation). The apo structure of the GC1 enzyme globally resembled that of the P99 enzyme structure, with an RMSD of 0.6 A for the Cα; most significantly, the GC1 apo structure showed a localized disorder at residues 213-215, including one residue of the insertion [9], suggesting an increase in dynamics in the apo structure relative to that of the P99 enzyme. This effect of increased dynamics is not seen in the AmpC omega loop insertion apo structure, where unambiguous density is seen for all residues of the omega loop region in the apo structure (Figure 2.5).

Intriguingly, the GC1 structure showed a dramatic conformational change upon binding to a transition-state analog of the extended-spectrum substrate cefotaxime; the omega loop region refolds to a more open conformation, which significantly displaces Tyr224 (numbered Tyr221 in the P99 and AmpC structures), moving the Tyr224 hydroxyl group by 12 Å, and the Tyr224 Ca by 6 Å [10]. Since this tyrosine is thought to sterically prohibit third-generation cephalosporins from adopting a conformation competent for deacylation, its displacement likely explains the extended-spectrum activity of GC1. Interestingly, the crystal structure of P99 in complex with this cefotaxime transition-state analog shows the enzyme only adopts the "closed" conformation for the omega loop in this complex [10]. It appears the three-residue insertion in GC1 causes not only an increase in dynamics, in the apo structure, but also an increase in flexibility relative to the wild-type enzyme, allowing the omega loop to adopt a refolded, open conformation, providing room for the bulky third-generation cephalosporins to adopt a catalytically competent conformation. As the increase in omega loop disorder only seen upon soaking AmpC omega loop insertion crystals with cefotaxime qualitatively resembles the increase in flexibility in the GC1/cefotaxime

transition-state analog structure, it seems likely that this AmpC mutant may also function not solely due to a change in the apo structure, but also a shift in the conformational ensemble accessible to the enzyme upon substrate-binding.

The T70I crystallographic structures – both the apo and transition-state analog-bound structure, derived from two monomers in the same crystal – also provide a unique demonstration of how enzymes may exist not as a static conformation, but rather, as a conformational ensemble of multiple structures of similar free energies, and how mutations may affect the distribution of this ensemble. The T70I apo structure has two notable conformational changes relative to that of the wild-type enzyme structure: density is missing for residues 193-221 in the active site "omega loop", and the beta turn in the active site, comprised of residues 318-322, has flipped into the active site, occupying the space where ligands would normally bind. The latter conformational change destroys the oxyanion hole, formed by the backbone nitrogens of the catalytic Ser64, and Ala318; as we know this mutant protein is still very catalytically active, the state enriched by crystallography cannot be the only conformation accessible to the protein -- other, catalytically active states must be present in the population at high frequency. However, the disorder of 24 residues in the omega loop forming one wall of the binding site, including one of the residues thought to sterically hinder deacylation, provides a clue as to how this mutation may cause an increase in catalytic activity against bulky third-generation cephalosporins; an increase in flexibility/dynamics of this loop region would enlarge the enzyme active site, allowing large substrates to adopt a conformation able to deacylate. In the presence of benzo(b)thiophene 2-boronic acid (BZB), this loop region re-orders and can be resolved. We do note little increase in active site volume was seen in the complex structure with BZB; however, it is possible that binding of a third-generation cephalosporin, like cefotaxime, would shift the conformational ensemble present in the absence of ligand, and that the increased flexibility/dynamics of this loop would be able to adopt larger conformations in the presence of a ligand larger than benzo(b)thiophene.

The structures presented here demonstrate a variety of ways that distant substitutions can cause evolution of a new catalytic function, and underscore the challenges faced by protein engineering and rational design.

3.3 Exploiting constraints to minimize drug resistance

If indeed native activity and protein stability constrain enzyme evolution, can we play into these constraints to minimize evolution of drug resistance? Is there a point where there are so many constraints that there are effectively no mutants in the neighborhood of the wild-type sequence to which the enzyme can evolve? Intelligent inhibitor design – playing into the maintenance of both native catalytic function and protein stability as constraints on enzyme evolution – may potentially minimize emergence of drug resistance.

Research on inhibitor resistance in HIV protease suggests that this may be possible [11; 12; 13]. By overlaying positions of substrates for HIV protease from crystal structures and determining the boundaries within which the substrates lay, a "substrate envelope" was delineated. Similarly, an "inhibitor envelope" was determined by superposing the crystallographic positions of inhibitors bound to the enzyme. By overlaying the substrate envelope with the inhibitor envelope, Schiffer and colleagues determined that active site substitutions in HIV protease that confer inhibitor resistance predominately occur in residues in regions where the inhibitor envelope protrudes from the substrate envelope [13]. By mutating those residues important for drug binding, but likely less vital for substrate function, the enzyme can presumably evolve inhibitor resistance with a decreased cost to catalytic activity. Designing inhibitors within the confines of the substrate envelope successfully led to inhibitors of HIV protease, some with subnanomolar affinity [11; 12]. This speaks to the need to maintain native catalytic function as a constraint on enzyme evolution, and to the hope that by playing into these constraints – in this case, by designing inhibitors that bind within the confines of the

native substrate envelope – we may potentially be able to minimize emergence of drug resistance, as subsequent evolution of drug resistance would also likely substantially impact native catalytic activity. It would be ideal to design new drugs in such a way where it would be difficult to evolve resistance against them without overwhelming the enzyme with structural demands on its stability and native function.

We can also imagine that by increasing the number and diversity of inhibitor chemical functional groups against which enzymes are being selected, we could place too many structural and stability demands on the enzyme and raise its mutational burden to a point where evolution of drug resistance dramatically decreases**.** A practical implication of these studies is that it may be possible to design courses of therapy that involve enough constraints to make resistance, at least at the enzyme level, more difficult to develop.

3.4 *In vivo* evidence for the stability-function hypothesis

In accordance with the function-stability hypothesis and how stability and function may constrain enzyme evolution, naturally occurring "restabilizing" and "recatalyzing" substitutions have been found *in vivo*, in conjunction with mutations conferring drug resistance, in order to compensate for activity and stability losses occurring as a side effect of the primary drug-resistant mutations [1; 14; 15; 16]. In TEM beta-lactamase, extended-spectrum mutants with increased activity against third-generation cephalosporins are found to have decreased thermodynamic stability [1]. In several extended-spectrum clinical isolates of TEM, a secondary substitution (Met182Thr) is found quite distant from the active site, 15 Å away; this substitution has little effect on catalytic activity, but restabilizes the antibiotic resistant mutant enzymes by 2.7 kcal/mol and compensates for the loss of stability caused by the increase in extended-spectrum activity [1; 14; 15]. In HIV protease, two prominent mutations (M46I/L63P) distant from the active site are found clinically in patients treated with protease inhibitors; it was found that these two mutations do not affect binding, but instead confer catalytic activity

exceeding that of the wild-type enzyme by 110-360%, compensating for catalytic activity lost through primary inhibitor-resistant substitutions [16]. In addition, recent work demonstrated that chaperonin overexpression *in vivo* doubled the number of mutations accumulated during *in vitro* evolution of four enzymes, presumably by buffering and alleviating the decreased stability of the mutant enzymes evolved [17]. Could an enzyme successfully evolve to trade more stability for a dramatic increase in a new catalytic function essential for its survival? Where are the limits on how much stability an enzyme can sacrifice, and how does it depend on the amount and essentiality of new function gained, and native function lost? These areas remain to be investigated.

3.5 Conclusion

In summary, our work characterizes the biophysical constraints on enzyme evolution. We can imagine the ultimate fitness conferred to an organism by an enzyme as a convolution of both its catalytic activity for its native function and for new functions against new chemical challenges presented, and the level of soluble, active enzyme in the cell. Thus it seems logical that the three biophysical properties investigated here – new catalytic activity, native activity, and thermodynamic stability, and the resulting interplay between them – may together constrain enzyme evolution.

3.6 References

1. Wang, X., Minasov, G. & Shoichet, B. K. (2002). Evolution of an Antibiotic Resistance Enzyme Constrained by Stability and Activity Trade-Offs. *J. Mol. Biol.* **320**, 85-95.
2. Beadle, B. M. & Shoichet., B. K. (2002). Structural bases of stability-function trade-offs in enzymes. *J. Mol. Biol.* **321**, 285-296.
3. Shoichet, B. K., Baase, W. A., Kuroki, R. & Matthews, B. W. (1995). A Relationship Between Protein Stability and Protein Function. *Proc. Nat. Acad. Sci USA.* **92**, 452-456.
4. Aharoni, A., Gaidukov, L., Khersonsky, O., Mc, Q. G. S., Roodveldt, C. & Tawfik, D. S. (2005). The 'evolvability' of promiscuous protein functions. *Nat Genet* **37**, 73-6.
5. Goodey, N. M. & Benkovic, S. J. (2008). Allosteric regulation and catalysis emerge via a common route. *Nat Chem Biol* **4**, 474-82.
6. Ota, N. & Agard, D. A. (2005). Intramolecular signaling pathways revealed by modeling anisotropic thermal diffusion. *J Mol Biol* **351**, 345-54.
7. Lockless, S. W. & Ranganathan, R. (1999). Evolutionarily conserved pathways of energetic connectivity in protein families. *Science* **286**, 295-9.
8. Tokuriki, N. & Tawfik, D. S. (2009). Protein dynamism and evolvability. *Science* **324**, 203-7.
9. Crichlow, G. V., Kuzin, A. P., Nukaga, M., Mayama, K., Sawai, T. & Knox, J. R. (1999). Structure of the extended-spectrum class C beta-lactamase of Enterobacter cloacae GC1, a natural mutant with a tandem tripeptide insertion. *Biochemistry* **38**, 10256-61.
10. Nukaga, M., Kumar, S., Nukaga, K., Pratt, R. F. & Knox, J. R. (2004). Hydrolysis of third-generation cephalosporins by class C beta-lactamases. Structures of a transition state analog of cefotoxamine in wild-type and extended spectrum enzymes. *J Biol Chem* **279**, 9344-52.
11. Altman, M. D., Ali, A., Reddy, G. S., Nalam, M. N., Anjum, S. G., Cao, H., Chellappan, S., Kairys, V., Fernandes, M. X., Gilson, M. K., Schiffer, C. A., Rana, T. M. & Tidor, B. (2008). HIV-1 protease inhibitors from inverse design in the substrate envelope exhibit subnanomolar binding to drug-resistant variants. *J Am Chem Soc* **130**, 6099-113.
12. Chellappan, S., Kiran Kumar Reddy, G. S., Ali, A., Nalam, M. N., Anjum, S. G., Cao, H., Kairys, V., Fernandes, M. X., Altman, M. D., Tidor, B., Rana, T. M., Schiffer, C. A. & Gilson, M. K. (2007). Design of mutation-resistant HIV protease inhibitors with the substrate envelope hypothesis. *Chem Biol Drug Des* **69**, 298-313.
13. King, N. M., Prabu-Jeyabalan, M., Nalivaika, E. A. & Schiffer, C. A. (2004). Combating susceptibility to drug resistance: lessons from HIV-1 protease. *Chem Biol* **11**, 1333-8.

14. Huang, W. & Palzkill, T. (1997). A natural polymorphism in beta-lactamase is a global suppressor. *Proc Natl Acad Sci U S A* **94**, 8801-6.
15. Sideraki, V., Huang, W., Palzkill, T. & Gilbert, H. F. (2001). A secondary drug resistance mutation of TEM-1 beta-lactamase that suppresses misfolding and aggregation. *Proc Natl Acad Sci U S A* **98**, 283-8.
16. Schock, H. B., Garsky, V. M. & Kuo, L. C. (1996). Mutational anatomy of an HIV-1 protease variant conferring cross-resistance to protease inhibitors in clinical trials. Compensatory modulations of binding and activity. *J Biol Chem* **271**, 31957-63.
17. Tokuriki, N. & Tawfik, D. S. (2009). Chaperonin overexpression promotes genetic variation and enzyme evolution. *Nature* **459**, 668-73.

Gloss to Appendix A

In 2006, Timothy Palzkill's laboratory at the Baylor College of Medicine approached our lab about a possible collaboration, where our lab would do some crystallography and protein stability measurements in a project investigating a possible "global suppressor" in TEM-1 β-lactamase. The initial goal of their project was to investigate the R244 position in TEM-1, where it was known that a positive charge was important to bind both β-lactam substrates and inhibitors. Due to this, inhibitor-resistant substitutions found in the clinic, such as R244S, replaced this positive charge to avoid inhibition – but at cost to the enzymatic activity against its native substrates, resulting in a loss of resistance against substrates such as ampicillin. To investigate the plasticity of this positive charge, the Palzkill lab designed a screen to look for mutations at secondary sites in the protein that could perhaps compensate for the loss of positive charge in a designed mutant, R244A, and thus restore resistance against ampicillin. To their surprise, they isolated a mutation, L201P, that increased steady-state expression levels of the R244A mutant, increasing its resistance against ampicillin. They went on to investigate the ability of the L201P substitution to compensate for other mutations with decreased function – such as the L76N mutant, which disrupts the hydrophobic core of the protein. Though this mutant only has a small effect on in vitro catalytic efficiency, it is expressed poorly *in vivo* due to protease degradation (when expressed in a protease-deficient cell line, its expression level is similar to wild-type), and thus confers decreased resistance to ampicillin *in vivo*. The L76N mutant is therefore used as a sensitive test to investigate the ability of suppressor mutations to compensate for its decreased expression – and was the original system used to investigate the first TEM-1 "global suppressor" investigated by the Palzkill lab – M182T, a secondary mutation found in the clinic which compensates for the deleterious effects of primary substitutions conferring antibiotic resistance, which was then shown to restabilize the wild-type enzyme by 2.67 kcal/mol, restabilizing the

enzyme after the primary destabilizing substitutions conferring resistance to antibiotics. Indeed, the Palzkill lab found that the L201P mutation could compensate for the decreased expression levels of the L76N mutant, as well as other mutations.

The Palzkill Lab approached our lab to see if we would be willing to collaborate and to determine both the protein stability of the L201P protein, to see if it functioned by increasing the stability of the protein, and thus compensating for decreased expression levels of the R244A mutant and other mutants. In addition, they wanted us to determine the stability of several other related mutants – the R244A, L201P/R244A, M182T/R244A, and M182T/L201P. They also asked us if we could attempt the crystallography of the L201P mutant, in order to understand structurally how this mutation may act to suppress deleterious effects of other mutations.

Yu Chen, a postdoc in our lab, successfully crystallized L201P, and Brian Shoichet actually performed the protein stability measurements himself for L201P – and showed that this mutation actually did stabilize the protein relative to wild-type, by 0.8 kcal/mol by the method of Becktel and Schellman, at least at its melting temperature (53.4º C). However, we noted that the van't Hoff enthalpy of denaturation was actually ~30 kcal/mol lower for L201P than for the wild-type – so we were careful to note the caveat that we were hesitant to extrapolate these changes in stability back to lower temperatures, such as 37º C, the temperature where the *in vivo* experiments had been performed.

I volunteered to perform the stability measurements on the rest of the mutant proteins the lab was investigating. Since R244A had decreased steady-state expression levels relative to the wild-type enzyme, and since L201P restored expression levels back to that of wild-type, and since L201P appeared more stable than wild-type, at least in the region of its melting temperature – I and perhaps others expected to see that R244A was destabilized to wild-type, and that L201P would restore the stability to wild-type levels. Much to my surprise, however, R244A actually had a *higher* melting temperature

(54.0º C) than the wild-type enzyme (51.5º C). However, R244A had a significantly decreased van't Hoff enthalpy of denaturation (78.1 kcal/mol) relative to the wild-type enzyme (139.5 kcal/mol) – again leading us to caution against extrapolating changes in stability (stabilized by 1.08 kcal/mol by the Becktel and Schellman method at the melting temperature) back to 37º C, and noting that the relative stabilities may even be reversed at lower temperatures. Both L201P and M182T did have stabilizing effects on the R244A mutant, at least in the region of their melting temperature.

Brian suggested I investigate methods to depress the melting temperature of these mutant enzymes – such as performing thermal denaturation in the presence of various concentrations of chemical denaturants, such as guanidine hydrochloride (GdnHCl) -- to get a better idea of their relative stabilities in the vicinity of 37º C. Unfortunately, the resulting data was confusing and hard to interpret, as the thermal melts no longer looked two-state – and we found that it was known that TEM-1 does not denature in a two-state fashion with GdnHCl. Therefore we stuck to the initial thermal denaturation data for the paper.

What I liked about this project was its integration of *in vitro* thermodynamics and protein effects *in vivo*. The Palzkill Lab did a great deal of *in vivo* work with these mutant enzymes, including determination of the minimum inhibitory concentration for ampicillin against *E. coli* strains harboring these mutant enzymes, competition assays, and survival curves. This project was also an excellent training project for me, as it forced me to carefully consider protein stability curves and equations, and how changes in the van't Hoff enthalpy of denaturation can affect our interpretation of changes in stability as we attempt to extrapolate farther away from the melting temperature, and also led me to consider other methods for obtaining relative stability data at lower temperatures. In addition, it has had a long-standing impact on the way that I view protein stability, and the integration between *in vitro* and *in vivo* protein stability measurements.

This appendix originally appeared in the *Journal of Molecular Biology* in 2008.

Appendix A:

Genetic and structural characterization of an L201P global suppressor substitution in TEM-1 β-lactamase

David C. Marciano[1], Jeanine M. Pennington[2], Xiaohu Wang[2], Jian Wang[3], Yu Chen[4], Veena L. Thomas[4], Brian K. Shoichet[4] and Timothy Palzkill[1,2,3].

[1]Department of Molecular Virology and Microbiology, [2]Department of Pharmacology, [3]Program in Structural and Computational Biology and Molecular Biophysics, BCM, Houston, Texas 77030. [4]Department of Pharmaceutical Chemistry, UCSF, San Francisco, CA 94158-2330.

A.1 Abstract

The TEM-1 β-lactamase confers bacterial resistance to penicillin antibiotics and has acquired mutations that permit the enzyme to hydrolyze extended spectrum cephalosporins or avoid inactivation by β-lactamase inhibitors. However, many of these substitutions have been shown to reduce activity against penicillin antibiotics and/or result in a loss of stability for the enzyme. In order to gain more information concerning the trade-offs associated with active site substitutions, a genetic selection was used to find second site mutations which partially restore ampicillin resistance levels conferred by an R244A active site TEM-1 β-lactamase mutant. An L201P substitution distant from the active site was identified that enhanced ampicillin resistance levels and increased protein expression levels of the R244A TEM-1 mutant. The L201P substitution also increases the ampicillin resistance levels and restores expression levels of a poorly expressed TEM-1 mutant with a core-disrupting substitution. *In vitro* thermal denaturation of purified protein indicated that the L201P mutation increases the T_m of the TEM-1 enzyme. The X-ray structure of the L201P TEM-1 mutant was determined to gain insight into the increase in enzyme stability. The proline substitution occurs at the N-terminus of an α-helix and may stabilize the enzyme by reducing the helix dipole as well as lowering the conformational entropy cost of folding due to the reduced number of conformations available in the unfolded state. Collectively the data suggest that L201P promotes tolerance of some deleterious TEM-1 mutations by enhancing protein stability of these mutants.

A.2 Introduction

The most prevalent plasmid encoded β-lactamase in Gram-negative bacteria, TEM-1, provides resistance to penicillins and early generation cephalosporins [1]. The TEM-1 β-lactamase has evolved in response to the introduction of the extended spectrum β-lactams and β-lactamase inhibitors by acquiring substitutions which modify the substrate profile of the enzyme to match the new selection environment. Many of these active site substitutions alter the substrate profile of the TEM-1 enzyme at the cost of reduced hydrolysis of penicillin β-lactams such as ampicillin, amoxicillin and benzylpenicillin [2; 3; 4; 5; 6; 7; 8; 9].

In addition to sacrificing high-levels of catalytic efficiency against penicillin β-lactams, substitutions near the active site of TEM-1 frequently result in a loss of stability of the enzyme [10]. For example, a G238S substitution confers extended-spectrum β-lactamase (ESBL) activity but reduces the protein's melting temperature (ΔT_m = -4.5 relative to wild-type TEM-1) translating to a 1.94 kcal/mol loss of stability [10]. Likewise, the R164S ESBL mutation results in a reduced melting temperature (ΔT_m = -1.7) and corresponding loss of stability ($\Delta\Delta G_m$ = -0.73 kcal/mol) [10]. The stability of M69 mutants conferring inhibitor resistance is dependent upon the substituting residue. The M69I substitution results in a loss of stability ($\Delta\Delta G_m$ = -1.3), while the M69L TEM-1 mutant is actually more thermodynamically stable than wild type TEM-1 ($\Delta\Delta G_m$ = +1.0) [10].

One substitution distant from the active site, M182T, has arisen among antibiotic resistant isolates repeatedly in the context of active site substitutions that reduce stability

(http://www.lahey.org/studies). A genetic selection for suppressors of a destabilized TEM-1 β-lactamase led to the identification of the M182T mutation as a general suppressor of folding and/or stability defects [11; 12]. The M182T substitution has since been repeatedly identified in clones isolated from directed evolution experiments of TEM-1, which is consistent with its importance in correcting enzyme stability defects associated with other substitutions [13; 14; 15; 16; 17; 18; 19]. In restoring stability to TEM-1 variants, the M182T substitution mitigates stability trade-offs associated with amino acid substitutions that provide for extended spectrum cephalosporin hydrolysis and inhibitor resistance [10].

Several TEM-1 variants with substitutions at position 244 have been found in clinical isolates resistant to certain β-lactam/inhibitor combinations [6; 7; 21; 22; 23; 24; 25; 26]. The arginine at position 244, however, also plays an important role in substrate binding and catalysis. The X-ray structure of TEM-1 β-lactamase with an acylated penicillin in the active site indicates that the positive charge of this arginine residue interacts, via a bridging water molecule, with the C3 carboxylate group that is common to all classes of β-lactam antibiotics [20]. Moreover, substitutions at position 244 increase the K_m for hydrolysis of penicillin and, to a lesser extent, cephalosporin antibiotics [7; 9]. Yet, substitutions that remove the positive charge from position 244 reduce inactivation by inhibitors as a result of the missing interaction with the C3 carboxylate group [6; 7; 21; 22; 23; 24; 25; 26]. Thus, the normally high level of catalytic efficiency towards penem substrates is sacrificed in these mutants in exchange for inhibitor resistance, due to the increase in K_m for hydrolysis of β-lactam antibiotics associated with these substitutions.

TEM-1 β-lactamase is a member of a gene family called class A β-lactamases based on primary amino acid sequence homology [27; 28]. The class A β-lactamases include a large number of enzymes from both Gram-positive and Gram-negative bacteria [29]. Several class A β-lactamases do not encode an arginine at position 244 but rather provide the positive charge that interacts with the C3 carboxylate from another position near the active site [30]. For example, the SME-1 and *S. albus* G β-lactamases provide positive charge from R220 while the Toho-1 β-lactamase has an arginine at position 276. The structures of these enzymes indicate that the guanidinium group from the arginine occupies a similar position in the active site whether it is provided by R220, R244 or R276 [31; 32; 33; 34]. Therefore, it appears there is structural and evolutionary plasticity in the placement of the arginine that provides the positive charge for substrate binding. To further investigate the loss of catalytic activity associated with substitutions at position 244 and the plasticity with regard to the positive charge, an R244A mutant of TEM-1 β-lactamase was generated. A selection for mutations that increased the ampicillin resistance of *E. coli* containing the active site mutant R244A was designed to identify second site mutations that restore the positive charge, and thereby the catalytic efficiency, of the enzyme for ampicillin hydrolysis. The selection, however, resulted in the isolation of an L201P substitution that improves fitness by increasing stability and steady-state protein levels of the R244A enzyme. Suppressor function was compared between the L201P substitution and the established, stabilizing, M182T substitution by combining each with other primary substitutions having decreased function. Both L201P and M182T compensate for several but not all primary substitutions and exhibit an overlapping but not identical pattern of suppression. Therefore, these suppressors are

"global" in that they act on many different primary substitutions, but they may not act universally to compensate for all defects associated with primary substitutions.

A.3 Results and Discussion

I. Genetic selection of a second site suppressor of the TEM-1 R244A mutant

In TEM-1 β-lactamase, the side chain of arginine at position 244 is directed towards the active site pocket were it interacts with the C3 carboxylate group of a β-lactam substrate via a water molecule [9; 10; 20]. In order to initiate study of this position, the arginine side chain was replaced with alanine *via* site-directed mutagenesis in the pET-TEM-1 expression vector [356]. The pET-TEM-1 vector expresses large quantities of soluble TEM-1 β-lactamase via transcription from a T7 promoter and encodes an ompA leader fused to the mature portion of the TEM-1 enzyme [35]. This $bla_{\text{TEM-1}}$ gene has subsequently been shown to contain a E28G substitution in mature TEM-1 near the signal cleavage site [35; 36]. The mature ompA-TEM-1 E28G β-lactamase is properly processed as determined by N-terminal protein sequencing and does not exhibit measurable changes in catalytic properties relative to wild type TEM-1 with its native signal sequence [36]. The R244A substitution results in a 4-8 fold loss of ampicillin resistance relative to TEM-1 E28G β-lactamase as determined by the minimum inhibitory concentration of this β-lactam antibiotic. The R244C mutant of TEM-1 has been shown to have a similar effect on amoxicillin resistance levels [21]. The loss of activity seen with these arginine 244 substitutions could be the result of displacement of an active site water molecule that

normally interacts with the β-lactam carboxylate, as suggested by the crystal structure of the R244S mutant of TEM-1 [10].

To study the plasticity of the positive charge in this region of the active site, a search was made for mutations which partially restore ampicillin resistance to the R244A mutant. This was accomplished by constructing a random library of point mutations of the TEM-1 E28G:R244A gene encoded in the pET-TEM-1 vector by error-prone PCR. From the E28G:R244A library, a suppressor distant from the active site was isolated with a single nucleotide substitution resulting in a L201P mutation. Interestingly, the L201P substitution has been observed previously upon selection for inhibitor-resistant TEM-1 β-lactamases from an error-prone library of TEM-1 enzymes [37]. In addition, the L201P substitution was recently identified as a suppressor among populations of highly mutagenized TEM-1 mutants propagated under conditions of neutral drift [38].

In order to ensure separation of function from potential mutations found elsewhere in the pET-TEM-1 plasmid or from the E28G substitution, the L201P:R244A double and R244A single mutants were reconstructed in the original pET-TEM-1 plasmid and the E28G substitution was reverted to wild type by site-directed mutagenesis. The E28G:R244A and R244A mutants in pET-TEM-1 exhibited the same ampicillin minimum inhibitory concentration (MIC = 512 μg/ml). In addition, the pBG66 plasmid that encodes wild type TEM-1 β-lactamase was used to create both the R244A and L201P:R244A TEM-1 mutants by site-directed mutagenesis. Unlike the T7 promoter driven expression of $bla_{\text{TEM-1}}$ from the pET-TEM-1 expression vector, $bla_{\text{TEM-1}}$ is constitutively transcribed by its native promoter in the pBG66 plasmid [39]. The reconstructed pET-TEM-1 L201P:R244A in *E. coli* BL21(DE3) exhibits similar

ampicillin resistance (MIC = 512 μg/ml) relative to the R244A mutant as determined by 2-fold antibiotic dilutions. However, a difference in resistance levels was apparent when additional ampicillin concentrations were examined near the minimum inhibitory concentration (MIC) value where R244A exhibited an MIC of 358 μg/ml while the L201P:R44A had an MIC of 512 μg/ml. Similarly, the ampicillin MIC for pBG66-R244A and pBG66-L201P:R244A was 256 μg/ml as determined by 2-fold ampicillin dilutions (Table A.1). MIC determinations using commercially available E-test strips containing amoxicillin and a β-lactamase inhibitor, however, indicated that the pBG66-L201P:R244A mutant exhibits an increased level of resistance relative to the pBG66 encoded R244A mutant (Table A.1).

In order to further examine the fitness advantage conferred upon R244A by the L201P substitution, competition experiments were performed between *E. coli* strains containing the pBG66 plasmid with either the R244A or L201P:R244A β-lactamase genes. These experiments made use of otherwise isogenic Ara^+ and Ara^- *E. coli* B strains that, when grown on tetrazolium agar (TA) plates yield pink and red colonies, respectively [40]. The R244A and L201P-R244A encoding plasmids were introduced into the Ara^+ and Ara^- strains and a culture of each was grown to saturation in the absence of ampicillin. Equal volumes of the cultures were then diluted into fresh media containing increasing concentrations of ampicillin and grown to saturation. The cultures were then spread on TA plates and the number of pink and red colonies was determined. The results in Figure A.1 clearly indicate that the L201P:R244A mutant out competes the R244A mutant as ampicillin concentrations are increased indicating the L201P substitution provides a fitness advantage.

Table A.1. Influence of L201P substitution on TEM-1 β-lactamase mediated MIC levels.

	Amp[a]	Amox+CV[b]
TEM-1	2048	24
L76N	32	6
M182T	2048	24
L201P	2048	24
R244A	256	32
M182T:L201P	2048	16
L201P:R244A	256	64
L76N:M182T	512	16
L76N:L201P	64	12
L76N:M182T:L201P	1024	16

[a] μg/ml ampicillin using broth dilution, pBG66 plasmid
[b] μg/ml amoxicillin with clavulanic acid in 2:1 ratio using E-test strip, pBG66 plasmid

As a further test of the relative fitness of the R244A versus the L201P:R244A mutant, bacterial cultures harboring each mutant on the pBG66 plasmid were spread on agar plates containing increasing concentrations of ampicillin and the number of colonies under each condition were counted to generate a survival curve for each mutant (Fig. 2A). Data from the survival curve experiments were also used to assign ampicillin IC_{90} values to each TEM-1 mutant, defined here as the concentration of ampicillin required to reduce viability (colony forming units) of TEM-1 expressing bacteria by ≥90% (Table A.2). The results indicate the L201P:R244A mutant exhibits enhanced survival relative

Figure A.1

A.

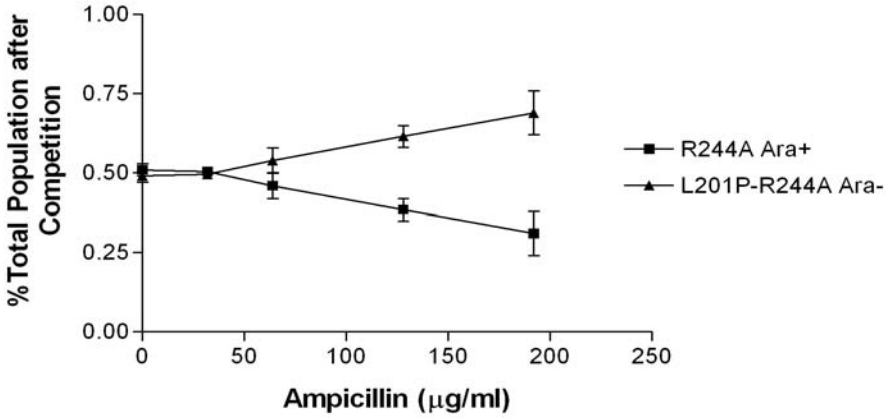

B.

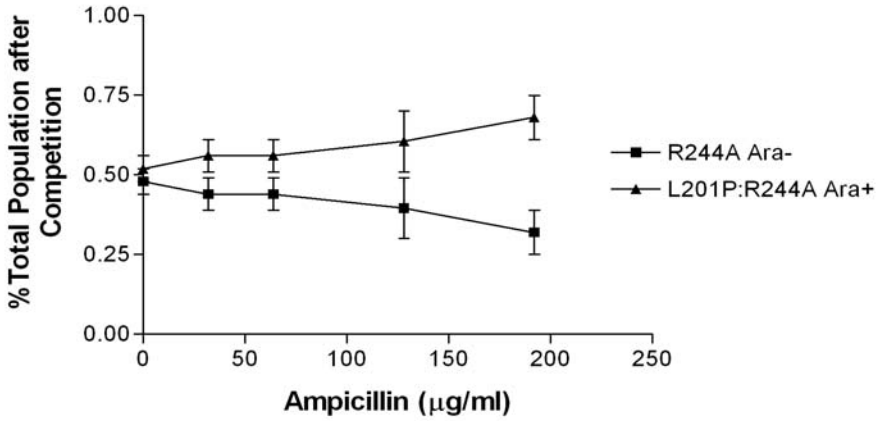

Figure A.1. Competition experiment between *E. coli* B cells containing pBG66-R244A and pBG66-L201P:R244A plasmids. **A.** Equal volumes of overnight cultures of *E. coli* Ara^+ pBG66 R244A and *E. coli* Ara^- pBG66 L201P:R244A were mixed and allowed to compete for growth overnight in LB medium containing the concentration of ampicillin indicated on the X-axis. The Y-axis indicates the percentage of the total culture of *E. coli* Ara^+ pBG66 R244A and *E. coli* Ara^- pBG66 L201P:R244A cells after the competition. **B.** Reciprocal competition experiment of *E. coli* Ara^- pBG66 R244A and *E. coli* Ara^+ pBG66 L201P:R244A strains.

Table A.2. Effect of stabilizer substitutions on TEM-1 β-lactamase mediated IC_{90} levels[a].

	Amp. (μg / mL)
TEM-1	>960
M182T	>960
L201P	>960
L76N	30
L76N:L201P	120
L76N:M182T	960
R244A	120
L201P:R244A	240
M182T:R244A	120
I47Y:E48C	240
I47Y:E48C:L201P	480
I47Y:E48C:M182T	480
H158S:V159S:T160H	30
H158S:V159S:T160H:L201P	30
H158S:V159S:T160H:M182T	960

[a]IC_{90} , defined as the concentration of ampicillin that reduces cfu per mL of culture by ≥90%, is derived directly from data measurements reported in Figure 2.

to the R244A mutant at increasing ampicillin concentrations. Expanded survival curves to an ampicillin concentration of 950 μg/ml are shown in Supplementary Fig. 1A. Taken together, the MIC determinations, competition experiments, and survival curves indicate that the L201P substitution confers enhanced ampicillin resistance to the R244A TEM-1, independent of plasmid and promoter context.

It is noteworthy that the M182T suppressor mutation was not identified among the suppressors of the R244A substitution, despite the fact that M182T has been identified previously as a suppressor of folding and/or stability defects of several different primary mutations [13; 14; 15; 16; 17; 18; 19]. One explanation is that the library of mutants constructed by PCR contained 1.8 x 10^5 clones, and the M182T mutant may not have been in this collection. Another possibility is that the M182T substitution does not enhance ampicillin resistance of the R244A primary mutant. To test this possibility, the M182T:R244A double mutant was constructed, and an ampicillin survival curve was generated. As seen in Fig. A.2A, the survival curves of the R244A and M182T:R244A are superimposable indicating that, at the resolution of this experiment, M182T does not enhance the ampicillin resistance of the R244A mutant. Therefore, the M182T mutation was not found among the R244A suppressor mutants because it does not alter the ampicillin resistance of R244A.

That the M182T suppressor substitution apparently does not act on the R244A enzyme suggests that the L201P mutation may be allele-specific, i.e., the mutation may increase ampicillin resistance only in combination with R244A. In order to investigate this possibility, double mutant constructs were made with the β-lactamase L76N substitution [11]. In TEM-1 β-lactamase, the completely buried leucine at position 76 is part of a

Figure A.2.

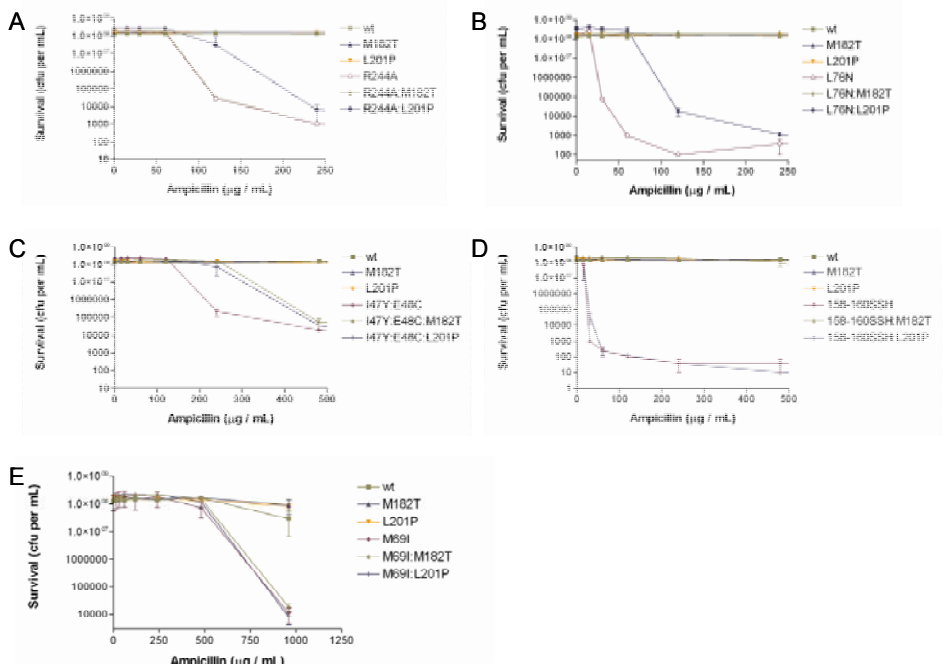

Figure A.2. Survival curves of *E. coli* with pBG66 plasmid encoding TEM-1 β-lactamase mutants. A. Colony forming units (cfu) on agar plates containing increasing concentrations of ampicillin for *E. coli* containing R244A, M182T, L201P single and double mutants. B. Cfu for *E. coli* containing L76N, M182T, L201P single and double mutants. C. Cfu for *E. coli* containing I47Y:E48C, M182T, L201P mutant combinations. D. Cfu for *E. coli* containing H158S:V159S:T160H, M182T, L201P mutant combinations. E. Cfu for *E. coli* containing M69I, M182T, L201P single and double mutants.

hydrophobic core of the enzyme [20; 41]. The L76N mutation has a modest effect on the catalytic properties of the enzyme *in vitro* but results in poor protein expression *in vivo.* This translates to a significant loss of resistance towards ampicillin [12]. Because of these qualities, the L76N mutant can be utilized as a sensitive test of the ability of second site amino acid substitutions to correct protein folding and/or stability defects [11; 12]. In addition, L76N was the original primary mutant used to identify M182T as a suppressor of folding and/or stability defects [11].

Both MIC and survival curve experiments were performed with *E. coli* containing the wild-type, M182T, L201P, L76N, L76N:M182T and L76N:L201P mutants encoded on the pBG66 plasmid. The addition of the M182T substitution restores the ampicillin resistance (MIC) of the pBG66 encoded L76N mutant to high levels (Table A.1). The pBG66-L76N:L201P mutant also displays a 2-fold increase of ampicillin resistance relative to pBG66-L76N alone (Table A.1). Moreover, the results in Fig. 2B and Table 2 show that the L201P substitution increases the survival of the L76N mutant in ampicillin. These data indicate that L201P can act on substitutions other than R244A. Because the L76N mutant enzyme is unstable, the result also suggests L201P acts to increase stability or improve folding of primary mutants. In addition, the M182T substitution acted as a suppressor of L76N, consistent with previous observations (Fig. A.2B) [11].

Several additional mutant combinations were constructed to examine the specificity of action of the M182T and L201P substitutions. The I47Y:E48C mutant was isolated from a library of random substitutions encompassing residues 46-48 of β-lactamase [39]. This mutant exhibits reduced ampicillin resistance and lower protein expression levels relative to wild-type TEM-1, and was used previously to demonstrate that M182T can suppress

the folding and/or stability defects of mutations other than L76N [11]. As seen in Fig. A.2C and Table A.2, *E. coli* containing either the I47Y:E48C: M182T or I47Y:E48C:L201P mutants exhibited increased survival on agar plates containing ampicillin compared to the I47Y:E48C parent mutant. This finding indicates both M182T and L201P improve the activity of the I47Y:E48C enzyme *in vivo*.

The H158S:V159S:T160H TEM-1 β-lactamase mutant was isolated from a library of random substitutions encompassing residues 158-160 [39]. This mutant was also chosen to test the suppression specificity of M182T and L201P based on its reduced ampicillin resistance and low protein expression levels. It was found that the M182T substitution strongly increased the ampicillin resistance levels of *E. coli* containing the H158S:V159S:T160H mutant, whereas the L201P substitution had no detectable effect on resistance levels of *E. coli* containing the mutant (Fig. A.2D, Table A.2).

Finally, neither M182T nor L201P increased the ampicillin resistance levels of the M69I mutant (Fig. A.2E). It was previously shown that the effect of the M182T substitution on the M69I enzyme could only be detected by measuring the specific activity of enzyme lysates at increasing temperatures [11].

The results of the double mutant experiments described above indicate that the TEM-1 L201P substitution can increase the ampicillin resistance of *E. coli* containing TEM-1 with primary mutations at different locations on the enzyme. This finding is consistent with L201P acting as a global suppressor mutant. However, it was also found that the addition of L201P did not result in detectable changes in ampicillin resistance for the H158S:V159S:T160H or M69I mutants. Similarly, the addition of the M182T substitution increased the ampicillin resistance conferred by several β-lactamase mutants

but not M69I or R244A. The failure to observe a change in resistance levels when M182T or L201P are combined with certain mutants could be due to the failure of the assay to detect subtle effects. For example, *E. coli* containing either M69I:M182T or M69I:L201P did not exhibit increased resistance relative to the M69I parent (Fig. A.2E). However, previous studies examining temperature sensitivity have shown that the M69I:M182T enzyme is more active than the M69I parent enzyme at elevated temperatures [11]. Therefore, the failure to observe a change in ampicillin resistance levels does not rule out an effect on the stability of the enzyme. Nevertheless, the patterns of suppression of the M182T and L201P substitutions display differences. In general, the M182T substitution is a stronger suppressor than L201P given that M182T confers higher levels of ampicillin resistance in most of the β-lactamase mutants tested. The notable exception is the failure of M182T to enhance the ampicillin resistance of the R244A mutant.

II. Immunoblot analysis of steady-state levels of β-lactamase mutants

The effect of the L201P substitution on steady-state protein levels of several TEM-1 mutants was quantified by immunoblot analysis of the perplasmic contents of the cell. The protein core-disrupting L76N substitution greatly reduces expression of TEM-1 β-lactamase (Fig. A.3 and reference [11]). A previous study found that the reduced expression level of the L76N mutant is due to periplasmic degradation in that the L76N mutant expression levels are similar to wild-type TEM-1 when expressed in an *E. coli* strain deficient in four periplasmic proteases [11]. Because unstable proteins are rapidly

Figure A.3

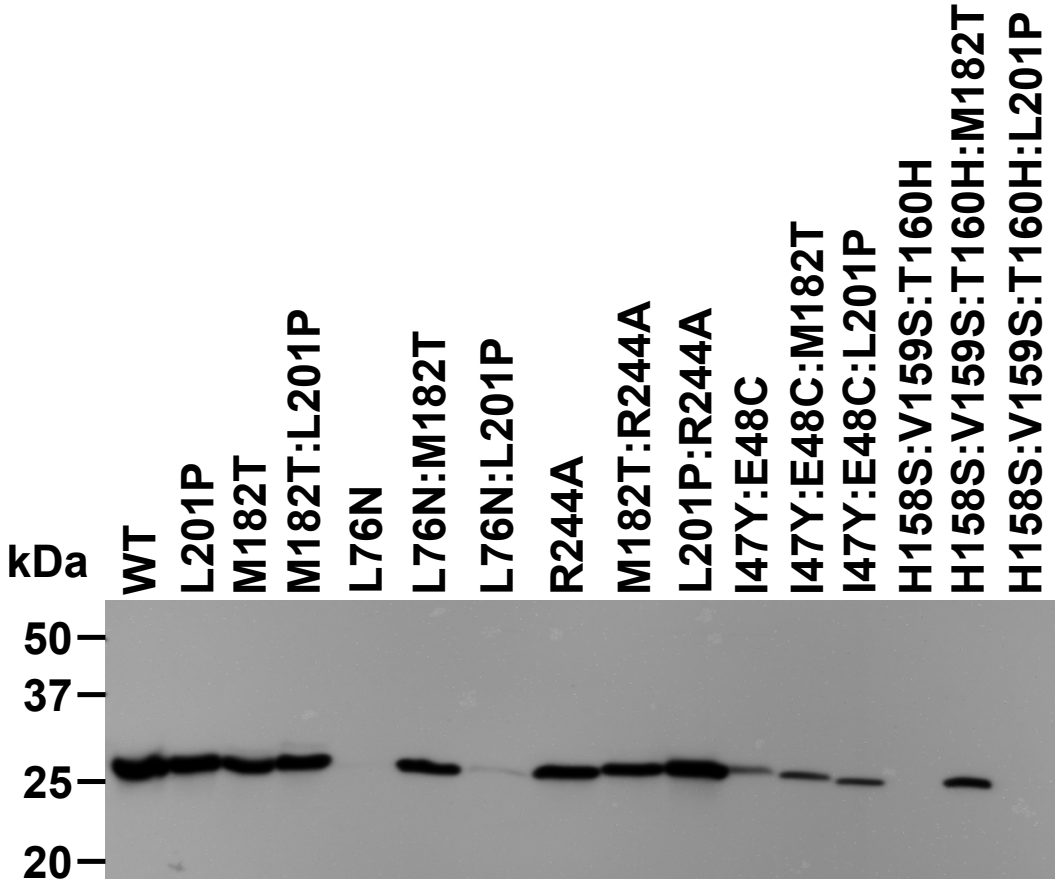

Figure A.3. Steady-state protein levels of wild-type and mutant TEM-1 β-lactamases as determined by immunoblot of *E. coli* periplasmic protein. Positions are: 1, wt TEM-1; 2,L201P; 3, M182T; 4, M182T:L201P; 5, L76N; 6, L76N:M182T; 7, L76N:L201P; 8, R244A; 9, M182T:R244A; 10, L201P:R244A; 11, I47Y:E48C; 12, I47Y:E48C:M182T; 13, I47Y:E48C:L201P; 14, H158S:V159S:T160H; 15, H158S:V159S:T160H:M182T; 16, H158S:V159S:T160H:L201P.

proteolyzed in *E. coli*, steady-state levels of expression relative to wild type can be used as an indicator of the effect of a mutation on protein stability [42].

The levels of protein expression of TEM-1 β-lactamase wild type and mutants was monitored by immunoblots of the periplasmic contents of *E. coli* expressing the enzymes from the pBG66 plasmid using anti-β-lactamase polyclonal antisera [11]. Consistent with previous results, the introduction of the M182T substitution rescues steady-state protein levels of the L76N mutant (Fig. A.3) [11]. The L201P substitution also improves steady-state L76N protein expression levels, which is consistent with it acting as a stability enhancing mutation similar to M182T (Fig. A.3) and is also consistent with the increased ampicillin resistance observed in the survival curve (Fig. A.2B). The R244A mutation had little effect upon steady-state protein levels suggesting that any effect upon protein folding associated with this active site substitution is modest in comparison to the effect of the L76N mutation (Fig. A.3). However, the L201P:R244A clone displayed a higher level of protein expression relative to the R244A clone (Fig. A.3, lanes 10 versus 8) while the M182T:R244A clone displayed similar levels as the R244A clone (Fig. A.3, lanes 9 versus 8). These observations are consistent with the results of the survival curve experiments with M182T:R244A and L201P:R244A. The higher level of protein expression of L201P:R244A may explain the increased ampicillin resistance which resulted in the isolation of this mutant in the second site mutation selection. The ability of L201P to increase expression levels of both the R244A and L76N mutants of TEM-1 β-lactamase provides evidence that L201P can act on more that one primary mutation in the enzyme.

The results of the survival curve experiments in Fig. 2 suggest that L201P can suppress defects associated with the I47Y:E48C mutant enzyme but not the H158S:V159S:T160H enzyme while the M182T substitution can act on both mutants (Fig. A.2C and D, Table A.2). The immunobloting results correlate well with these

findings in that the I47Y:E48C:L201P enzyme exhibits increased expression relative to the parent enzyme while the H158S:V159S:T160H:L201P enzyme levels are not altered relative to the parent enzyme (Fig. A.3). In addition, the expression levels of the I47Y:E48C:M182T and H158S:V159S:T160H:M182T enzymes are higher than the parent enzymes (Fig. A.3). Taken together, the survival curve and immunoblotting analyses indicate that both the M182T and L201P substitutions can act on more than one primary mutation, and that the set of mutants that can be suppressed by each overlap but is not identical.

Finally, the M182T and L201P substitutions both increase protein expression levels of other mutants and therefore it was of interest to examine the effect of the combination of M182T and L201P in a double mutant. It was observed that the M182T:L201P double mutant has similar expression levels as the wild type or the M182T or L201P single mutants (Fig. A.3).

III. Enzyme kinetic parameters of TEM-1 β-lactamase mutants

The M182T substitution rescues β-lactamases containing destabilizing mutations but has little influence on enzyme catalytic activity [10; 12]. Although ~25 Å distant from the active site, the L201P suppressor could increase enzymatic activity by altering the active site via a long-range structural change propagated down helix α9. To address this issue, the R244A and L201P:R244A enzymes were expressed and purified for kinetic analysis with ampicillin as substrate. No major differences in k_{cat} or K_m were found between R244A and L201P:R244A (Table A.3). However, as stated above, the L201P substitution is able

Table A.3. Enzyme kinetic parameters for TEM-1 β-lactamase and mutant derivatives for ampicillin hydrolysis.

	TEM-1	L201P	R244A	R244A-L201P
K_m (μM)	55.2±5.0	58.9±7.0	2704±492	3076±649
k_{cat} (s^{-1})	641±51	844±8	1747±359	1706±383
k_{cat}/K_m ($\mu M^{-1} \cdot s^{-1}$)	11.735±2.091	14.480±1.890	0.645±0.029	0.554±0.016

to increase *in vivo* ampicillin resistance levels of the R244A TEM-1 mutant in both the pET-TEM-1 and pBG66 genetic contexts. The finding that the L201P substitution does not enhance enzyme activity via a change in catalytic efficiency but does restore function of both the L76N and R244A mutants *in vivo*, supports the hypothesis that the L201P substitution acts by increasing the stability of the TEM-1 enzyme and thereby increases steady-state enzyme levels.

IV. Thermodynamic stability of TEM-1 β-lactamase mutant enzymes

To directly address the effect of the L201P substitution upon TEM-1 stability, the L201P, R244A, L201P:R244A and M182T:L201P TEM-1 enzymes were purified for the purpose of obtaining thermal denaturation curves. Measuring the helical signal by circular dichroism, all mutant proteins denatured reversibly in an apparently two state manner, as previously observed for the wild-type enzyme [43]. The TEM-1 L201P enzyme exhibited an increased melting temperature relative to wild type TEM-1, by 1.9 ºC, indicating increased stability at higher temperatures [10; 43] (Table A.4). Typically such a substantial change in the T_m may be interpreted as an increase in the stability of the protein across its folded temperature range. Using the method of Schellmann [44], which analyzes stability changes in the area of the T_m, L201P would be 0.8 kcal/mol more stable than the wild

Table A.4. Thermodynamic parameters for TEM-1 β-lactamase mutations affecting stability

	T_m[a] (^oC)	ΔT_m (^oC)	ΔH (kcal/mol)	$\Delta\Delta G_u$ (kcal/mol)	ΔS_u (kcal/mol*K)
TEM-1[b]	51.5±0.1	—	139.5±7.9	—	0.43
M182T[c]	57.7±0.1	6.2±0.2	160.3±4.3	2.67±0.13	0.48
L201P	53.4±0.1	1.9±0.2	111.4±0.7	0.80±0.08	0.34±0.002
L201P:M182T	58.0±0.2	6.5±0.3	96.9±5.9	2.80±0.13	0.29±0.01
R244A	54.0±0.3	2.5±0.4	78.1±5.5	1.08±0.17	0.24±0.02
L201P:R244A	54.7±0.3	3.2±0.4	85.8±1.7	1.38±0.17	0.26±0.004

a. Relative to TEM-1.
b. From ref [Wang, Minasov & Shoichet, Proteins 2001]
c. From ref [Wang, Minasov & Shoichet, JMB 2002]

lower temperatures where the enzyme is maximally stable. What we can certainly say is that L201P is more stable at higher temperatures than wild type TEM-1.

We also determined the T_m of the R244A enzyme, which was 2.5 ºC higher than wild type, and therefore even more stable than L201P, at least at the temperature of melting. However, the van't Hoff enthalpy of denaturation for R244A (78.1 kcal/mol) is much more depressed than was that of L201P, suggesting that this increase of stability can only be trusted at the temperature of melting, and that at lower temperatures the relative stabilities might well be reversed. Moreover, the L201P:R244A double mutant has a T_m that is 0.7 degrees higher than R244A and so the L201P substitution does further

stabilize the R244A enzyme. In this double mutant, moreover, the van't Hoff enthalpy of denaturation is partly restored towards its wild type value, consistent with a stabilization throughout the temperature range of folded protein, and not only at higher temperatures, relative to R244A. This result is consistent with the MIC and survival curve results, and with increased steady state periplasmic expression levels of the L201P:R244A enzyme compared to the R244A enzyme. The reduced hydrolytic activity associated with the R244A substitution results in a significant reduction in ampicillin resistance. The reduction in resistance levels leads to ampicillin MICs being more sensitive to small changes in β-lactamase stability and expression levels [45]. This may have provided the sensitivity necessary for the ampicillin selection to identify a suppressor that enhanced steady state expression levels via an increase in the stability of the enzyme.

The M182T and L201P each stabilize TEM-1 β-lactamase. Therefore it was of interest to assess the effects on enzyme stability of a double mutant containing both substitutions. The M182T:L201P double mutant exhibits a 6.5 degree increase in T_m relative to wild type and is marginally more stable than M182T alone, at least around the temperature of melting. Still, the increase in stability of the double relative to the single mutants is much less than additive, which is surprising given how distant the two substitutions are in space in the structure. On closer inspection, residues 201 and 182 both sit at the N-termini of sequential helices, which are connected by a four residue loop. Thus, whereas each of these substitutions can act independently as stabilizers of destabilizing substitutions, together the two substitutions exhibit negative additivity. This in turn suggests that the two helices on which they reside may affect one another. To better understand this

Table A.5. Data collection and refinement statistics.

Data collection	
Space group	$P2_12_12_1$
Cell dimensions	
a, *b*, *c* (Å)	41.218 59.140 87.802
α, β, γ (°)	90.00 90.00 90.00
Resolution (Å)	50.00-1.92 (1.99-1.92)[a]
R_{merge} (%)	6.1 (35.4)
$I / \sigma I$	14.0 (2.48)
Completeness (%)	92.0 (83.3)
Refinement	
R_{work} / R_{free}	19.6 % / 24.2%
R.m.s deviations	
Bond lengths (Å)	0.013
Bond angles (°)	1.473
Ramanchandran plot [b]:	
Most favored region (%)	93.0
Additionally allowed (%)	6.6
Generously allowed (%)	0.4

[a] Values in parenthesis represent highest resolution shells.

[b] Calculated by PROCHECK, excluding glycine and proline [54].

observation, and to investigate the effects of Leu201→Pro at atomic resolution, we determined the structure of L201P by x-ray crystallography.

V. Structure determination of L201P β-lactamase

The L201P TEM-1 enzyme was crystallized in conditions similar to that of native TEM-1. Its structure was determined to 1.92 Å by x-ray, and the structure was modeled and refined with good statistics (Table A.5). The electron density at and around the point of

Figure A.4

A

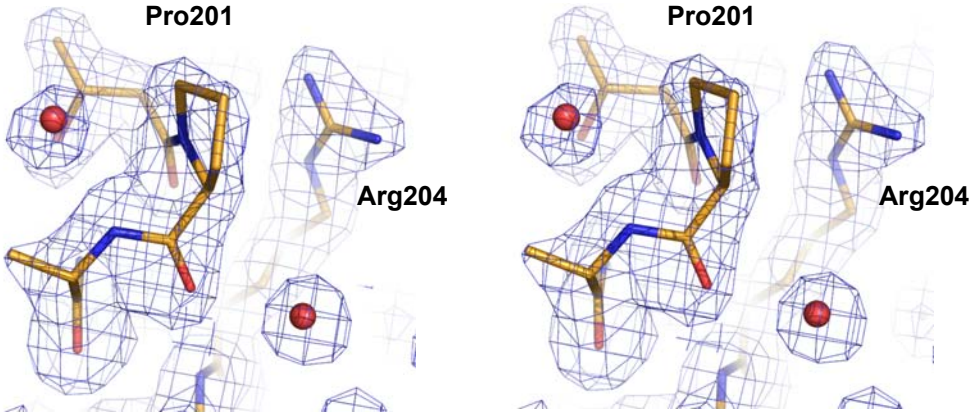

B

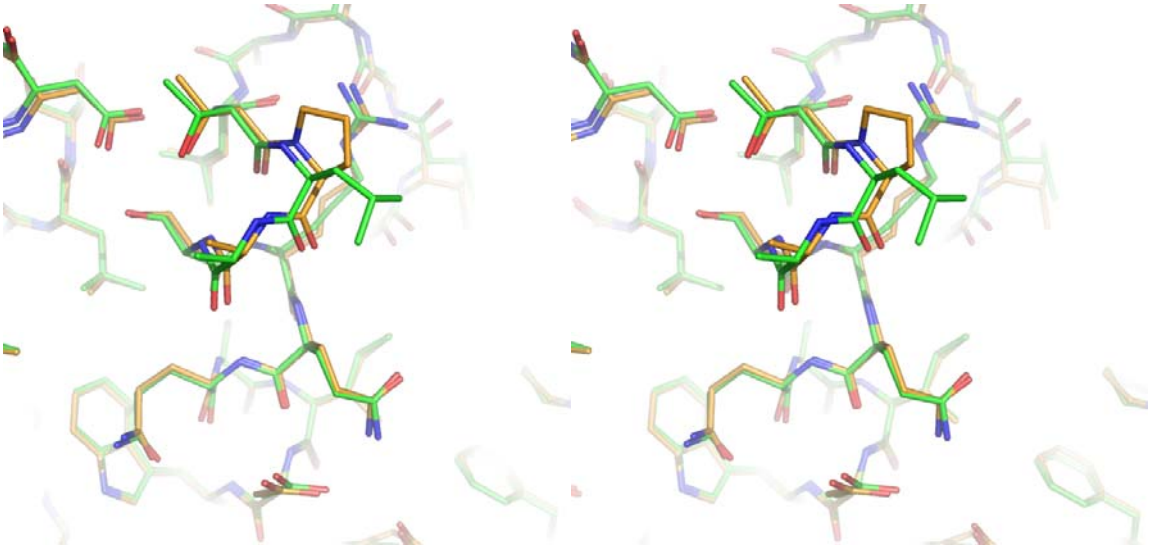

C

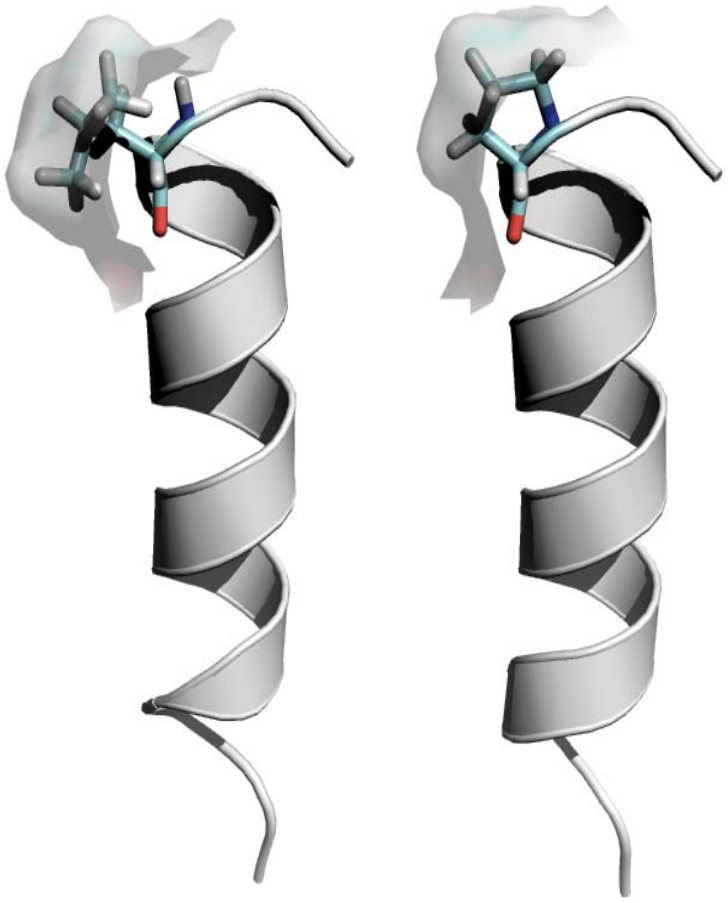

Figure A.4. Structure of the L201P mutant of TEM-1 β-lactamase. **A.** 2Fo-Fc electron density map, contoured at 1σ, shows the mutated residue 201 and surrounding environment, including two ordered water molecules (red spheres) that interact with the protein backbone. Carbon atoms are colored in gold, oxygen atoms in red and nitrogen atoms in blue. **B.** Overlay of the TEM-1 WT structure (carbons in green) and the L201P mutant (carbons in gold) in the region of the Leu201→Pro substitution. **C.** Wild-type TEM-1 (PDB-1AXB) helix α9 is shown next to α9 of the L201P structure. The residue at position 201 is presented in stick format and the solvent exposed surface associated with residue 201 is presented in each structure.

substitution, Leu201→ Pro, was unambiguous, allowing us to compare the protein environment in the native and mutant enzymes (Fig. A.4A). Residue 201 is at the N-terminus of the α9 helix in TEM-1; in both the native and mutant structures the residue is surface exposed, making only van der Waals contacts with Arg204 in both structures. The structures of the native (pdb 1AXB) and mutant overlap closely in the region of substitution (Fig. 4B), and the overall Cα RMSD between the two structures is only 0.31 Å, and in the local region of the substitution (residues 197-205) it is 0.08 Å. Thus the increased temperature stability of the mutant enzyme is not easily explained by changes in interactions in the folded form of the enzyme. Rather, the proline substitution removes the uncompensated main chain amide proton of Leu201, lying as it does at the N-terminus of helix α9, replacing it with a non-polar carbon of the proline. This reduces the cost of desolvating this group on folding. Consistent with such a role, there is a high propensity for proline at the first (N1) position of α helices [46]. Also, the reduced flexibility of the proline side and main chain will increase the free energy of the unfolded form, further increasing the relative stability of the folded enzyme. This entropic effect is thought to be responsible for a ~1 kcal/mol increase in stability observed with proline substitutions in T4 lysozyme and ribonuclease Sa [47]. Thus, the L201P substitution may enhance the stability of TEM-1 β-lactamase via both helix dipole and entropic mechanisms.

A.4 Conclusions

The frequent appearance of the M182T substitution in combination with destabilizing active site mutations in TEM-1 β-lactamase variants from clinical isolates provides a medically relevant example of evolutionary pressures acting upon protein stability (http://www.lahey.org/studies) [10; 11; 16]. The L201P substitution was previously identified during an *in vitro* selection experiment for inhibitor resistant TEM-1 mutants[37] and it was also recently identified as a suppressor from selection experiments with populations of highly mutagenized TEM-1 genes [38]. Unlike the M182T substitution, however, the L201P change has not been identified in natural isolates. The L201P substitution exhibits properties similar to M182T in that it increases stability and steady state protein expression levels and is not strongly allele specific, i.e., it can increase the stability of enzymes with different primary substitutions. The results also indicate, however, that both the M182T and L201P display some specificity with regard to their ability to stabilize enzymes containing destabilizing primary mutations. For example, the M182T substitution had no detectable impact on the R244A mutant, and the L201P substitution had no detectable effect on the H158S:V159S:T160H triple mutant.

Both the M182T and L201P increase the thermodynamic stability of the wild type enzyme. Therefore, M182T and L201P could generally increase stability ($-\Delta\Delta G$) and act additively with the primary mutations such that the double mutant has increased stability compared to the enzyme containing the primary mutation. The cases where either the M182T or L201P substitutions do not enhance stability could be explained as non-additivity with the primary substitution. By this view, the degree of allele-specificity of a suppressor mutation (substitution) is a function of its additivity relationships with various

primary mutations. The exact mechanisms by which M182T and L201P substitutions act and how they communicate with other residue positions in terms of additivity are currently unknown. It is possible that global suppressors actually act on subsets of residue positions and these subsets may overlap completely, partially (as for the targets of M182T and L201P), or not at all. The exact physical mechanism by which the substitutions act on the enzyme would determine additivity relationships. For example, the global stabilizer substitutions could differ with regards to acting upon the native folded protein or certain intermediates on the β-lactamase folding pathway which, in turn, could influence proteolysis or aggregation of the intermediates *in vivo*. If stabilizer substitutions acted in the same way, they would exhibit a similar pattern of suppression of primary mutations whereas a different pattern of suppression would be observed for stabilizer substitutions that act by different mechanisms. Further experiments are required clarify these questions. Nevertheless, it is clear from these experiments and other recent observations [38] that the Leu201→Pro substitution provides an important additional example of a stabilizer in TEM β-lactamase that acts on multiple primary mutations and suggests that multiple, single-point restabilizing substitutions may be accessible as a protein evolves new activity, increasing its ability to do so without catastrophic loss of stability.

A.5 Materials and Methods

I. Bacterial strains and plasmids

E. coli XL1-Blue strain (*recA1 endA1 gyrA96 thi-1 hsdR17 supE44 relA1 lac* [F'*proAB lacI*^{q}*ZΔM15 Tn10* (Tet^{r})]) was obtained from Stratagene (La Jolla, CA) and utilized in

site-directed mutagenesis and determination of steady-state protein expression levels. The *E. coli* BL21(DE3) strain (F^- *ompT gal [dcm] [lon] hsdSB* (r_B^- m_B^-) (λ DE3)) was employed in MIC determination and protein purification. The pET-TEM-1 vector encodes an ompA leader-TEM-1 fusion gene driven by the T7 promoter [35]. The ompA-TEM-1 fusion in pET-TEM-1 also contains an E28G substitution in TEM-1 near the signal cleavage site. The pET-TEM-1 E28G construct was used as template for library construction and for selection of the L201P suppressor mutation. Although no phenotypic changes have been described for the E28G substitution, the substitution was reverted by site-directed mutagenesis prior to subsequent purification of proteins used in enzyme kinetics as well as thermal denaturation experiments and crystallization of the L201P mutant. The pBG66 plasmid encodes wild type TEM-1 β-lactamase under the transcriptional control of its native promoter. Mutations were made in the pBG66 background by site-directed mutagenesis and used in MIC determinations and immunoblot analysis of steady-state protein levels.

II. Site-directed mutagenesis

All TEM-1 β-lactamase site-directed mutants were created using Stratagene's (La Jolla, CA) QuickChange kit according to the manufacturer's protocol. Primers were obtained from Integrated DNA Technologies (Coralville, IA). The following top strand primers were used to introduce mutations (underlined) into the TEM-1 gene: M182T (5'-CGAGCGTGACACCACGA<u>CG</u>CCTGCAGCAATGGC-3'), L201P (5'-GGCGAACTACTTACTC<u>CG</u>GCTTCCC-3') and R244A (5'-GCGTGGGTCT<u>GCT</u>GGTATCATTGCAGCACTGGG-3'). The L201P and R244A

containing pBG66 TEM-1 mutants were constructed upon the previously described wild-type, M69I, I47Y:E48C, H158S:V159S:T160H, L76N, M182T and L76N:M182T mutants [11]. Constructs were sequenced in-house using an Applied Biosystems Instruments (Foster City, CA) Prism Big Dye DNA sequencing kit with an ABI 3100 automated sequencing instrument or by Lonestar Labs (Houston, TX). The pET-TEM-1 E28G mutation was corrected using the top strand primer 5'-CGTAGCGCAGGCCCACCCAGAAACGCTGGTGAAAGTAAAAGATGC-3'.

III. Library construction and selection

A library of random point mutations was constructed by error-prone PCR using the pET-TEM-1 E28G:R244A gene as template. Mutagenic PCR via inclusion of $MnCl_2$ was performed with 5U *Taq* polymerase (Promega, Madison, WI), 0.2 mM dATP, 0.2 mM dCTP, 0.4 mM dGTP, 0.4 mM dTTP (dNTPs from Bioline, Randolph, MA), 1.5 mM $MgCl_2$, 1X Taq polymerase buffer (Promega, Madison, WI), 100 ng of outside primers and 45 ng of pET-TEM-1 E28G:R244A plasmid as template in a 100 µl reaction. A series of mutagenic PCR reactions were performed utilizing either 0.0625, 0.125 or 0.25 mM $MnCl_2$ (three reactions performed in triplicate). The PCR reaction parameters were as follows: 95 ^{o}C for 1 min; followed by 30 cycles of 95 ^{o}C for 1 min, 50 ^{o}C for 2 min, and 72 ^{o}C for 3 min; ending with 72 ^{o}C for 10 min. All 9 mutagenic PCR reactions were pooled and column purified using a Qiagen PCR purification kit (Qiagen Inc., Valencia, CA) before digestion with restriction enzymes *Xho*I/*Nde*I/*Dpn*I obtained from New England Biolabs (Ipswich, MA). Insert DNA was gel purified and ligated into pET-TEM-1 digested with *Xho*I/*Nde*I that was also treated with calf intestinal alkaline

phosphatase (CIP) obtained from New England Biolabs (Ipswich, MA). The DNA in the ligation reaction was extracted with phenol/chloroform, transformed into electrocompetent *E. coli* BL21(DE3) and spread onto LB plates containing kanamycin. A total of 1.8×10^5 cfu's were pooled. The library was subjected to selection on 350 μg/ml ampicillin. DNA was isolated from individual clones and sequenced to reveal a t → c mutation resulting in the L201P substitution. The L201P:R244A mutant was recovered and sequenced 6 times. It is not known if the 6 mutants were independent, or if they represent clonal expansion. In addition, the P62L:R244A, A86T:R244A and I208L:R244A mutants were recovered one time each. Only the P62L:R244A mutant (and L201P:R244A) reproducibly improved MIC relative to R244A. The L201P:R244A mutant was pursued because it was detected in multiple clones and it exhibited the most significant increase in ampicillin resistance.

IV. Minimum inhibitory concentration (MIC) determinations

a. MIC determinations for pET-TEM-1 plasmids- E. coli

BL21(DE3) was utilized as the host strain for determining the ampicillin MIC of the pDM122 (pET-TEM-1-R244A), pDM123 (pET-TEM-1-R244A:L201P) pDM124 (pET-TEM-1-L201P), and pET-TEM-1 (wt) constructs. Briefly, overnight cultures were grown at 37°C in LB broth containing 25 μg/ml kanamycin to maintain the plasmid and 100 μM IPTG to induce expression from the T7 promoter. The overnight cultures were diluted $1{:}10^4$ (~10^5 bacteria/ml) and 90 μl was inoculated into 1.75 ml fresh LB broth containing 25 μg/ml kanamycin, 100 μM IPTG, and various concentrations of ampicillin. The concentrations of ampicillin tested were 179, 230, 256, 282, 307, 333, 358, 384, 410, 435,

461, 486, 512, 563, 666, 860, 1024, 1106 μg/ml. The cultures were then incubated at 37^{o}C with shaking for ~18 hours and the MIC was determined by examining the minimum inhibitory concentration of ampicillin for bacterial growth.

b. MIC determinations for pBG66 plasmids

Overnight cultures were grown in LB broth containing 12.5 μg/ml chloramphenicol to maintain the pBG66 plasmid. The overnight cultures were diluted 1:10^{4} (~10^{5} bacteria/ml) and 90 μl was inoculated into 1.75 ml fresh LB broth containing 12.5 μg/ml chloramphenicol and various concentrations of ampicillin. The concentrations of ampicillin tested were 4, 8, 16, 32, 64, 128, 256, 512, 1024, 1536, 2048, 4096 and 8192 μg/ml. The cultures were then incubated at 37^{o}C with shaking for ~18 hours and examined to determine the minimum inhibitory concentration of ampicillin for bacterial growth. For MIC determination using amoxicillin + clavulanic acid E-test strips (AB Biodisk, Solna, Sweden), a one tenth dilution of an overnight culture of *E. coli* XL1-Blue transformed with a pBG66 construct was spread upon LB plates before placement of the E-test strip on the bacterial lawn. Plates were allowed to incubate overnight at 37^{o}C before scoring for growth. Each assay was conducted in at least duplicate using independent overnight cultures.

V. Competition Experiments using *E. coli* B Ara^{+} and Ara^{-} strains

Competition experiments were performed between *E. coli* B Ara^{+} and Ara^{-} cells containing the pBG66 plasmid encoding either the TEM-1 R244A or L201P:R244A β-lactamases. For these experiments, pBG66-TEM-1 R244A and pBG66-TEM-1 L201P:R244A plasmids were transformed into both the *E. coli* B Ara^{+} and Ara^{-} strains.

Reciprocal experiments were performed, i.e., Ara^+ R244A versus Ara^- L201P:R244A and Ara^+ L201P:R244A versus Ara^- R244A for each ampicillin concentration. For simplicity, the methods described below are for the Ara^+ R244A versus Ara^- L201P:R244A experiment but they were the same for the reciprocal experiment. A culture of each strain was grown overnight in LB medium containing 12.5 μg/ml chloramphenicol to select for the presence of the pBG66 plasmid. Equal volumes of each overnight culture were mixed and diluted to a final concentration of 1×10^4 cells per ml in LB medium containing 12.5 μg/ml chloramphenicol with or without ampicillin. A zero time point was taken from this culture and spread on tetrazolum (TA) agar plates containing 12.5 μg/ml chloramphenicol. After overnight growth at 37°C, Ara^+ R244A colonies are white/pink and Ara^- L201P:R244A are red. By counting pink versus red colonies it was possible to estimate the number of Ara^+ R244A and Ara^- L201P:R244A cells in the culture. Competition experiments were performed by adding various concentrations of ampicillin to the Ara^+:Ara^- mixed starting culture and allowing the cells to compete for growth overnight at 37°C. The cultures were then spread on TA agar plates and pink and red colonies were counted after overnight growth at 37°C.

VI. Bacterial cell survival on ampicillin agar

E.coli XL1-Blue containing the pBG66 plasmid that encodes TEM-1 or a TEM-1 β-lactamase mutant were grown overnight in LB broth containing 12.5 μg/mL chloramphenicol. Overnight cultures were diluted 1:100 into LB broth containing 12.5 μg/mL chloramphenicol and incubated for 4 hours at 37°C to mid-log phase (OD_{600} = 0.4-0.6). Ten-fold serial dilutions of each culture were made, and 100 μl of each dilution

were spread onto LB agar plates containing 0 μg/mL, 15 μg/mL, 30 μg/mL, 60 μg/mL, 120 μg/mL, 240 μg/mL, 480 μg/mL, or 960 μg/mL of ampicillin. After incubation for 24 hours at 37°C, colony forming units (cfu) on each plate were counted. This data was used to calculate the cfu per mL of culture, or survival on a given concentration of ampicillin.

VII. Immunoblot analysis

The effect of the M182T and L201P substitutions upon steady-state expression levels of TEM-1 β-lactamase was determined by immunoblot analysis of *E. coli* XL1-Blue periplasmic contents as previously described [48]. Briefly, overnight cultures transformed with pBG66 encoding wild type TEM-1 or a mutant thereof were diluted 1/50 in fresh LB media containing chloramphenicol and allowed to grow to an OD_{600} of ~0.3. 1.5 mL of culture was pelleted by centrifugation, resuspended in 200 μl of spheroplast buffer (50 mM Tris-HCl [pH 8], 1mM EDTA, 20% sucrose) and incubated on ice for 10 minutes. The cells were again pelleted by centrifugation, and resuspeded in 200 μl of cold H_20 to release the periplasmic contents of the culture. The concentration of soluble protein in each sample was measured using the Bio-Rad Bradford protein assay reagent (Hercules, CA), and approximately 15 μl of sample (adjusted according to protein concentration to ensure equal loading between wells) was resolved on a 12% SDS-PAGE gel. *E. coli* proteins were electro-transferred to a nitrocellulose membrane (Amersham, GE Heathcare, Piscataway, NJ) using a Bio-Rad (Hercules, CA) semi-dry transfer apparatus. The membrane was blocked overnight in 5% milk before probing with rabbit polyclonal anti-TEM-1 antibody. A donkey anti-rabbit horseradish peroxidase conjugate was

utilized with the Amersham ECL chemiluminescent detection reagent (GE Healthcare, Piscataway, NJ) to visualize TEM-1 proteins. This procedure was performed in duplicate using independent cultures.

VIII. Protein purification

The L201P, R244A, M182T:L201P and L201P:R244A β-lactamases were purified to ~90% homogeneity. *E. coli* BL21(DE3) cells transformed with the relevant mutant construct were grown in LB broth with 300 mM sorbitol, 250 mM betaine and 25 μg/ml kanamycin to OD_{600} 0.8, and transcription was induced with 0.4 mM IPTG. The induced culture was grown overnight with shaking at room temperature. Cells were harvested by centrifugation and the periplasmic contents were obtained by osmotic shock. The periplasmic fraction was dialyzed overnight at 4^{o}C before loading onto a Hi-Trap zinc chelating column (Amersham, GE Heathcare, Piscataway, NJ) charged with $ZnCl_2$ [5; 49]. The β-lactamase containing fraction was eluted by a pH gradient and purity was determined by SDS-PAGE gel electrophoresis. Buffer exchange into 50 mM PO_4 pH 7.0 was facilitated by use of a Centricon centrifugal filter (Millipore, Billerica, MA). Mutant β-lactamases L201P, R244A, M182T:L201P and L201P:R244A used in thermal denaturation and crystallization procedures were further purified to ~99% purity by size-exclusion chromatography. Protein concentrations were determined with the Bio-Rad Bradford protein assay reagent (Hercules, CA).

IX. Enzyme kinetics

Michaelis-Menten steady-state kinetic parameters were determined on a Beckman-Coulter spectrophotometer model DU 800 (Fullerton, CA). Ampicillin hydrolysis was monitored at 235 nm. Reactions were performed at 30^{o}C in 50 mM phosphate buffer (pH 7.0). K_m and k_{cat} values were determined by fitting initial velocity rates over a range of substrate concentrations to a Michaelis-Menten curve using SigmaPlot. Measurements were performed in triplicate.

X. Thermal denaturation

Thermal denaturation was carried out in 200 mM potassium phosphate, pH 7.0, as described [43]. The enzymes were denatured by raising the temperature in 0.1°C increments at a ramp rate of 2^{o}C/min on a Jasco J-715 spectropolarimeter with a Jasco PTC-348WI Peltier-effect temperature controller and an in-cell temperature probe and stir bar were used, as described. All T_m and ΔH_{VH} values were calculated with the program EXAM [50]; the change in heat capacity upon denaturation (ΔC_p) was set to 3.8 kcal/mol•K for each enzyme.[Wang, Minasov & Shoichet, 2001; Wang, Minasov & Shoichet, 2002] Denaturation was marked by an obvious transition in the far-UV CD signal, monitored at 223 nm. Reversibility was measured by the return of folded CD signal divided by the amount of signal lost on unfolding: all enzymes showed greater than 90% reversibility after denaturation. Values of $\Delta\Delta G_u$ were determined by the method of Schellman [44], using the entropy of unfolding of the wild-type (WT) enzyme, as determined previously.[Wang, Minasov & Shoichet, 2001; Wang, Minasov & Shoichet, 2002]

$$\Delta\Delta G_u = \Delta T_m \bullet \Delta S_{WT\text{-}enzyme} \quad (1)$$

XI. Structure determination of L201P β-lactamase

L201P was crystallized in 1.6M potassium phosphate buffer (pH 8.7) using a hanging drop method [10]. Diffraction data were collected at ALS (Advanced Light Source, Lawrence Berkeley National Lab, Berkeley, CA) Beamline 8.3.1 to 1.92 Å resolution and processed with HKL2000 [51]. An initial model was obtained through molecular replacement based on the structure of and a TEM-1 M182T mutant structure (1JWP) using EPMR [52]. Refinement was performed with CCP4 to a final R value of 19.6% and R_{free} 24.2% [53]. Full statistics are provided in Table 5. The coordinates have been deposited in the Protein Data Bank with access code 3CMZ.

A.6 Acknowledgments

This project was supported by NIH grants AI32956 to TP and GM63815 to BKS. We thank Marvin Makinen for providing the pET-TEM-1 plasmid.

A.7 References

1. Shah, A. A., Hasan, F., Ahmed, S. & Hameed, A. (2004). Characteristics, epidemiology and clinical importance of emerging strains of Gram-negative bacilli producing extended-spectrum beta-lactamases. *Res. Microbiol.* **155**, 409-421.

2. Canica, M. M., Caroff, N., Barthelemy, M., Labia, R., Krishnamoorthy, R., Paul, G. & Dupret, J. M. (1998). Phenotypic study of resistance of beta-lactamase-inhibitor resistant TEM enzymes which differ by naturally occurring variations and by site-directed substitution at Asp276. *Antimicrob. Agents Chemother.* **42**, 1323-1328.

3. Cantu III, C. (1998). The role of residue 238 of TEM-1 β-lactamase in the hydrolysis of extended-spectrum antibiotics. *J. Biol. Chem.* **273**, 26603-26609.

4. Cantu III, C., Huang, W. & Palzkill, T. (1996). Selection and characterization of amino acid substitutions at residues 237-240 of TEM-1 β-lactamase with altered substrate specificity for aztreonam and ceftazidime. *J. Biol. Chem.* **271**, 22538-22545.

5. Cantu III, C., Huang, W. & Palzkill, T. (1997). Cephalosporin substrate specificity determinants of TEM-1 b-lactamase. *J. Biol. Chem.* **272**, 29144-29150.

6. Chaibi, E. B., Sirot, D., Paul, G. & Labia, R. (1999). Inhibitor-resistant TEM beta-lactamases: phenotypic, genetic and biochemical characteristics. *J. Antimicrob. Chemother.* **43**, 447-458.

7. Delaire, M., Labia, R., Samama, J. P. & Masson, J. M. (1992). Site-directed mutagenesis at the active site of Escherichia coli TEM-1 b-lactamase. Suicide inhibitor-resistant mutants reveal the role of arginine-244 and methionine-69 in catalysis. *J. Biol. Chem.* **267**, 20600-20606.

8. Thomas, V. L., Golemi-Kotra, D., Kim, C., Vakulenko, S. B.,

Mobashery, S. & Shoichet, B. K. (2005). Structural consequences of the inhibitor-resistant Ser130Gly substitution in TEM beta-lactamase. *Biochemistry* **44**, 9330-9338.

9. Zafaralla, G., Manavathu, S., Lerner, A. & Mobashery, S. (1992). Elucidation of the role of arginine-244 in the turnover processes of class A beta-lactamases. *Biochemistry* **31**, 3847-3852.

10. Wang, X., Minasov, G. & Shoichet, B. K. (2002). Evolution of an antibiotic resistance enzyme constrained by stability and activity trade-offs. *J. Mol. Biol.* **320**, 85-95.

11. Huang, W. & Palzkill, T. (1997). A natural polymorphism in β-lactamase is a global suppressor. *Proc. Natl. Acad. Sci. USA* **94**, 8801-8806.

12. Sideraki, V., Huang, W., Palzkill, T. & Gilbert, H. F. (2001). A secondary drug resistance mutation of TEM-1 beta-lactamase that suppresses misfolding and aggregation. *Proc. Natl. Acad. Sci. USA* **98**, 283-288.

13. Barlow, M. & Hall, B. G. (2002). Predicting evolutionary poteintial: In vitro evolutions accurately reproduces natural evolution of the TEM β-lactmase. *Genetics* **160**, 823-832.

14. Barlow, M. & Hall, B. G. (2003). Experimental prediction of the evolution of cefepime resistance from the CMY-2 AmpC β-lactamase. *Genetics* **164**, 23-29.

15. Hecky, J. & Muller, K. M. (2005). Structural perturbation and compensation by directed evolution at physiological temperature leads to thermostabilization of beta-lactamase. *Biochemistry* **44**, 12640-12654.

16. Orencia, M. C., Yoon, J. S., Ness, J. E., Stemmer, W. P. & Stevens, R. C. (2001). Predicting the emergence of antibiotic resistance by directed evolution and structural analysis. *Nat. Struct. Biol.* **8**, 238-242.

17. Osuna, J., Perez-Blancas, A. & Soberon, X. (2002). Improving a circularly permuted TEM-1 beta-lactamase by directed evolution. *Protein Eng.* **15**, 463-470.

18. Stemmer, W. (1994). Rapid evolution of a protein *in vitro* by DNA

shuffling. *Nature (London)* **370**, 389-391.

19. Zaccolo, M. & Gherardi, E. (1999). The effect of high-frequency random mutagenesis on *in vitro* protein evolution: A study on TEM-1 β-lactamase. *J. Mol. Biol.* **285**, 775-783.

20. Strynadka, N. C. J., Adachi, H., Jensen, S. E., Johns, K., Sielecki, A., Betzel, C., Sutoh, K. & James, M. N. G. (1992). Molecular structure of the acyl-enzyme intermediate in b-lactam hydrolysis at 1.7 A resolution. *Nature* **359**, 700-705.

21. Bret, L., Chaibi, E. B., Chanal-Claris, C., Sirot, D., Labia, R. & Sirot, J. (1997). Inhibitor-resistant TEM (IRT) beta-lactamases with different substitutions at position 244. *Antimicrob. Agents Chemother.* **41**, 2547-2549.

22. Bret, L., Chanal, C., Sirot, D., Labia, R. & Sirot, J. (1996). Characterization of an inhibitor-resistant enzyme IRT-2 derived from TEM-2 beta-lactamase produced by *Proteus mirabilis* strains. *J. Antimicrob. Chemother.* **38**, 183-191.

23. Imtiaz, U., Manavathu, E., Mobashery, S. & Lerner, S. (1994). Reversal of clavulanate resistance conferred by a ser-244 mutant of TEM-1 beta-lactamase as a result of a second mutation (arg to ser at position 164) that enhances activity against ceftazidime. *Antimicrobial Agents and Chemotherapy* **38**, 1134-1139.

24. Lemozy, J., Sirot, D., Chanal, C., Huc, C., Labia, R., Dabernat, H. & Sirot, J. (1995). First characterization of inhibitor-resistant TEM(IRT) beta-lactamases in *Klebsiella pneumoniae* strains. *Antimicrob. Agents Chemother.* **39**, 2580-2582.

25. Stapleton, P. D., Shannon, K. P. & French, G. L. (1999). Construction and characterization of mutants of the TEM-1 beta-lactamase containing amino acid substitutions associated with both extended-spectrum resistance and resistance to beta-lactamase inhibitors. *Antimicrob. Agents Chemother.* **43**, 1881-1887.

26. Vedel, G., Belaaouaj, A., Gilly, L., Labia, R., Philippon, A., Nevot, P. & Paul, G. (1992). Clinical isolates of *Escherichia coli* producing TRI β-lactamases: novel TEM-enzymes conferring resistance to β-lactamase inhibitors. *J. Antimicrob. Chemother.* **30**, 449-462.

27. Ambler, R. P. (1980). The structure of beta-lactamases. *Phil. Trans. Ry. Soc. London, Ser. B* **289**, 321-331.

28. Ambler, R. P., Coulson, F. W., Frere, J.-M., Ghuysen, J.-M., Joris, B., Forsman, M., Levesque, R. C., Tiraby, G. & Waley, S. G. (1991). A standard numbering scheme for the class A β-lactamases. *Biochem. J.* **276**, 269-272.

29. Bush, K., Jacoby, G. A. & Medeiros, A. A. (1995). A functional classification scheme for b-lactamases and its correlation with molecular structure. *Antimicrob. Agents Chemother.* **39**, 1211-1233.

30. Matagne, A., Lamotte-Brasseur, J. & Frere, J. M. (1998). Catalytic properties of class A beta-lactamases: efficiency and diversity. *Biochem. J.* **330**, 581-598.

31. Dideberg, O., Charlier, P., Wery, J. P., Dehotty, P., Dusart, J., Erpicum, T., Frere, J.-M. & Ghuysen, J.-M. (1987). The crystal structure of the beta-lactamase of *Streptomyces albus* G at 0.3nm resolution. *Biochemistry Journal* **245**, 911-913.

32. Ibuka, A. S., Ishii, Y., Galleni, M., Ishiguro, M., Yamaguichi, K., Frere, J. M., Matsuzawa, H. & Sakai, H. (2003). Crystal structure of extended-spectrum beta-lactamase Toho-1: Insights into the molecular mechanism for catalytic reaction and substrate specificity expansion. *Biochemistry* **42**, 10634-10643.

33. Matagne, A., Misselyn-Baudin, A.-M., Joris, B., Erpicum, T., Granier, B. & Frere, J.-M. (1990). The diversity of the catalytic properties of class A beta-lactamases. *Biochemistry Journal* **265**, 131-146.

34. Sougakoff, W., L'Hermite, G., Pernot, L., Naas, T., Guillet, V., Nordmann, P., Jarlier, V. & Delettre, J.

(2002). Structure of the imipenem-hydrolyzing class A β-lactamase SME-1 from *Serratia marcescens*. *Acta Cryst.* **D58**, 267-274.

35. Sosa-Peinado, A., Mustafi, D. & Makinen, M. W. (2000). Overexpression and biosynthetic deuterium enrichment of TEM-1 beta-lactamase for structural characterization by magnetic resonance methods. *Protein Expr. Purif.* **19**, 235-245.

36. Savard, P. Y. & Gagne, S. M. (2006). Backbone dynamics of TEM-1 determined by NMR: evidence for a highly ordered protein. *Biochemistry* **45**, 11414-11424.

37. Vakulenko, S. B., Geryk, B., Kotra, L. P., Mobashery, S. & Lerner, S. A. (1998). Selection and characterization of beta-lactam-beta-lactamase inactivator-resistant mutants following PCR mutagenesis of the TEM-1 beta-lactamase gene. *Antimicrob. Agents Chemother.* **42**, 1542-1548.

38. Bershtein, S., Goldin, K. & Tawfik, D. S. (2008). Intense neutral drifts yield robust and evolvable consensus proteins. *J. Mol. Biol.* **379**, 1029-1044.

39. Huang, W., Petrosino, J., Hirsch, M., Shenkin, P. S. & Palzkill, T. (1996). Amino acid sequence determinants of β-lactamase structure and activity. *J. Mol. Biol.* **258**, 688-703.

40. Lenski, R. E., Simpson, S. C. & Nguyen, T. T. (1994). Genetic analysis of a plasmid-encoded, host genotype-specific enhancement of bacterial fitness. *J. Bacteriol.* **176**, 3140-3147.

41. Minasov, G., Wang, X. & Shoichet, B. K. (2002). An ultrahigh resolution structure of TEM-1 beta-lactamase suggests a role for Glu166 as the general base in acylation. *J. Am. Chem. Soc.* **124**, 5333-5340.

42. Mayer, S., Rudiger, S., Ang, H. C., Joerger, A. C. & Fersht, A. R. (2007). Correlation of levels of folded recombinant p53 in *Escherichia coli* with thermodynamic stability *in vitro*. *J. Mol. Biol.* **372**, 268-276.

43. Wang, X., Minasov, G. & Shoichet, B. K. (2002). Noncovalent interaction energies in covalent

complexes: TEM-1 β-lactamase and β-lactams. *Proteins: Struc. Func. Genet.* **47**, 86-96.

44. Becktel, W. J. & Schellman, J. A. (1987). Protein stability curves. *Biopolymers* **26**, 1859-1877.

45. Bershtein, S., Segal, M., Bekerman, R., Tokuriki, N. & Tawfik, D. S. (2006). Robustness-epistasis link shapes the fitness landscape of a randomly drifting protein. *Nature* **444**, 929-932.

46. Penel, S., Hughes, E. & Doig, A. J. (1999). Side-chain structures in the first turn of the alpha-helix. *J. Mol. Biol.* **287**, 127-143.

47. Matthews, B. W., Nicholson, H. & Becktel, W. J. (1987). Enhanced protein thermostability from site-directed mutations that decrease the entropy of unfolding. *Proc. Natl. Acad. Sci. USA* **84**, 6663-6667.

48. Palzkill, T., Le, Q.-Q., Venkatachalam, K. V., LaRocco, M. & Ocera, H. (1994). Evolution of antibiotic resistance: several different amino acid substitutions in an active site loop alter the substrate profile of ß-lactamase. *Mol. Microbiol.* **12**, 217-229.

49. Bowden, G. A., Paredes, A. M. & Georgiou, G. (1991). Structure and morphology of protein inclusion bodies in *Escherichia coli*. *Biotechnology* **9**, 725-730.

50. Kirchhoff, W. (1993). EXAM: A two-state thermodynamic analysis program., Gaithersburg, MD.

51. Otwinowski, Z. & Minor, W. (1997). Processing of X-ray diffraction data collected in oscillation mode. In *Methods in Enzymology: Macromolecular Crystallography, Part A* (Carter, C. W. & Sweet, R. M., eds.), pp. 307-326. Academic Press, New York.

52. Kissenger, C. R., Smith, B. A., Gehlhaar, D. K. & Bouzida, D. (2001). Molecular replacement by evolutionary search. *Acta Crystallographica* **D57**, 1474-1479.

53. Collaborative Computational Project, N. (1994). The CCP4 suite: programs for protein crystallography. *Acta Cryst.* **D50**, 760-763.

54. Laskowski, R. A., MacArther, M. W., Moss, D. S. & Thornton, J. M. (1993). PROCHECK: a program to check the stereochemical quality of protein structures. *J. Applied Crystall.* **26**, 283-291.

Supplementary Figure A.1

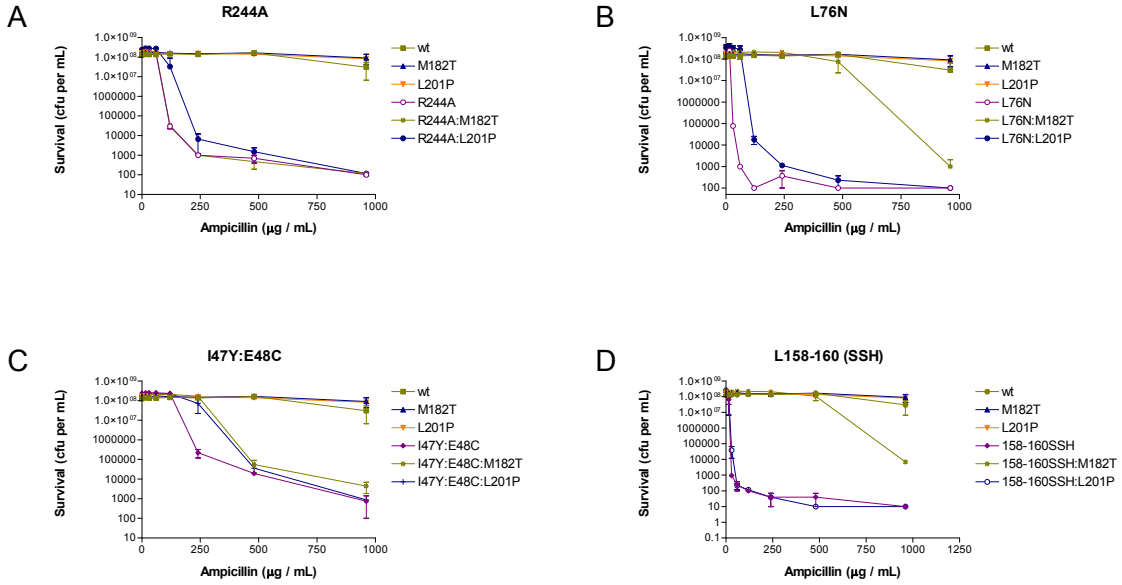

Supplementary Figure A.1. Expanded survival curves of *E. coli* with pBG66 plasmid encoding TEM-1 β-lactamase mutants, showing survival up to an ampicillin concentration of 950 µg/mL. **A.** Colony forming units (cfu) on agar plates containing increasing concentrations of ampicillin for *E. coli* containing R244A, M182T, L201P single and double mutants. **B.** Cfu for *E. coli* containing L76N, M182T, L201P single and double mutants. **C.** Cfu for *E. coli* containing I47Y:E48C, M182T, L201P mutant combinations. **D.** Cfu for *E. coli* containing H158S:V159S:T160H, M182T, L201P mutant combinations.

Publishing Agreement

It is the policy of the University to encourage the distribution of all theses, dissertations, and manuscripts. Copies of all UCSF theses, dissertations, and manuscripts will be routed to the library via the Graduate Division. The library will make all theses, dissertations, and manuscripts accessible to the public and will preserve these to the best of their abilities, in perpetuity.

Please sign the following statement:

I hereby grant permission to the Graduate Division of the University of California, San Francisco to release copies of my thesis, dissertation, or manuscript to the Campus Library to provide access and preservation, in whole or in part, in perpetuity.

Author Signature

12/14/09

Date